Power Transmission Capacity Enhancement of East-West Interconnectors Using Series-Shunt Compensation

by

Md. Shafiul Alam

A Thesis Submitted to the Department of Electrical and Electronic Engineering of Bangladesh University of Engineering and Technology in Partial Fulfillment of the Requirement for the Degree of

Master of Science in Electrical and Electronic Engineering

Department of Electrical and Electronic Engineering

BANGLADESH UNIVERSITY OF ENGINEERING AND TECHNOLOGY

Dhaka-1000, Bangladesh

February, 2012

The thesis titled "**Power Transmission Capacity Enhancement of East-West Interconnectors Using Series-Shunt Compensation**" submitted by Md. Shafiul Alam, Roll No. 0409062111P, Session: April, 2009, has been accepted as satisfactory in partial fulfillment of the requirement for the degree of **Master of Science in Electrical and Electronic Engineering** on February 27, 2012.

BOARD OF EXAMINERS

1. ____

Dr. Abdul Hasib Chowdhury — Chairman (Supervisor)
Associate Professor
Department of Electrical and Electronic Engineering
BUET, Dhaka-1000, Bangladesh

2. ____

Dr. Md. Saifur Rhaman — Member (Ex-officio)
Professor and Head
Department of Electrical and Electronic Engineering
BUET, Dhaka-1000, Bangladesh

3. ____

Dr. Md. Quamrul Ahsan — Member
Professor
Department of Electrical and Electronic Engineering
BUET, Dhaka-1000, Bangladesh

4. ____

Dr. Kazi Mujibur Rahman — Member
Professor
Department of Electrical and Electronic Engineering
BUET, Dhaka-1000, Bangladesh

5. ____

Dr. Ashikur Rahman Bhuiya — Member (External)
Senior Engineer
Alberta Electric System Operator
Calgary, Canada

Declaration

It is hereby declared that this thesis titled "**Power Transmission Capacity Enhancement of East-West Interconnectors Using Series-Shunt Compensation**" or any part of it has not been submitted elsewhere for the award of any degree or diploma.

Signature of the Candidate

Md. Shafiul Alam

Acknowledgements

The author would like to express heartiest gratitude to his supervisor Dr. Abdul Hasib Chowdhury, Associate Professor, Department of Electrical and Electronic Engineering, BUET, Dhaka, for his whole hearted support and co-operation to materialize this thesis. It is also acknowledged that without his advice, guidance and support this thesis work would not have been possible.

Next author would like to thank Dr. J. H. Chow, Professor, Department of Electrical and Computer Systems Engineering, Rensselaer Polytechnic Institute, New York, USA, for his continuous support through e-mail to work with the software Power System Toolbox (PST). The Author also thanks Professor Dr. C. A. Canizares, Department of Electrical and Computer Engineering, University of Waterloo, Canada, for supporting this work with the simulation tool UWPFLOW.

The author also thanks Md. Jan-E-Alam, PhD Student, Department of Computer and Telecommunications Engineering, University of Wollongong, Australia, for his kind support at the beginning of this work.

The author thanks his friend Nur Mohammad, Assistant Manager, Power Grid Company of Bangladesh (PGCB) and other PGCB officials for helping to model East West Interconnected System (EWIS) of Bangladesh Power System (BPS) network.

Finally, I thank my parents, close relatives and friends for their continuous inspiration towards the completion of this works.

Abstract

Utilization of the existing transmission line capacity to its fullest is most important due to the continuous growth of the demand and rising cost of new transmission infrastructures. Due to the problems associated with voltage drop and stability limits, a transmission line can not be loaded up to its thermal limit. The potential benefits of installing Flexible AC Transmission System (FACTS) devices on the system for enhancing power transmission capacity and stability are well known. Two main members of FACTS family like thyristor controlled series capacitor (TCSC) and static var compensator (SVC) have been widely studied and reported in technical literature and have been shown as effective as well as time saving alternative to building new transmission lines for enhancing power transmission capacity. This thesis examines the application of series-shunt compensation by means of TCSC and SVC to enhance power transmission capacity of two East-West Interconnectors (EWIs) of Bangladesh Power System (BPS). Two SVCs are connected in parallel with two buses in the western region of the interconnectors and two TCSCs are connected in series with the interconnectors. Modal analysis is performed to tune parameters of damping controllers of these FACTS devices. Bifurcation, steady state, and transient analyses clearly demonstrate positive effect of series-shunt compensation on transmission capacity and stability in BPS network.

Table of Contents

Chapter 3: Test System Modeling

Chapter 4: Simulation Results and Analyses

Chapter 5: Conclusion

List of Figures

List of Tables

List of Abbreviations

ACS	Advanced Series Compensation
ATC	Available Transfer Capacity
BPS	Bangladesh Power System
CPF	Continuation Power Flow Analysis
EWI	East West Interconnector
EWIS	East West Interconnected System
FACTS	Flexible AC Transmission System
HB	Hopf Bifurcation
kV	Kilo Volt
LF	Loading Factor
MVA	Mega Volt Ampere
MVAR	Mega Volt Ampere Reactive
MW	Mega Watt
PGCB	Power Grid Company of Bangladesh
PST	Power System Toolbox
RE	Sending End
SE	Receiving End
SNB	Saddle Node Bifurcation
SVC	Static VAR Compensator
TCS	Thyristor Controlled Reactor
TCSC	Thyristor Controlled Series Compensation
TSC	Thyristor Switched Capacitor
UWPFLOW	University of Waterloo Power Flow

List of Symbols

δ	Transmission angle
λ	Loading factor
$f(\cdot)$	Vector function
$g(\cdot)$	Algebraic equation
J	System jacobian
A	State matrix
θ	Angular position of rotor in radian
T_m	Mechanical torque supplied by the prime mover in N-m
Te	Electrical torque output of the alternator in N-m
x_l	Leakage reactance
ω	Rotor speed
D	Damping constant
τ_j	Inertia time constant
α	Thyristor firing angle
x_e	Equivalent reactance of TCSC
ε_V	Error signal

CHAPTER 1

Introduction

1.1 Introduction

It is important to optimize the utilization of the existing transmission systems in a competitive market environment due to the challenges associated with constructing new transmission lines. Growth of different commercial schemes for the electric power industry, particularly deregulation of market, has made this requirement even stronger [1]. A transmission line can be loaded up to its thermal limit however, practically if the receiving zones do not have compensating reactive elements, the voltage can drop below the limit constant by quality criteria [2]. In such situation, it is advisable to limit the transmission of these lines to prevent excessively low voltages in the receiving end as well as to prevent a possible voltage collapse [3].

Power transmission capacity can be enhanced directly by using series and shunt compensation [4]. The objective of Flexible AC Transmission System (FACTS) technology is to bring a system under control and to transmit power as premeditated by control centre; it also improves the system stability. The use of FACTS controlled series compensation and shunt compensation; especially thyristor controlled series capacitor (TCSC) and static var compensator (SVC), for stability enhancement have been reported in [5].

Most of the thermal capacity of east-west interconnectors (EWIs) of Bangladesh Power System (BPS) is unexploited [6]. Application of controlled series compensation has been studied and it has been found that even with highest level of series compensation 15% capacity of first EWI and 45% capacity of second EWI are left unused [6]. Combined application of series and shunt compensation can be studied to enhance transmission capacity. TCSC and SVC damping controller can be employed to damp system oscillation.

An application of series-shunt compensation using TCSC and SVC has been studied in this work for power transmission capacity enhancement of EWIs of BPS network. This work also investigates the improvement of stability of the system with proper tuning of damping controller parameters of TCSC and SVC for EWIs.

1.2 Background and Present State of the Problem

Realizing maximum power transfer at the lowest possible cost is one of the greatest challenges today for transmission system operators. In meeting this challenge, early researchers explored the possibility of using series compensation of transmission line. In [7], R.E. Marbury et. al. introduced series capacitor as an element connected in series with the line to improve the voltage by interleaving negative reactance. A series capacitor installation process consists of a bank of capacitors that is connected in series with each phase of transmission or distribution line, each bank having the reactance necessary to cancel the desired portion of inductive reactance of each phase in order to handle maximum continuous and momentary line currents. In most of the circuits to which series capacitors are connected the fault currents are more than twice of the continuous current rating. Due to this reasons it is necessary to use capacitors with continuous current rating equal to one half of maximum current which may flow during a fault.

In [8], Starr and Evans demonstrated that high voltage transmission circuits can be operated at their optimum loading only when their equivalent impedances or lengths are reduced. This reduction in transfer impedance can be accomplished most cost-effectively through the use of series capacitor. Series capacitor can be connected at any point of the transmission line, but mid point of the transmission path is preferable, as this minimizes the problems of exciting inrush currents and reduces the voltages to the ground. When the system with series capacitor subjected to faults, high voltage drops across the capacitor are produced so measures against high voltage drops must be provided. Authors proposed two types of capacitors as measures such as non limited and limited voltage capacitors. Non-limited voltage type capacitor has desirable feature of always being able to provide reactive compensation even under stressed conditions of the system but it is not cost effective. Limited voltage type capacitor is less expensive and small in size but can not provide desired reactive compensation during fault conditions.

In [9], S. B. Crary, L. E. Saline discussed several methods of applying series capacitor. One method adopted by the authors is switching out a parallel bank of capacitors to increase compensation. The other is to insert an additional series bank after the faulted section of parallel circuit has been isolated. Although the two methods are roughly equivalent, the latter may result in less expensive and more trustworthy switching. A switch of lower recovery-voltage rating could be engaged, and the troublesome problem of breaker restriking on capacitor back-to-back switching would be minimized. If all capacitor components are considered to operate at rated voltage under maximum system load conditions, the series arrangement also requires about 20 percent less total capacitor kilovolt-amperes for the same net compensation. The authors also showed that series capacitors reduce the over-all line reactance, and hence allow a larger sTable transfer of power and increase system transient stability. The most economical and practical location of series capacitors was proven by the authors in the intermediate switching stations as mentioned in [8].

To improve the stability of the pacific regional system, 500 kV series capacitor was installed in the pacific intertie of California [10]. At the time of installation there were no industry standards for 500 kV series capacitor banks. In order to take the advantage of existing manufacturing techniques, capacitor units of 100-125 kVAR were used in series parallel combination. Upon the loss of one line, system studies indicated the possibility of subsequent power swings which could produce up to 4800 amperes on the remaining line for a period of about 10 seconds. Loading on the line and capacitor bank would be gradually decreased over a time to 1800 amperes which is 12.5% higher than the bank nominal nameplate rating. In order to eliminate this problem provision were kept for increasing current rating 12.5% by adding series parallel capacitor units without significantly modifying the basic protective and control system for the bank.

The concepts of thyristor assisted FACTS was introduced by N. G. Hingorani [11]. Several merits and demerits of High Voltage DC (HVDC) transmission were discussed and due to the high cost of HVDC converters, FACTS was introduced to decrease transmission cost, which is a collection of thyristor based controllers, including phase shifter, advanced static VAR compensator, dynamic brake, modulator series capacitor, load tap changer, and fault current limiter.

J. J. Paserba et. al. [12] presented a model of TCSC for transient and oscillatory studies. The model has option for an open loop auxiliary signal which could be the input from an external power flow controller. The model also comprises a small-signal modulation input. The reference signal to this model is the initial operating point of the TCSC. All of these inputs are added which is put through a first-order lag. This lag is correlated with the firing controls and natural response of the TCSC and is represented by a single time constant. The output of first order lag is the desired reactance of the TCSC. An overload management function was added to this model to switch from transient overload capability studies to long-term dynamic stability studies.

S. G. Jalali et. al. [13] presented a new model of Advanced Series Compensation (ASC) for stability analysis. In the model slow response time is created by the joint effect of the parallel capacitors and the Thyristor Controlled Reactor (TCR) which act together to produce desired effective impedance. The differential equations of the ASC capacitor and the TCR are solved to present this stability model. To ensure the correct response of the model during power swings authors included power oscillation damping algorithms which can be optimized for the particular system being studied.

Z. Xu et. al. [14] discussed on the controllable impedance range of TCSC from the theoretical derivation. Authors derived an equivalent reactance equation of TCSC in terms of thyristor firing angle and ratio (K) of capacitive and inductive reactance of TCSC at fundamental frequency. There can be several resonant points if K can take any values. In order to avoid such difficulty and to have one resonant point K is restricted to a certain value. In real operation, K is fixed, and the equivalent reactance of TCSC is determined by the conduction angle. The rate of change of equivalent reactance of TCSC with respect to thyristor conduction angle is defined as Impedance Sensitivity Factor (ISF). Near the resonant point the ISF is large, thus small change in conduction angle will cause large change in equivalent reactance of TCSC which will influence sTable operation of power system. So authors emphasized to restrict the range of conduction angle so that the value of ISF is within the allowable range.

In [15], A. D. Rosso et. al. proposed a TCSC damping controller to damp power system oscillations, which consists of a washout filter, a dynamic compensator, and a limiter. The function of the washout filter is to avoid controller response to the dc offset of the input signal. To provide the necessary phase-lead characteristics dynamic compensator consists two or more lead-lag blocks. Open loop eigenvalue and mode observability analysis were conducted to tune damping controller parameters. In [16], A. D. Rosso et. al. modified [15] with TCSC set point variations upon occurrence of large disturbance.

In [17], L. Rouco and F. L. Pagola analyzed the design of hierarchical TCSC controller taking into account interactions between stability control loop and power flow control loop. The power flow control loop is considered to be disabled after large disturbance with TCSC steady state reactance at a fixed value, at this instant stability control loop provides maximum compensation level so that synchronizing torque is increased to improve first swing stability of the system, as well as provide proper modulation to damp the subsequent power oscillations. Variable post-contingency set point of TCSC showed improved transient performance of the test system. Modal controllability is determined for the modulation of series capacitor reactance. Modal observability factor is calculated as the product of the observability vector and the vector that contains components of right eigenvector corresponding to the components of the terminal of the device. As reviewed in [15], authors also calculated controllability and observability to tune damping controller parameters but in this work authors multiplied controllability and observability and termed this multiplication as “engenvalue sensitivity”. The sensitivity of eigenvalues informs about the amount and direction of eignevalue displacement.

Jovcic and Pillai [18] derived a new linear continuous TCSC model in state-space form. The fundamental frequency model of a TCSC is derived first to facilitate initialization of the steady-state parameters. In this model voltage across the TCSC capacitor comprises an uncontrolled and a controlled component and it is assumed that the line current is constant over one fundamental cycle. The uncontrolled component is unaffected by thyristor switching and it is also constant over a fundamental cycle since it is directly proportional to the amplitude of the line current. The controlled component is represented as a nonlinear function of the uncontrolled component and thyristor firing angle. To calculate thyristor firing angle in order to show dynamic compensation effect by the above developed model, controller included a second order feedback filter, PI controller, PLL (Phase-Locked-Loop) and a transport delay model which were not included in the previous models [12,13,14].

A Fixed level of series compensation with TCSC can improve transient stability of power system; but for enhancing more transient stability, a damping controller can be added with TCSC for modulating the reactance of TCSC [15, 19].

To suppress inter-area mode oscillations and to improve power system damping in [19], J. X. Ling et. al. proposed adaptive TCSC damping controller based on oscillation energy. In the proposed method no detailed information about system data and configuration of the studied power system is required. Implementation of this controller involves only active power flow along the tie line as feedback where the TCSC is installed. Following a disturbance in the system kinetic energy and potential energy of the oscillations as well as their sum increases from zero until the disturbance is cleared. Conversion rate of potential to kinetic and kinetic to potential energy determines the magnitude of oscillations.

Q. Liu et. al [20] presented a new method for Supplementary Damping Controller (SDC) of TCSC based on Linear Parameter Varying (LPV). An LPV damping controller for TCSC is designed based on a single Lyapunov function under some realistic constraints. The active power is used as feedback control signal for controller in this work among the different locally measurable feedback control signals like the active power flow of the tie line, the magnitude of the voltage at the TCSC. To construct the LPV model for the power system, some scheduling parameter is first selected. Then for each scheduling point indicated in terms of real and reactive power loads, real power generation scheduled at generator buses, and voltage magnitude at certain buses, a power flow solution is obtained. Initial value of each state is calculated with this power flow solution and then the system is linearized at this equilibrium. The proposed LPV technique guarantees the stability of the system with the obtained LPV controller during the arbitrarily fast change of the measured scheduling parameter.

For a hybrid power system which have both TCSC and series capacitors, a SDC is proposed by X. Zheng, Z. Xu, and J. Zhang [21] to mitigate subsynchronous resonance (SSR) caused by the series capacitors. The controller is based on the reactance versus firing angle characteristic. The proposed damping controller is composed of a bandpass filter, a gain, two or more lead-lag blocks and a limiter. The authors used the deviation of the generator speed as the input signal than that of bus voltage magnitude, line current, active power etc. as reported in [19, 20]. A bandpass filer is added to remove low frequency signal and high frequency harmonics and to pass only subsynchronous frequency band. The lead-lag blocks are then used for the phase shift compensation. A limiter is employed to avoid the parallel resonance.

Shunt compensation has been widely used for many years to provide voltage support on long transmission line. The basic power flow equation through a transmission line shows that modulating the voltage influences the flow of the active power.

In [22], L. Gyugyi and E. R.Taylor presented and compared shunt compensation by means of fixed capacitor banks and synchronously switchable capacitor banks. The steady-state characteristic and the response of the compensators to small disturbances i.e. when the resultant terminal voltage excursions remain in the liner operation range are practically identical by both compensation schemes. But Superior operating behavior is attained by synchronously switchable capacitor banks than that of fixed capacitor banks when subjected to large disturbances. The authors also showed that the fixed type capacitor has high loss at zero VAR output which decreases with the increase of VAR output. Switchable capacitor shows just complementary behavior with fixed type capacitor. So in the power system where the dynamic characteristics of the compensator are mainly used to improve transient stability, to support voltage and to restrain overvoltage, the average VAR output may be usually low and therefore the switched capacitor type compensator can have a considerable economic advantage in loss evaluation over fixed capacitor type compensator.

In [23], A. A. Edris proposed VAR compensator to enhance loadability of low capacity power system. In the test system transmission voltage is selected to be 130 kV, the load is assumed a composite one with 50 % static part of impedance character and 50 % dynamic part represented by an equivalent induction motor. Loading margin of this system is obtained through repeated time simulations of the receiving end voltage-time response following a 200 ms three phase short circuit fault at this end under both fixed value VAR compensator, static VAR compensator (SVC) and it is found that SVC has 1.5 times greater loadability limit than that of fixed type VAR compensator. Finally, author derived a mathematical formula defining the sensitivity of the receiving end voltage to the shunt compensation with the help of this formula regulator gain of the used SVC is calculated to improve transient performance.

Power transmission capacity and system stability improvement by Static Var Compensator (SVC) have been presented in [24]. To control bus voltage, SVC involves voltage control loop which is composed of voltage regulator, TCR and Thyristor Switched Capacitor (TSC) firing circuit, and voltage magnitude transducer. The primary control function is carried out by voltage regulator. The output of the voltage regulator denotes the controllable susceptance of SVC. The firing circuits include nonlinearity to convert this controllable susceptance value to firing angle command for TCR. The function of the voltage magnitude transducer is to sense the voltage of SVC bus. The middle of the transmission line is suggested as the best location for SVC installation to enhance transmission capacity and to damp electromecanical oscillations. A supplementary damping controller named "SVSTAB" is connected with SVC. Different types of locally measureable signals like frequency, voltage magnitude, and active current or power flow on the major lines are tested as input of this supplementary damping controller.

In [25], E. Lerch et. al. developed a new method for SVC damping controller. As stated by the authors the purpose of locally measurable signals like frequency, voltage magnitude and in addition active current or power in the incoming lines to the node of SVC is to calculate phase angle difference for damping power system oscillation by the use of this phase angle difference. Instead of using frequency, voltage magnitude and active current or power as input signals to the damping controller [24], a signal for phase angle of generators with respect to the SVC node is used in this work [25]. The phase angle difference is obtained by elimination of the reference angle of the SVC node. Additional filters are needed to filter out interference signals from the relevant frequency range of oscillation from 0.3 to about 2 Hz. After additional filters, the authors employed a bang-bang control to their proposed controller to wash out harmonic content from the phase angle difference signal.

Zhao and Jiang [26] presented a new SVC damping controller by formulating and solving power system damping control problem using robust optimization technique. Challenge for supplementary damping controller is to damp out system oscillations in a particular frequency band, to meet this challenge it is necessary to formulate the controller design problem based on the $H_\propto$ optimization technique. Another demand to supplementary control is that it needs to introduce excessive variations so that fluctuations of voltage, transferred power are within the desired limits, in order to meet this demand, the authors choose appropriate weighting functions. Having chosen appropriate weighting functions damping controller was designed by minimizing cost function in the frequency domain.

Q. Wang et. al. [27] showed the enhancement of power transmission capacity of long transmission line by means of shunt compensation. This work took into account the line losses as well as the Sending End (SE), Receiving End (RE) impedances in the presence of the shunt compensator like SVC. Transmission line is modeled in the form of π-circuit. Having derived the equation of real power and angle of transmission line for a two machine system, the authors modified line section susceptance by means of variable SVC susceptance and showed the improvement of transmission capacity of the line with reduced machine angle difference.

In real power system reactance of the transmission path and the time constant of SVC regulator may contain uncertainties. Retuning the SVC controller is necessary when these uncertainties are large enough. Moreover power system parameters and variables are changed due to the change in system structure over time. In order to minimize above difficulties, R. Yan et. al. [28] proposed a new nonlinear robust adaptive SVC controller which can deal with both constant and time varying systems [24, 25]. The design is started from state space model of the system. In the design procedure transmission line reactance is considered as unknown constant parameter and two different cases for regulator time constant of SVC are regarded that are unknown constant or unknown time varying uncertainty. By choosing appropriate values for the design parameters, tracking error is minimized sufficiently.

H. K. Tyll [29] presented detailed information about how SVC can play an important role in real power system by appropriate reactive power compensation. The author demonstrated that at all load conditions like heavy load, light load, outage of any line during heavy load condition, load rejection at the end of the line, SVC can minimize voltage deviations and can maintain good voltage profile. In the stressed system the first peak cannot be influenced because the SVC control must first observe the increase and can only react afterwards. Having sensed first peak of oscillation by the SVC damping controller, system stability margin is maintained within the prescribed limits by damping the oscillations of the system than that of without SVC.

M. N Noroozian et. al. [30] presented a new robust control strategy for both TCSC and SVC which respond to any network conditions like system loading, network topology, fault type and location. In [26], the authors proposed robust controller design for SVC only but in this work [30] the effect of both TCSC and SVC on each other is taken into account for the robust controller design. The control strategies for these devices are based on energy function methods and derived controls use local input signals. The control strategies are started with formulation of energy function in which TCSC is modeled as series combination of fixed and controllable reactance and SVC is modeled as parallel combination of fixed and controllable shunt admittance. In order to damp electromechanical oscillations series and shunt components are controlled in such a way that the total energy function decreases. Finally control laws for TCSC and SVC are derived form this condition.

In [31], R. Griinbaum et. a. presented several examples of benefits of FACTS like TCSC and SVC in power transmission systems. For the system with increasing transmission line loading over long distances, TCSC and SVC are shown to be very robust and effective means to improve damping. The damping effect of TCSC and SVC has different benefits like the effectiveness of these FACTS members for controlling of power swings increases with high levels of power transfer, improvement of voltage regulation, reactive balance and transient stability improvements.

Blackout of the power system is directly related with Voltage collapse phenomena. This voltage collapse problem can be restated as an optimization problem where the objective is to maximize certain system parameters classically associated to load levels [8]. This voltage collapse techniques may also be employed to compute the maximum power that can be transmitted through the transmission system also known in the new competitive energy market as Total

Transfer Capability (TTC) or as Available Transfer Capability (ATC). Several FACTS devices like TCSC and SVC can be employed in the existing power network to improve its power handling capacity thus increasing ATC of the transmission line [5].

TCSC and SVC controllers are basically based on variable series and shunt compensation of transmission system respectively hence it is important to study the effect of these controllers on ATC. Effect of TCSC and SVC controller on maximizing ATC has been studied in [32]. Bifurcation theorem is used in this study for computing ATC which is directly associated with voltage collapse conditions i.e. saddle node bifurcations. Effect of constant PQ and voltage dependent load modeling has been studied in this work with the Italian test system.

Both the works [5, 32] concluded that TCSC and SVC have positive effect on the ATC enhancement of the transmission line at optimum cost.

Power systems are now large, complex and interconnected systems, which consist of thousands of buses and hundreds of generators and lines. Due to the growth of demand on such large system, electric utilities have to rely on power export/import arrangements through transmission capacity enhancement by constructing new lines. But new transmission lines are expensive and take considerable amount of time to construct. This leads the utility planners to utilize full capacity of the existing transmission lines and resources. The recent improvement and use of FACTS devices like TCSC and SVC in power transmission system have led to many applications not only to increase the voltage stability of the existing system but also to provide of greater operating flexibility. The literature presented above encourages studying the application of TCSC and SVC to enhance transmission capacity and stability in BPS network particularly in the EWIs of BPS network.

1.3 Thesis objective

The main goal of this work is to improve power transmission capacity of EWIs in BPS while improving system stability by means of the series-shunt compensation through appropriate controller design for TCSC and SVC.

1.4 Scope of Work

Bangladesh power system is geographically divided into five operational regions namely- Dhaka, Central, Southern, Northern and Western region. Dhaka, Central, Southern- these three regions jointly form the greater Eastern Grid, on the other hand Northern and Western region form Western Grid. Bulk power is generated in the Eastern Grid and transmitted to the Western grid by means of two EWIs that are Ghorasal to Ishurdi (1^{st} EWI) and Ashuganj to Sirajganj (2^{nd} EWI). This work investigates power transmission capacity enhancement of these two EWIs by means of series-shunt compensation. The specific objectives include: determination of maximum loading point of EWIs, investigation of oscillatory behavior of the system, calculation of damping controller parameters to improve damping of electromechanical oscillation of the system by means of series-shunt compensation.

In this work Continuation Power Flow (CPF) analysis is performed with gradually increased loading in the western zone to determine maximum loading point associated with the voltage collapse. Modal analysis is performed to tune damping controller parameter of TCSC and SVC. Time domain simulation is carried out to observe the improvement in transient stability with series-shunt compensation.

1.5 Organization of This Thesis

The paper is structured as follows. **Chapter 1** presents several aspects of series-shunt compensation and current state of work. Analytical techniques are presented in **Chapter 2**. **Chapter 3** presents test systems, dynamic modeling of systems, and simulation tools. Results of analyses have been presented and discussed in **Chapter 4.** Conclusion and future research suggestions are provided in **Chapter 5. Appendix A** presents data format and two area test system data. Finally, **Appendix B** presents East West Interconnected System (EWIS) data.

CHAPTER 2

Analytical Techniques

2.1 Introduction

This chapter briefly introduces several analytical techniques used in this work. To capture static and dynamic behavior of the EWIs without and with series-shunt compensation- steady state, bifurcation and transient analysis have been performed. Steady state analysis can be performed to determine transmission angle between sending and receiving end buses. Transient stability analysis can be conducted to determine system stability upon occurrence of a large disturbance. Static voltage collapse phenomena may be explained as a dynamic effect of a generic saddle-node bifurcation. Continuation Power Flow (CPF) analysis can be used to find out such saddle-node bifurcation [5, 33].

2.2 Steady State Analysis

The load flow problem represents the nonlinear relationships among bus power injections, power demands, and bus voltages and angles, with the network constants providing the circuit parameters. It is the heart of most system-planning studies and also the initial point for transient and dynamic stability studies. In this work Newton-Raphson (N-R) method is used for solving the load flow equations.

Load flow analysis involves calculation of line power flow, bus voltage magnitude, voltage angle to investigate steady state operation of system and for future expansion of system. For a given transmission path, there is a maximum power level which can be transmitted from sending end to receiving end while maintaining stability is known as steady state limit. This stability limit is determined by the angle difference between the sending and receiving end voltage. This angle is known as transmission angle. A system is said to have better stability when transferring same amount of power with lower transmission angle [34].

Typical power and transmission angle relation is described in the following equation (2.1) [35, 36].

$$P = \frac{V_S V_R}{X_L} sin\delta \tag{2.1}$$

Where,

P = transmitted power from sending to receiving end

V_S= sending end voltage

V_R= receiving end voltage

X_L= inductive reactance of the transmission line

δ = transmission angle

Application of series-shunt compensation can improve power transmission with lower transmission angle [45]. Detailed on this matter of stability is reported in some of the text books [36, 37, 38]. Relation of steady state power transmission and degree of series shunt compensation can be understood by the equation (2.2) as reported in [37].

$$P' = P\sqrt{\frac{1-K_{sh}}{1-K_{se}}} \tag{2.2}$$

Where,

P', P= modified and natural power transfer respectively

$k_{sh}= \frac{b_{sh}}{b_c}$ =degree of shunt compensation

$k_{se}= \frac{x_{Cse}}{x_L}$ =degree of series compensation

2.3 Bifurcation Analysis

Voltage stability problems in the power system may be analyzed by bifurcations theory. Generally two types of bifurcations are of interest to the power system researchers. These are characterized by changes in the eigenvalues of the system equilibria as certain parameters change in the system. Typically, system loading level is used as bifurcation parameters, which is varied slowly, moving the system from one equilibrium point to another. To locate bifurcation points system is modeled by suiTable mathematical equation.

Power system is a highly non linear system; dynamic behavior of such a system may be represented by the following general mathematical description [5].

$$\dot{x} = f(x, y, \lambda, p)$$
$$o = g(x, y, \lambda, p) \quad (2.3)$$

Where, $x \in \Re^n$ represents the system state variables, associated with dynamic states of generators, loads, and any other time varying element in the system, such as TCSC and SVC controllers, exciter governor of the machines etc.; $y \in \Re^n$ corresponds to the algebraic variables, usually related to the transmission system and steady-state element models, such as some generating sources and loads in the network; $\lambda \in \Re^{\mathrm{m}}$ corresponds to set of variables that are not controllable, varied continuously, typically loading factor is one of the parameter which varies as system load changes, and leads the system into bifurcation; $p \in \Re^k$ stands for some directly controllable parameters such as degree of series shunt compensation; *f(·)* and *g(·)* represent vector function of algebraic equation and system constraints function respectively.

Many analysis methodologies have been proposed and are currently being used for the study of voltage collapse phenomena. These techniques are associated with identification of system equilibria where the corresponding Jacobians become singular; these equilibrium points are typically referred to as points of voltage collapse and can be mathematically associated with Saddle-Node Bifurcation (SNB) points [2, 35]. Based on equation (2.3), under certain assumptions, corresponding equilibrium point can be defined by equation (2.4).

$$\begin{bmatrix} f(x_o, y_o, \lambda_o p_o) \\ g(x_o, y_o, \lambda_o p_o) \end{bmatrix} = F(z_o, \lambda_o p_o) = 0 \quad (2.4)$$

And its jacobian $D_z F|_o$ has a zero eigenvalue [35].

Determination of SNB points related to voltage collapse phenomena is associated with finding out collapse points (x_o, y_o, λ_o) for a given set of controllable parameters p_o, typically corresponds to the maximum loading level or loadability margin in p.u. or MW.

A typical nose curve/PV curve/bifurcation diagram is shown in Figure 2.1, where the loading factor, λ, is increased from 0 until system voltage collapse.

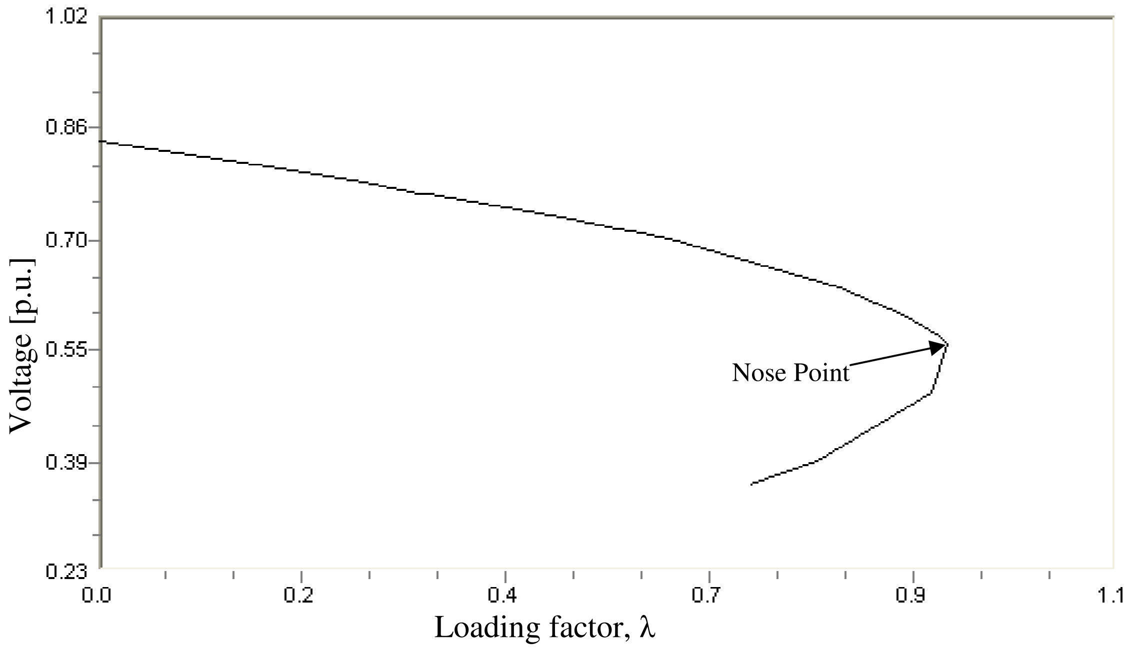

Figure 2.1: Typical bifurcation diagram

To explain the bifurcation diagram shown in Figure 2.1, let us consider a radial two bus power system. Bus-I is a generator bus and bus-II is a load bus as shown in Figure 2.2.

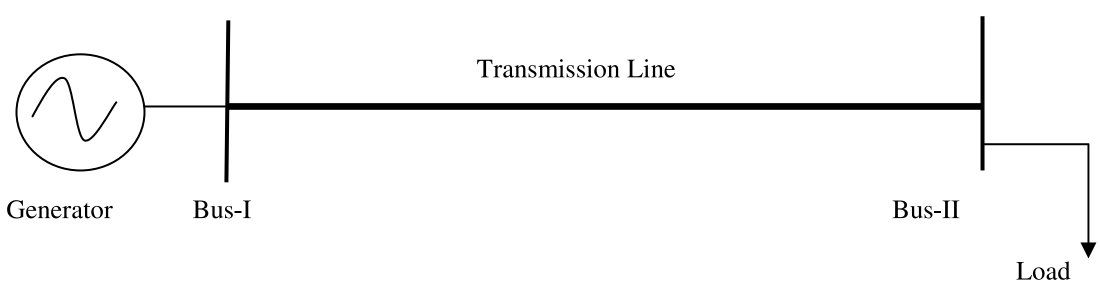

Figure 2.2: Simple two bus system

To clarify SNB on such simple two bus system, assume base case active and reactive load on bus-II to be P_0 and Q_0 respectively, which is increased gradually as loading factor (λ) is increased in the following manner.

$$P = P_0 (1+ \lambda) \quad (2.5A)$$

$$Q = Q_0 (1+ \lambda) \quad (2.5B)$$

Keeping all others system parameters unchanged, if loading in bus-II is increased with a loading factor (λ) gradually, voltage at bus-II decreases progressively, and at a point further increase in loading factor causes a sharp and quick fall in system voltage, this point is known as nose point, shown in Figure 2.1. This voltage collapse phenomenon is also known as Saddle Node Bifurcation (SNB) which represents maximum loading point of the system [36, 39, 40].

There are many possible ways of determining such SNB where corresponding power flow Jacobians becomes singular [2, 35, 41]. One of the simple methods is to use an ordinary power flow and to gradually increase loads until convergence is no longer obtained. But this process needs manual intervention and most of the cases this approach often experiences from convergence difficulties and one is never sure where the actual limits are.

Another method of determining SNB in dynamic system is CPF technique. Continuation power flow technique consists of three step approach of determining equilibrium points as one of the system parameter like loading parameter (λ) changes. These steps are predictor, corrector and parameterization.

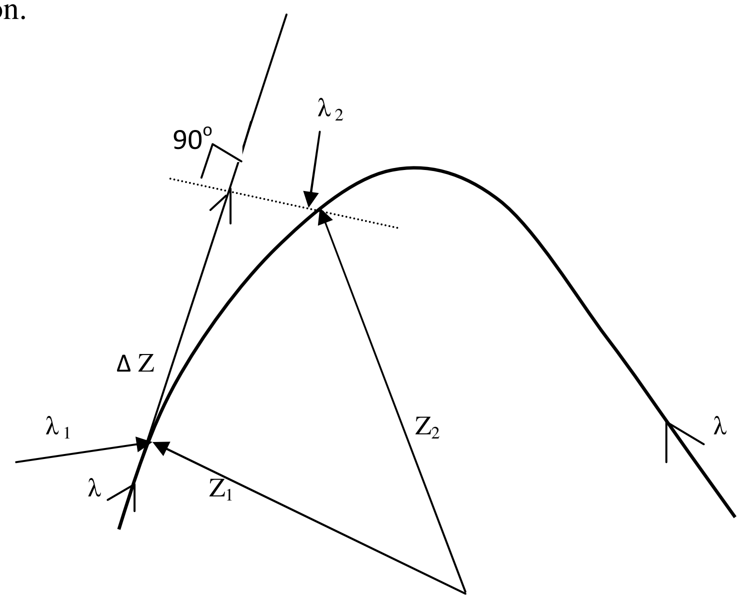

Figure 2.3: Continuation method geometry in state space and load parameter space

At the predictor step arbitrary steps of loading parameter and state variables are chosen to predict a new equilibrium point from the previous known equilibrium point. Corrector step is used to find intersection between the perpendicular plane to the tangent vector at the preceding equilibrium and branch as shown in Figure 2.3. Step size is reduced if the process does not converge. As the system closes to the solution of power flow equations by varying loading parameter, system Jacobian becomes ill-conditioned, then parameterization involves switching loading parameter to the new variables of the system that presents highest changes, guarantees the Jacobian of the power flow equations is non singular at saddle node bifurcation point [42]. The software package used in this work is based on CPF analysis, and uses voltage as switching variable from loading factor in the parameterization step.

Before experiencing voltage collapse corresponding to saddle node bifurcation, power system may experience another local bifurcation termed as “Hopf Bifurcation (HB)” which may cause oscillatory instability [40]. Hopf Bifurcation analysis is based on an eigenvalue analysis, also referred to as small signal stability or steady state stability analysis in power systems, as some system parameters (λ, p) in the differential and algebraic equation (2.3) changes.

Determination of HB point is started with linearization of equation (2.3) about an operation point (x_o, y_o) for a given set of parameters (λ_o, p_o) which yields equation (2.6) as reported in [43].

$$\begin{bmatrix} \Delta\dot{x} \\ 0 \end{bmatrix} = \begin{bmatrix} J_1 & J_2 \\ J_3 & J_4 \end{bmatrix} \begin{bmatrix} \Delta x \\ \Delta y \end{bmatrix} \tag{2.6}$$

Where, J is the system Jacobian. System eignevalues can be computed by eliminating Δy in the above equation which gives equation (2.7).

$$\Delta\dot{x} = (J_1 - J_2 J_4^{-1} J_3)\Delta x = A\Delta x \tag{2.7}$$

Where, A is the state matrix of the system. Now HB point in the system is determined by observing eigenvalues of state matrix A, as some of the parameters (λ, p) of the system change.

HB is identified as a point when a pair of complex conjugate eigenvalues having non zero real part of the system state matrix crosses the imaginary axis of the complex plane [40, 43].

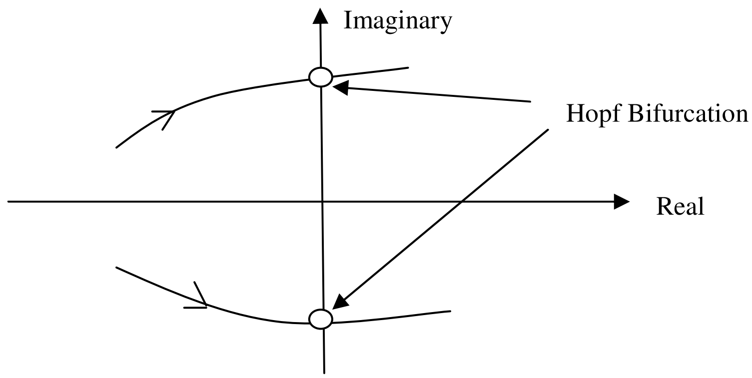

Figure 2.4: Locus of eigenvalues on hopf bifurcation

As loading of the system is increased, critical eigenvalues shifts to right half from left half region of s-plane as shown in Figure 2.4. Once real part of critical eigenvalues becomes zero, it indicates oscillatory behavior of the system.

Application of series-shunt compensation moves critical eigenvalues again into the left half region of s-plane, and hence improve oscillatory instability of the system [44, 45]. Dynamic Loading Margin (DLM) related to HB and Static Loading Margin (SLM) related to SNB of EWIs without and with compensation have been determined by modal analysis and CPF technique as reported in [45].

2.4 Transient Stability Analysis

In this work transient stability analysis has been performed to show performance of damping controllers of TCSC and SVC. Transient stability analysis is part of dynamic security analysis of power system which involves the evaluation of the ability of a power system to maintain synchronism under severe disturbances. When subjected to large disturbances, linearization technique is not allowed in solving non linear differential and algebraic equations, and thus iterative method is used to solve the equations [37, 38]. In transient stability analysis linear differential and algebraic equations are solved to determine bus voltage, machine angle, line power flow etc. upon occurrence of large disturbances. The motion of machine rotor is given by the equation (2.8) as reported in [37, 38].

$$J\frac{d^2\theta}{dt^2} = T_m - T_e \tag{2.8}$$

Where,

J = total moment of inertia of the rotor mass in kgm^2

T_m = mechanical torque supplied by the prime mover in N-m

T_e = electrical torque output of the alternator in N-m

θ = angular position of the rotor in radian

In transient stability analysis, equation (2.8) is solved using step by step technique.

2.5 Summary of Analytical Techniques

In this chapter, several analytical techniques have been introduced briefly that are used in the enhancement of transmission capacity of EWIs as well as stability of the system. CPF analysis has been introduced to find out SNB related to voltage collapse. This analysis is used to trace the solution of the power flow equations along with dynamic states of generator, loads, and any other time varying elements in the system such as FACTS controller. Transmission angle between sending and receiving end buses can be determined by steady state analysis. Eigenvalues and eigenvectors can be determined by means of modal analysis and the transient stability analysis can be conducted to determine system stability upon occurrence of a large disturbance.

CHAPTER 3

Test System Modeling

3.1 Introduction

This chapter introduces description of two test systems one is well known two area system and second one is EWIS of BPS network. Detailed system modeling for EWIS is introduced along with brief description of simulation tools. Two area system modeling is not presented in this work because this test system has been used in many literatures for stability analysis [37, 46].

3.2 Test Systems

Transmission capacity and stability enhancement by applying series-shunt compensation have been observed in this work on two test power systems one is two area test system and another is the EWIS of BPS network which is the main focus of this work. A standard two area system has been considered as a test bed before using the EWIS.

3.2.1 Two Area System

The two area system consists of two regions each having two generators and one load as shown in Figure 3.1. These two regions are connected by a double circuit transmission line. Two capacitive shunts are connected with two load busses in order to support reactive power. At base case condition Area-II has generation lack of 367 MW that is supplied by the surplus of area-I.

This test system has been used in many references [37, 46] for the purpose of stability analysis.

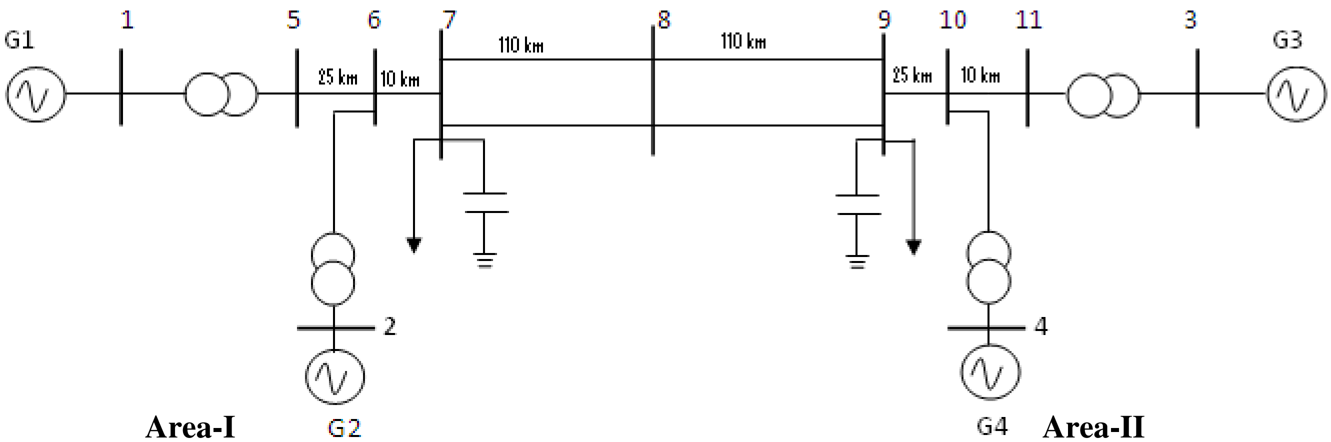

Figure 3.1: Two area test system

In order to apply series compensation on the tie-line by means of TCSC an additional bus is connected next to sectioning bus and shunt compensation is applied by SVC connected at the load bus of area-II.

3.2.2 East West Interconnected System

Bulk power is generated in the eastern grid of BPS network. This power is transmitted to the western grid by means of two tie line that are Ghorasal to Ishurdi (1st EWI) and Ashuganj to Sirajganj (2nd EWI). Figure 3.2 shows EWIS system of BPS network. This topology has been derived from the actual network condition of BPS.

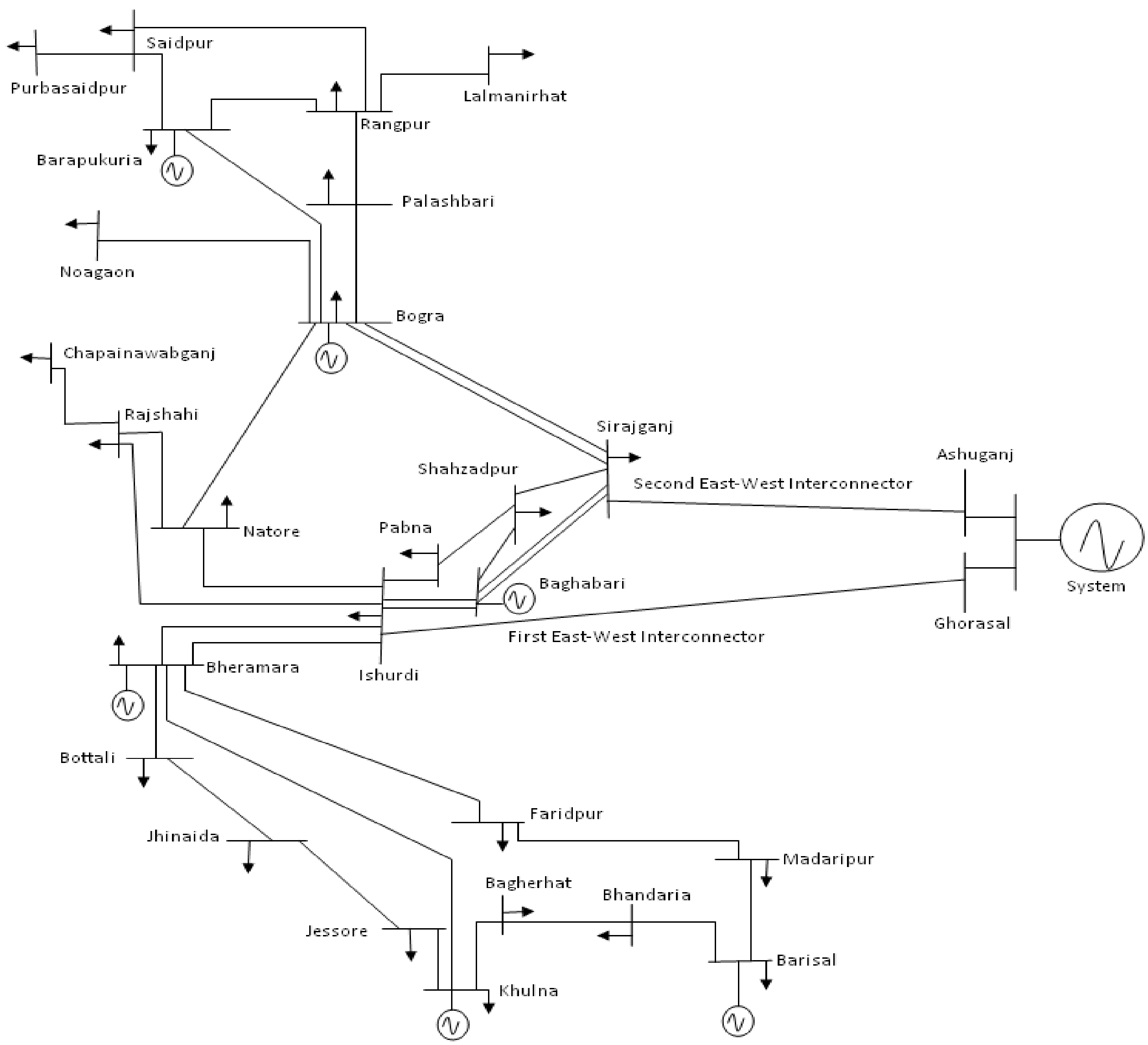

Figure 3.2: East West Interconnected System

In this study power transmission capacity enhancement of EWIs using TCSC and SVC has been observed so for the scope of study eastern grid has been represented by a single stand alone bus which has been taken as reference bus for load flow study. Until March 2009, there was only one interconnector between eastern and western grid that was Ghorasal to Ishurdi 230 kV line. After this line another 230 kV line has been constructed between Ashuganj to Sirajganj to enhance power transmission capability from eastern to western grid. At the same time power handling capability of the western grid was enhanced by extending 230 kV tapped from sirajganj to Barapukuria and sirajganj to Khulna. Natore to Bogra line creates mesh configuration at the middle part of the western grid as shown in Figure 3.2.

In this work series-shunt compensation is applied to the two existing interconnectors between eastern and western grid. In order to be able to apply series compensation in the EWIs by means of TCSC two additional buses are connected adjacent to the Ishurdi and Sirajganj buses. To apply shunt compensation in the EWIs, two SVCs are connected to the Ishurdi and Sirajganj buses. To minimize cost of compensation TCSCs and SVCs are connected to end of the interconnectors instead of middle of interconnectors.

3.3 System Modeling

System modeling includes modeling of synchronous machine, exciter, turbine-governor, transmission line, load, TCSC and SVC for EWIS.

3.3.1 Synchronous Machines

Synchronous machines at Baghabari, Bheramara and Bogra contribute to large generation in the western grid. Generation in the northern part of western grid is aggregated at in Barapukuria and machines at this station is considered somewhat higher than its actual rating because of some of the machines in Rangpur, Saidpur and Thakurgaon are not considered due to their lower availability. Two other generating stations of Khulna and Barisal are included in the western grid for this study.

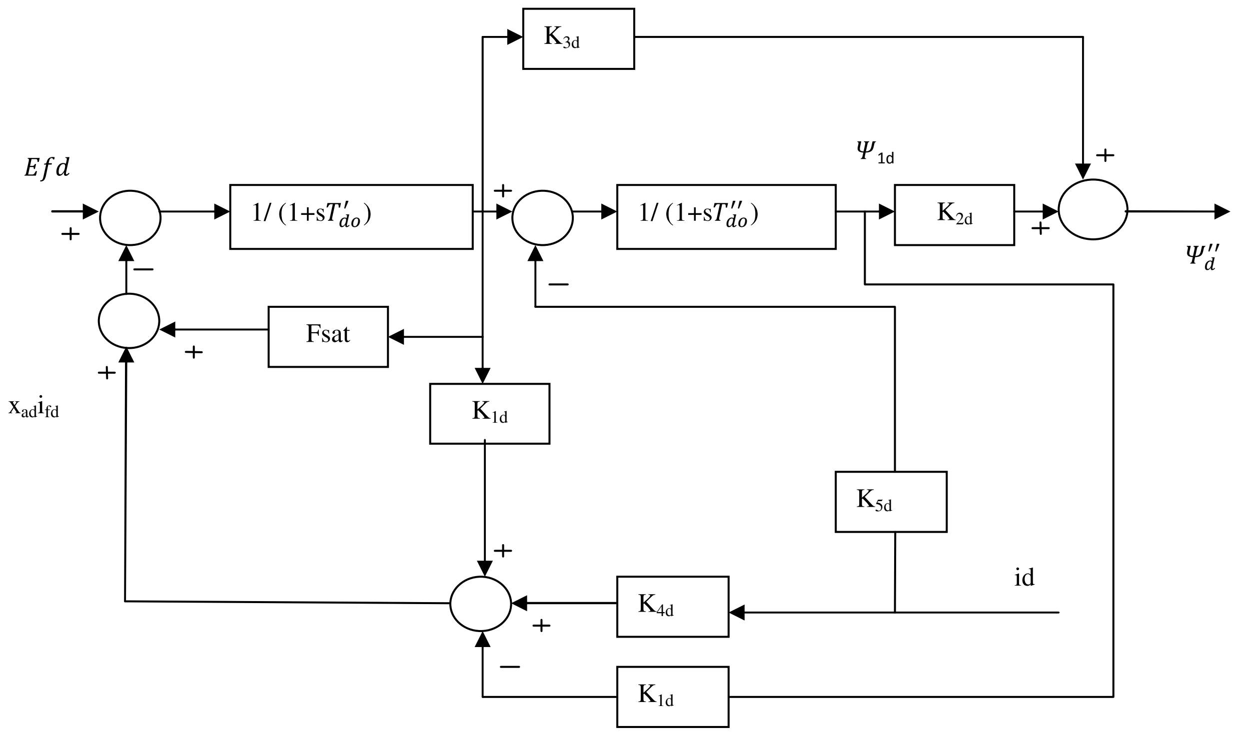

Figure 3.3: Block diagram for direct axis sub-transient model of synchronous machine

Sub-transient model of synchronous machines has been used in this work for dynamic analysis. Block diagram of direct and quadrature axis sub-transient models are shown in Figure 3.3 and 3.4 respectively. These models are available in the simulation reference [47].

The coefficients of the direct axis sub-transient model are given by following the equations-

$$K_{1d}=\frac{(X'_d-X''_d)(X_d-X'_d)}{(X'_d-X_l)^2} \tag{3.1}$$

$$K_{2d}=\frac{(X'_d-X''_d)}{(X'_d-X_l)} \tag{3.2}$$

$$K_{3d}=\frac{X''_d-X_l}{X'_d-X_l} \tag{3.3}$$

$$K_{4d}=\frac{(X_d-X'_d)(X'_d-X''_d)}{X'_d-X_l} \tag{3.4}$$

$$K_{5d}=X'_d-X_l \tag{3.5}$$

Where,

x_l = Leakage Reactance

x'_d = Direct-Transient Reactance

x''_d = Direct-axis Sub-Transient Reactance

T'_{do} = Direct-Axis Open Circuit Time Constant

T''_{do} = Direct-Axis Open Circuit Sub-Transient Time Constant

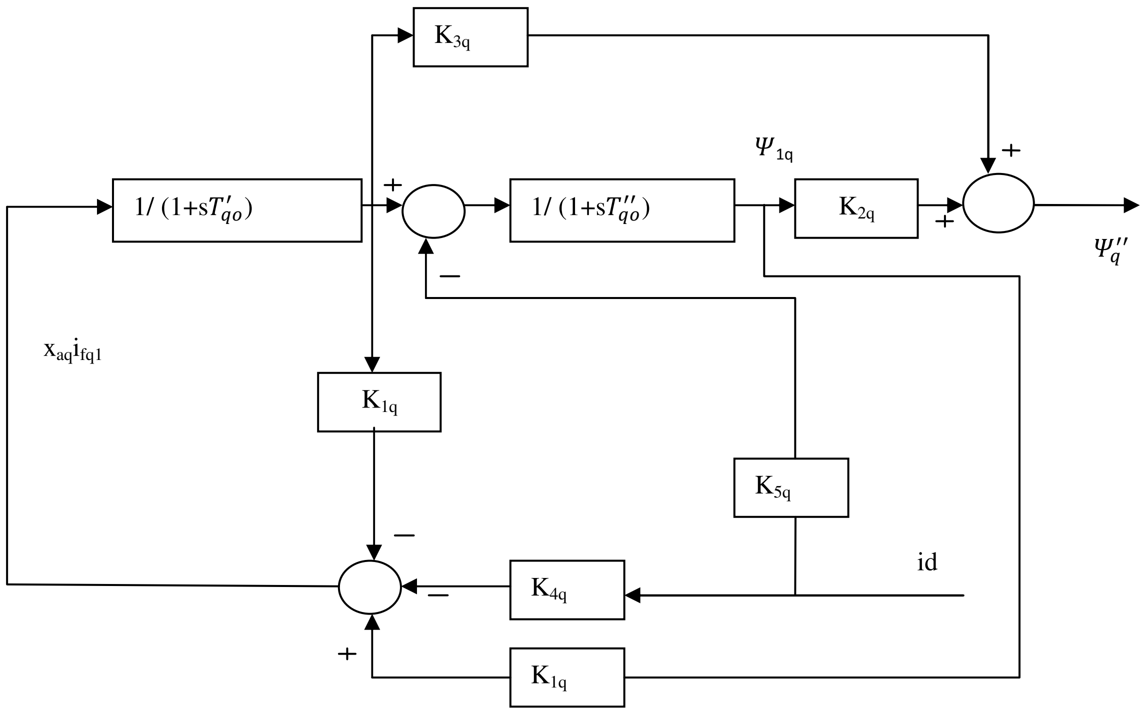

Figure 3.4: Block diagram for quadrature axis sub-transient model of synchronous machine

The coefficients of the quadrature axis sub-transient model are given by following the equations-

$$K_{1q} = \frac{(X'_q - X''_q)(X_q - X'_q)}{(X'_q - X_l)^2} \tag{3.6}$$

$$K_{2q} = \frac{(X'_q - X''_q)}{(X'_q - X_l)} \tag{3.7}$$

$$K_{3q} = \frac{X''_q - X_l}{X'_q - X_l} \tag{3.8}$$

$$K_{4q} = \frac{(X_q - X'_q)(X'_q - X''_q)}{X'_q - X_l} \tag{3.9}$$

$K_{5q} = X'_q - X_l$ (3.10)

Where,

x_l = Leakage Reactance

X'_q = Quadrature-Axis Transient Reactance

X''_q = Quadrature-Axis Sub-Transient Reactance

T'_{qo} = Quadrature-Axis Open Circuit Time Constant

T''_{qo} = Quadrature-Axis Open Circuit Sub-Transient Time Constant

Inertia equations of the machines used in this study have been represented in [35]. These equations are as follows-

$s\delta = \omega - 1$ (3.11)

$(D + \tau_j\ s)\ \omega = T_m - (E''_q Iq + E''_d I_d)$ (3.12)

Where,

δ = Rotor angle

ω = Rotor speed

D = Damping Constant

τ_j = Inertia time constant

T_m = Mechanical torque input

E''_d = Direct axis component of sub-transient EMF

E''_q = Quadrature axis component of sub-transient EMF

I_d, Iq are direct and quadrature axis component of armature current

Machine data for this study have been chosen based on sample data of nearest MVA size machine as provided in [48].

3.3.2 Exciter

Since most of the machines in EWIS are older type so the IEEE type-1 self excited DC exciter has been chosen. Block diagram of such exciter as per IEEE recommended practice [49] is shown in Figure 3.5. In such type exciter terminal voltage transducer output V_C is subtracted from the the set point reference V_{REF}, and power system stabilizer signal voltage V_S and stabilizing feedback voltage V_F are added with V_{REF} to produce error signal. Voltage regulator amplifies this resulting error signal with gain K_A. Voltage regulator includes non windup limits associated with saturation or amplifier power supply limitations. This voltage regulator utilizes power sources that are unaffected by the transients on the synchronous machines. Time constant T_B and T_C have been chosen zero in this work as per recommendation [49]. Voltage regulator output V_R controls the exciter that may be seperately or self excited. Shunt field rheostat setting is controlled using K_E. In some programs K_E is chosen zero which is automatically updated by the those programs for self excitation so K_E has been entered zero in this work. All other parameters of this exciter for this work have been chosen based on the sample data provided in [49].

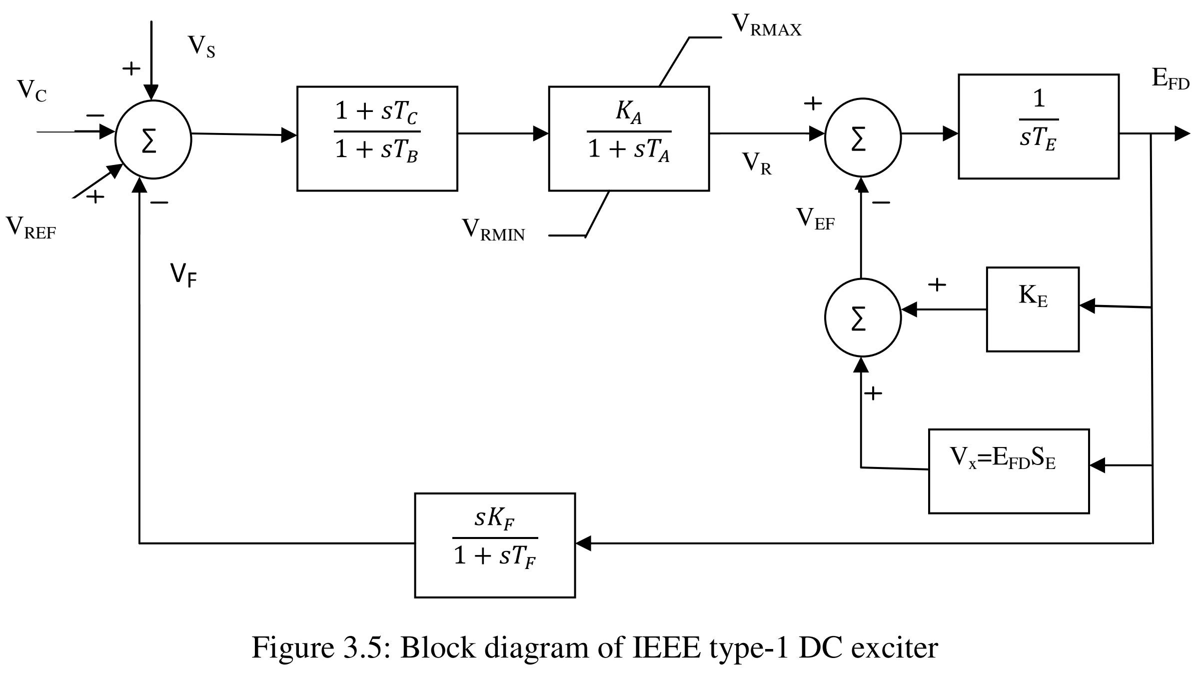

Figure 3.5: Block diagram of IEEE type-1 DC exciter

3.3.3 Turbine-Governor

Turbine-governor model used in this work is available in simulation package [47] shown in Figure 3.6. In such model turbine actual speed is subtracted from the set point speed in order to produce error signal. This error signal is then amplified with steady state gain 1/r where r is speed regulation.

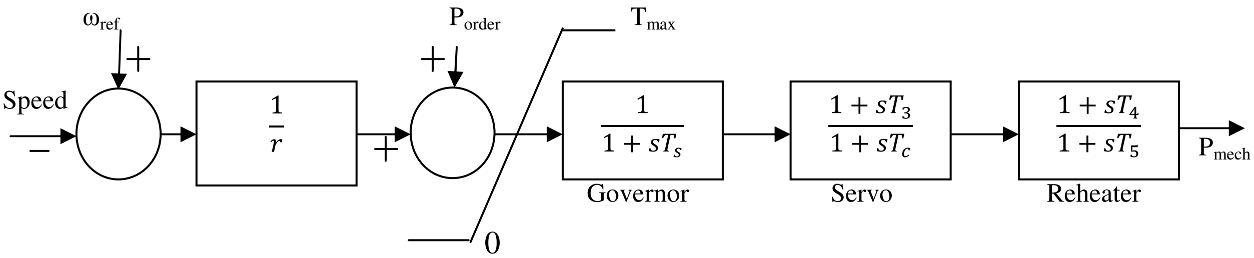

Figure 3.6: Turbine-governor model

Amplified error signal is then added with power signal. Summation of these two signals is limited by the maximum power order T_{max}, goes through the next subsequent dynamic blocks like governor, servo, reheater to produce required mechanical power output to govern turbine.

3.3.4 Transmission Line

For the medium transmission line in range 100 km to 250 km length can be represented by nominal T or π-model. Since length of both 1st and 2nd EWIs of BPS network lies within the range of medium transmission line, nominal π-model representation is used for this work. Typical π-model data for 2nd EWI is shown in Figure 3.7.

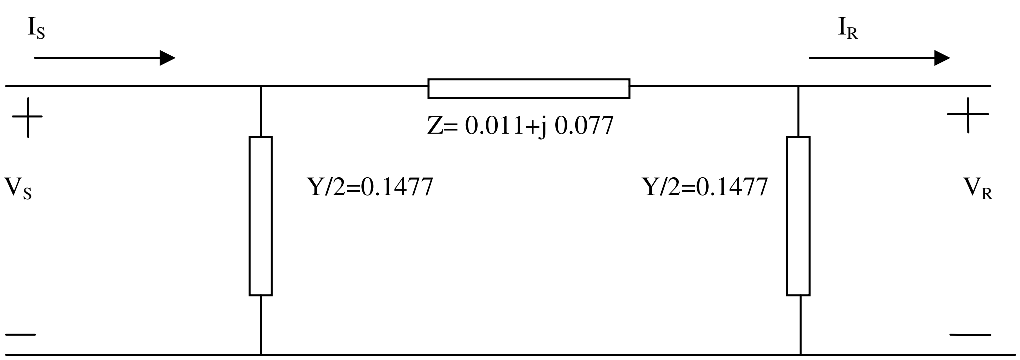

Figure 3.7: π model of 2nd EWI

The transmission line matrix representation in terms of ABCD constants [38] is given below –

$$\begin{bmatrix} V_s \\ I_s \end{bmatrix} = \begin{bmatrix} A & B \\ C & D \end{bmatrix} \begin{bmatrix} V_R \\ I_R \end{bmatrix} \tag{3.13}$$

Where,

$A = D = (1 + \frac{YZ}{2})$

$B = Z$

$C = Y\ (1 + \frac{YZ}{4})$

Y and Z represent line impedance and susceptance respectively. All other lines of EWIS are also represented with nominal π-model.

3.3.5 Load

Loads have been applied at several 132 kV buses in the western grid. Loads at these buses have been represented as constant PQ load. Constant active power load data have been collected from Power Grid Company of Bangladesh (PGCB). Power factor in BPS network varies from 0.85 to 0.95 [50], power factor at load busses for this study has been selected 0.928 lagging. Then using constant active power and power factor, reactive power is calculated.

3.3.6 Capacitive Shunt

Some capacitive shunts are preset in 33 kV sides in the western grid of BPS network. These capacitive shunts are included in the respective 33 kV buses for this work.

3.3.7 Thyristor Controlled Series Capacitor (TCSC) and its Control Scheme

The TCSC is the member of FACTS family that is used for the purpose of series compensation. The basic TCSC structure consists of a TCR module and a fixed capacitor connected in parallel as shown in Figure 3.8. This fixed capacitor and TCR branch act together to produced desired reactance.

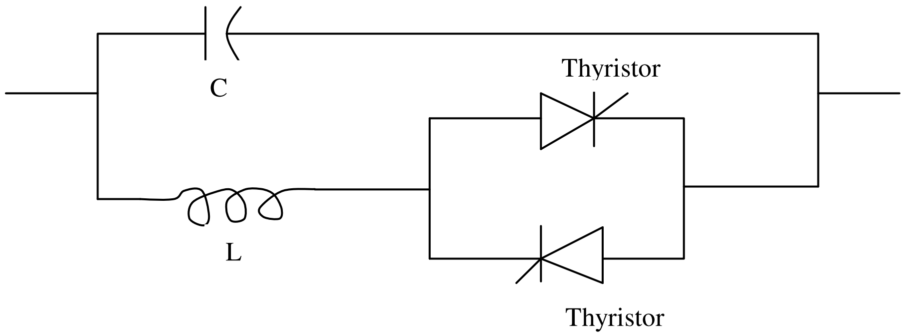

Figure 3.8: Common structure for TCSC and SVC

The equivalent reactance of TCSC represented as a function of the firing angle of thyristor (α) is given by the following equation [15].

$$x_e = -x_C\left[1 - \frac{K_x^2(\sigma+\sin\sigma)}{(K_x^2-1)\pi} + \frac{4K_x^2\ \cos^2(\sigma/2)}{\pi(K_x^2-1)^2}\left(k_x \tan\frac{K_x\sigma}{2} - \tan\frac{\sigma}{2}\right)\right] \tag{3.14}$$

Where,

$\sigma = 2(\pi - \alpha)$

$K_x = \sqrt{\frac{X_C}{X_L}}$

X_C and X_L represent capacitive and inductive reactance respectively at fundamental frequency. TCSC can be continuously controlled in the capacitive or inductive region by controlling thyristor firing angle (α) which is defined as the angle in electrical degrees between the positive going zero crossing of the voltage across the inductor and positive going zero crossing of the current through inductor. Since two thyristors are fired symmetrically the maximum possible firing angle is 180 degree. There is a value of firing angle (α) at which TCSC is in it resonant condition and this value of firing angle depends on the ratio K_x. A typical equivalent reactance (X_e) vs. firing angle (α) characteristic curve of TCSC is shown in Figure 3.9.

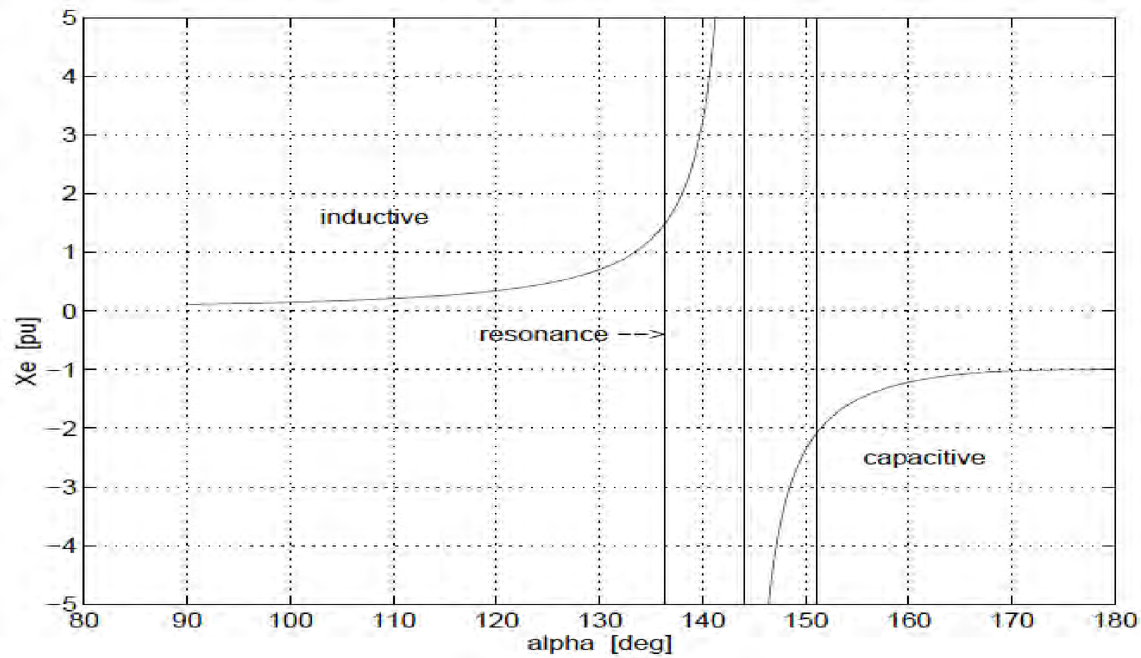

Figure 3.9: Reactance-firing angle curve of TCSC

For the purpose of series compensation TCSC must be operated in the capacitive region in order to apply negative reactance on the line where it is placed. To operate TCSC in the capacitive region firing angle of thyristor must be greater than the angle that causes resonance and must be equal to or less than 180 degrees [15].

In this work following TCSC model is used for stability studies [16].

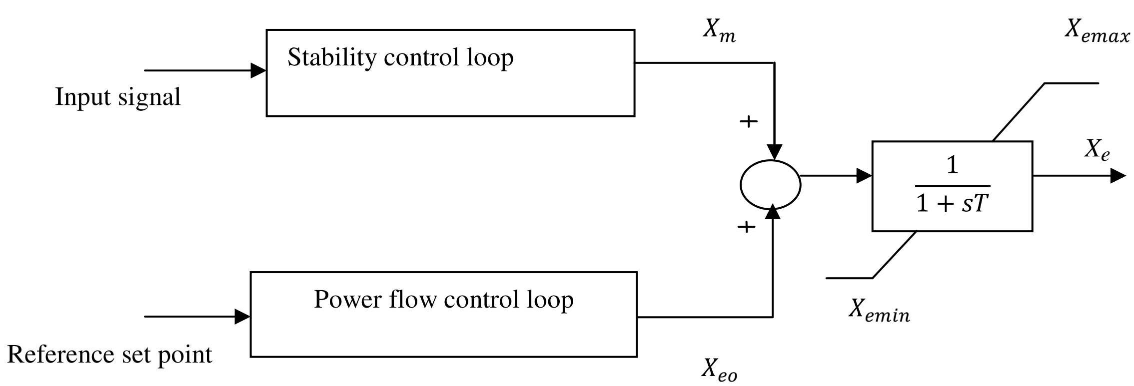

Figure 3.10: TCSC model for stability improvement

In Figure 3.10 fixed level of compensation by inserting negative reactance is provided with power flow control loop that is related to the reference set point of TCSC. In this work reference set point is varied manually to achieve different degree of compensation. Upon the occurrence of disturbance on the system degree of compensation is increased with the stability control loop. Stability control loop consists of a damping controller that is shown in Figure 3.11.

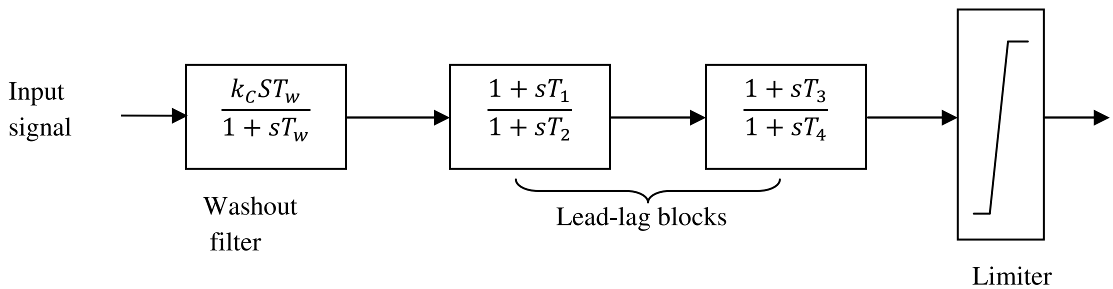

Figure 3.11: TCSC damping controller

TCSC damping controller consists of a washout filter, lead-lag blocks, and limiter. The washout filter is employed to avoid controller response to the dc offset of input signal. Lead-lag blocks provide necessary phase lead characteristic. Last of all, limiter is used to pick up controller response to the large deviation of the input signal. Selection of input signal to the TCSC damping controller is an important feature. The oscillation modes to be damped by the dynamic action of controller, the modes must be "observable" in the input signal, and must be "exciTable" by the output of that controller. These properties are known as "observability" and "controllability" respectively that are determined from the eigenvectors, input and output matrix of the linear representation of the system. Among the several locally measurable signals voltage, current and active power have been used in this work and the effect of using of these signals has been compared on the system stability.

Output of the stability control loop termed as modulation reactance X_m is added with TCSC set point or steady state reactance X_{eo} as shown in Figure 3.10. Summation of these two reactances is put through a first order lag to represent the natural response of the device which yields the equivalent capacitive reactance X_e. The model [Fig. 3.10] used in this study is valid for both dynamic and steady state stability analyzes.

3.3.8 Static Var Compensator (SVC)

SVC is the shunt compensation device whose main function is to regulate voltage at a chosen bus by controlling the reactive power injection. SVC increases steady state power transmission limit and hence enhances the transient stability of the system [51].

Common structure of SVC and TCSC is shown in Figure 2.8. The main differences between these two devices are: SVC is shunt connected to a bus whereas TCSC is series connected to the transmission line, and SVC connected to the bus through a step-down transformer whereas TCSC is directly connected to the transmission line.

The controllable reactance of TCR, X_V is given by [52].

$$x_V = x_L \frac{\pi}{2(\pi-\alpha)+sin2\alpha} \quad (3.15)$$

Where, x_L represents fundamental frequency inductive reactance of TCR.

If firing angle α is 90 degree, the TCR is in full conduction and its equivalent reactance is equal to X_L. At 180 degree firing angle TCR equivalent reactance becomes infinite and SVC injects the maximum reactive power to the bus at which it is connected.

The steady state control law for the SVC is the typical current-voltage characteristic represented by the equation (3.16) as reported in [53].

$$V = V_{REF} + X_{SL}I \quad (3.16)$$

Where, V_{REF} and X_{SL} represent reference voltage and slope respectively.

The slope is needed to evade hitting limits for small variations to the bus voltage and its typical value is in the range of 2% to 5% with respect to SVC base. A typical value for the controlled voltage range is 5% of V_{REF} [52].

Figure 3.12 represents V-I characteristic curve of SVC for the same inductive and capacitive range. SVC current (I_{SVC}) is usually expressed in per unit with respect to maximum current of the device.

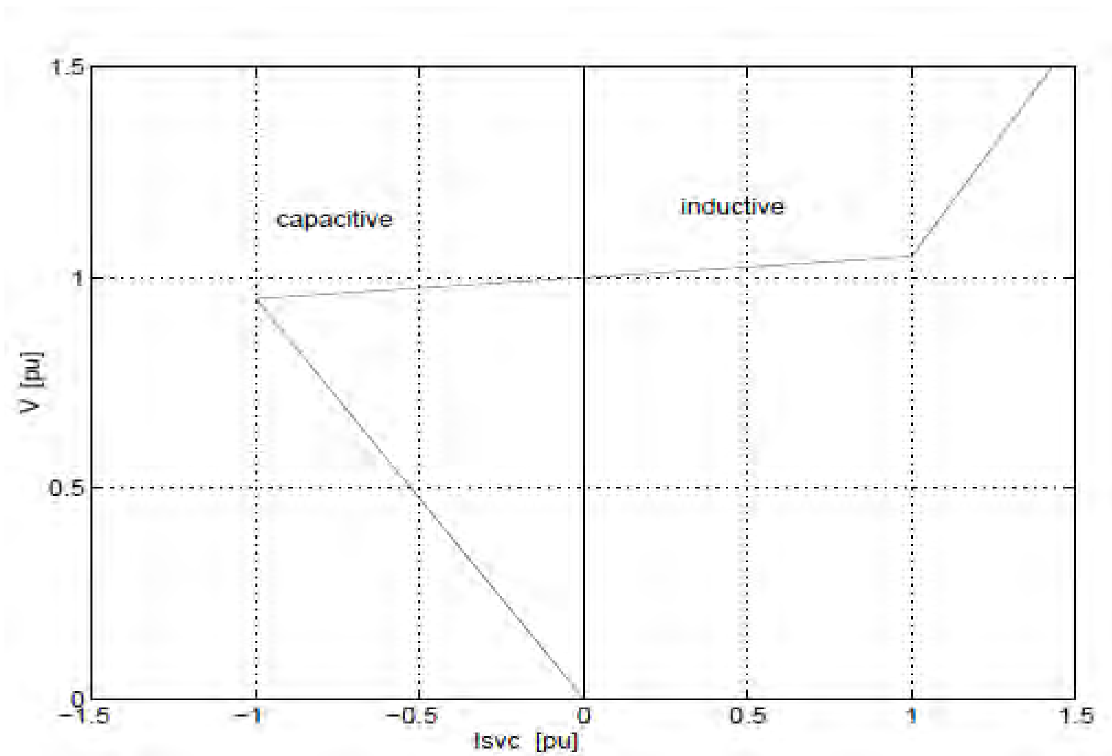

Figure 3.12: SVC V-I characteristic

For the SVC structure presented in Figure 3.8, the reactive power supplied by the device is given by [33].

$$Q_{SVC}=\frac{V^2}{X_V}-\frac{V^2}{X_C} \tag{3.17}$$

In the V-I characteristic of SVC presented in Figure 3.12, reactive power supplied by the device Q_{SVC} varies from Q_{MaxC} to Q_{MaxL} for the current limits $\pm I_{Max}$ while voltage of the SVC is varying from its minimum to maximum limits.

The SVC provides rapid and fine adjustment of voltage, which is desirable in power system control and operation. From the system point of view, SVC is a shunt connected static Var generator/load whose output is adjusted to exchange capacitive or inductive current so as to retain or control specific power system variables. SVC is similar to a synchronous compensator in that it is used to supply or absorb reactive power having no rotating part. It operates similar to an automatic voltage regulator system to set and maintain a target voltage level. The basic stability model of SVC as shown in Figure 3.13 has been used in this work and reported in [24].

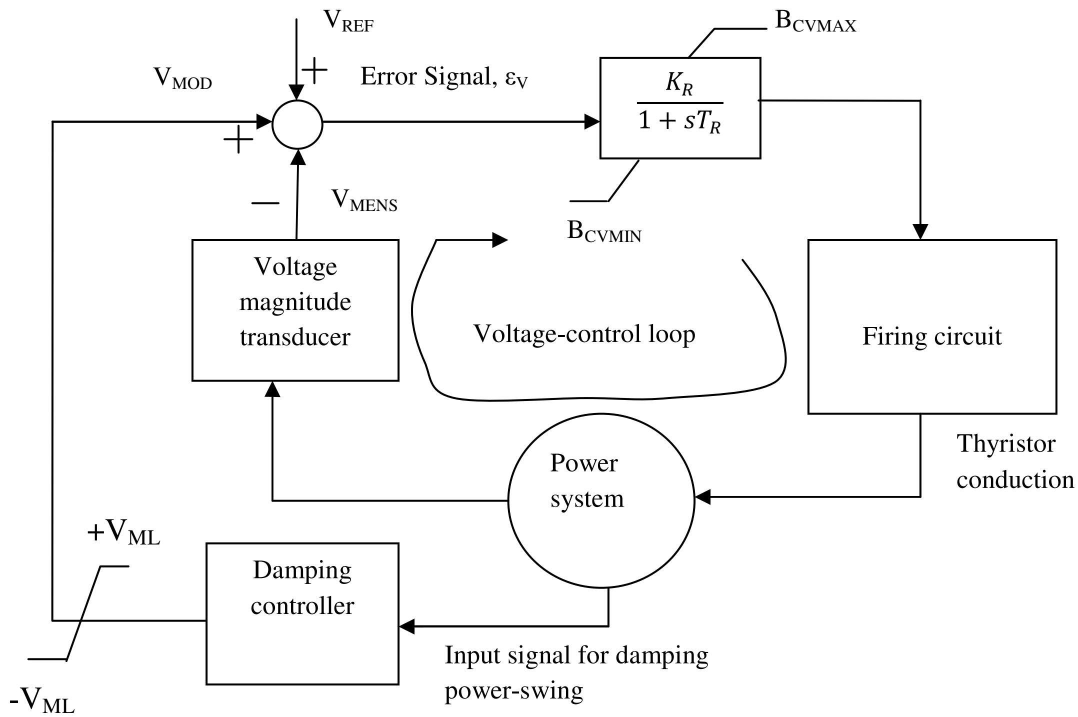

Figure 3.13: SVC control structure for voltage stability

To control bus voltage, SVC involves voltage control loop which is composed of voltage regulator, firing circuit, and voltage magnitude transducer. The primary control function is performed by voltage regulator. Depending on the desired susceptance value firing circuit is initiated to convert this numerical value of susceptance to thyristor conduction angle. Power swing damping controller produces modulation signal V_{MOD} depending on the different locally measurable input signals like bus voltage magnitude, active power, reactive power, current magnitude etc. This modulation signal V_{MOD} is added with reference voltage V_{REF} and subtracted with the output of voltage magnitude transducer output to produce error signal.

The power swing damping controller shown in Figure 3.14 as proposed in [24], has been used in this work.

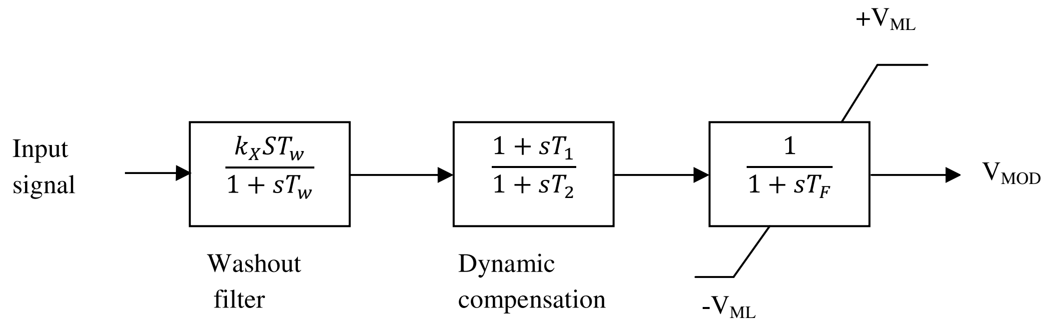

Figure 3.14: SVC power swing damping controller

To avoid controller response to dc offset of input signal washout filter is used. Dynamic compensator consists of two or more lead-lag blocks which provide dynamic compensation. Finally output of the lead-lag block is passed through first order lag to produce modulation signal.

3.4 Simulation Tools

Two simulation tools UWPFLOW and PST have been used in this work. CPF analysis has been performed in UWPFLOW environment to determine SNB point related to voltage collapse phenomena. PST has been used to perform load flow, eigenvalue and transient analysis. A short description of these tools has been given below.

3.4.1 UWPFLOW

This research tool has been developed by Prof. Claudio A. Canizares and Shu Zhang of the University of Waterloo, Ontario, Canada and Prof. Fernando L. Alvarado form University of Wisconsin-Madison Madison, USA. The program code has been written in C and C++ and runs under WINDOWS, and UNIX.

The program reads AC/DC power flow data in WSCC/BPA/EPRI formats and IEEE common format. TCSC and SVC data are in special format unique to this package. Additional unformatted data is required for bifurcation analysis, such as the generation and load data file. Loading factor is changed in program to investigate saddle node bifurcation point. Newton

Raphson method is used to solve load flow equation and CPF is conducted for static bifurcation analysis. A basic PV-curve plotting option is available in the tool to determine SNB related to voltage collapse. Detailed information of the tool is available in [54]. The program generates a series of output files that allow different analyses like tangent vectors, left and right eigenvectors at a singular bifurcation point, Jacobians, power flow solutions at different loading levels, voltage stability indices, etc.

3.4.2 PST

Power System Toolbox (PST) is a MATLAB based tool that can be used for dynamic analysis of AC/DC/FACTS power systems. This tool was first developed by Prof. J. H. Chow of Rensselaer Polytechnic Institute, New York, USA and was further developed by Graham Rogers of Cherry Tree Scientific Software, Ontario, Canada.

Load flow, eigenvalue, and transient analysis can be performed with PST. Newton Raphson method is used to perform load flow analysis within the program. PST provides models of machines and control systems for performing transient simulation of power system, and for building state variable models for small signal analysis and for damping controller design. The tool contains several driver program file for performing load flow, eigenvalue, and transient analysis. The most attractive feature of PST is that it is open source, so user can expand or modify PST program code to meet special modeling or simulation requirements. Detailed information about this tool is presented in [47].

CHAPTER 4

Simulation Results and Analyses

4.1 Introduction

Simulation results of different analyses performed on the two area test system and proposed model of EWIS as developed in chapter-3, are presented in this chapter.

First CPF analysis is performed to find out maximum loading point corresponding to SNB. Then eigenvalue analysis up to SNB point is performed to find out HB point. Finally steady state analysis is carried out to demonstrate improvement in transmission angle and bus voltage.

4.2 Two Area System

In the two area test system mentioned in Chapter-3, area-I has base case load of 967 MW and area-II has base case load of 1767 MW. Area-I and area-II have generation of 1400 MW and 1419 MW respectively. Area-II has shortfall of 348 MW and it is covered by the surplus power of area-I.

4.2.1 Bifurcation and Eigenvalue analysis

Bifurcation diagram shown in Figure 4.1 shows that the system without compensation experiences voltage collapse related to SNB at a loading factor (LF) of 0.145 i.e. with a 14.5% load increase.

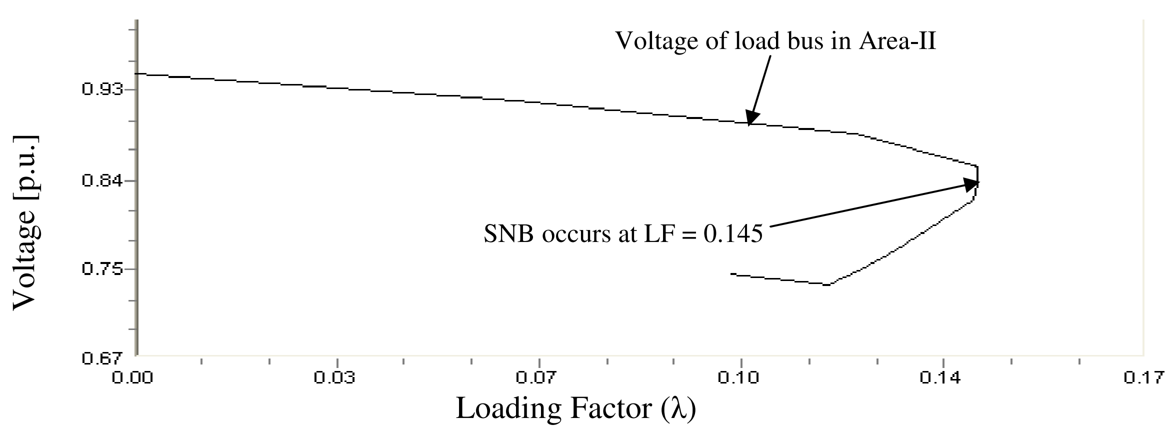

Figure 4.1: Bifurcation diagram of two area system without compensation

Modal analysis has been performed on the uncompensated system, and it is observed that at LF = 0.051, HB is triggered as shown in Figure 4.2, i.e. at LF = 0.051 a pair of complex conjugate eigenvalue with zero real part, crosses imaginary axis.

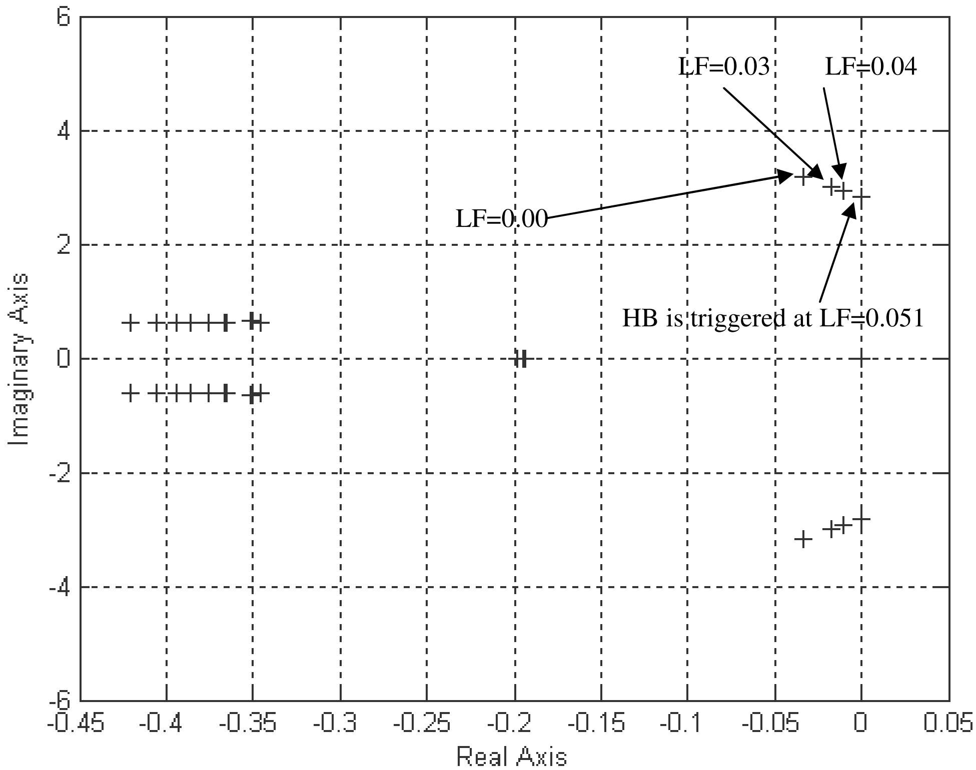

Figure 4.2: Critical eigenvalues of two area system without compensation

As the LF of the uncompensated system is increased, critical eigenvalue moves into the right half region of the complex plane. Now application of series/series-shunt compensation will force critical eigenvalue to move deeper into the left half region of the complex plane –demonstrating better dynamic stability.

Bifurcation diagrams with 40% series and 2 p.u. shunt compensation, with 70% series and 2 p.u. shunt compensation are shown in Figures 4.3 and 4.5 respectively. Critical eigenvaluses of two area system at different loading factors with 40% series and 2 p.u shunt compensation, with 70% series and 2 p.u. shunt compensation have been plotted in Figure 4.4 and 4.6 respectively to show improvement in HB with series-shunt compensation compared to the system without compensation as shown in Figure 4.2 .

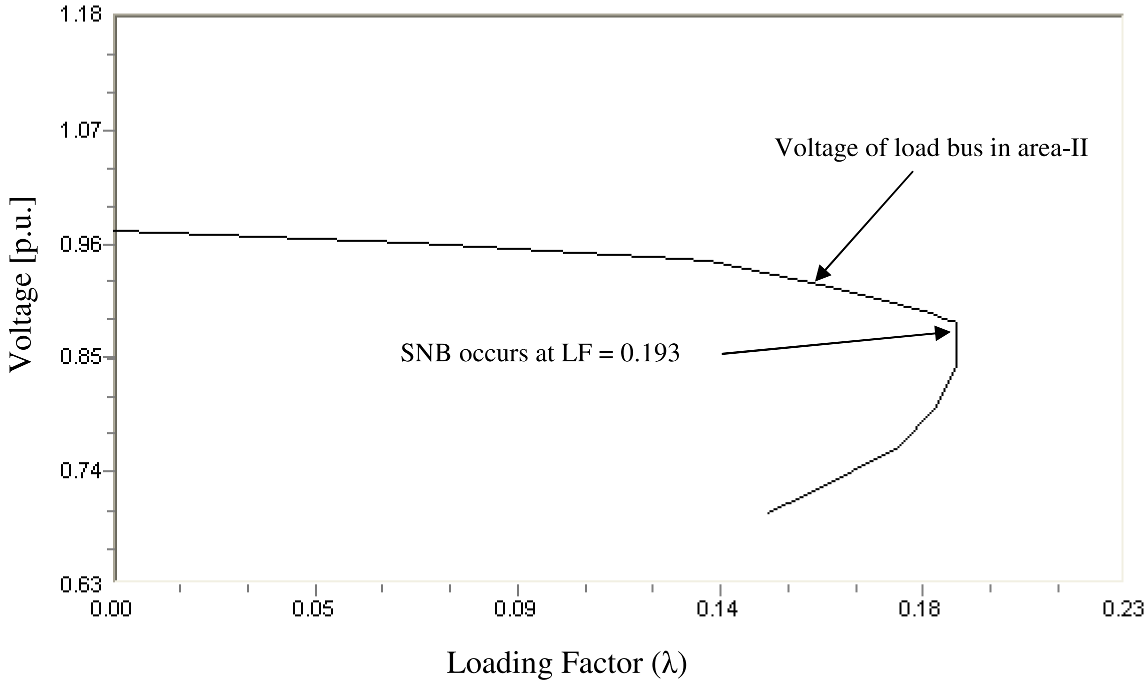

Figure 4.3: Bifurcation diagram of two area system with 40% series and shunt compensation

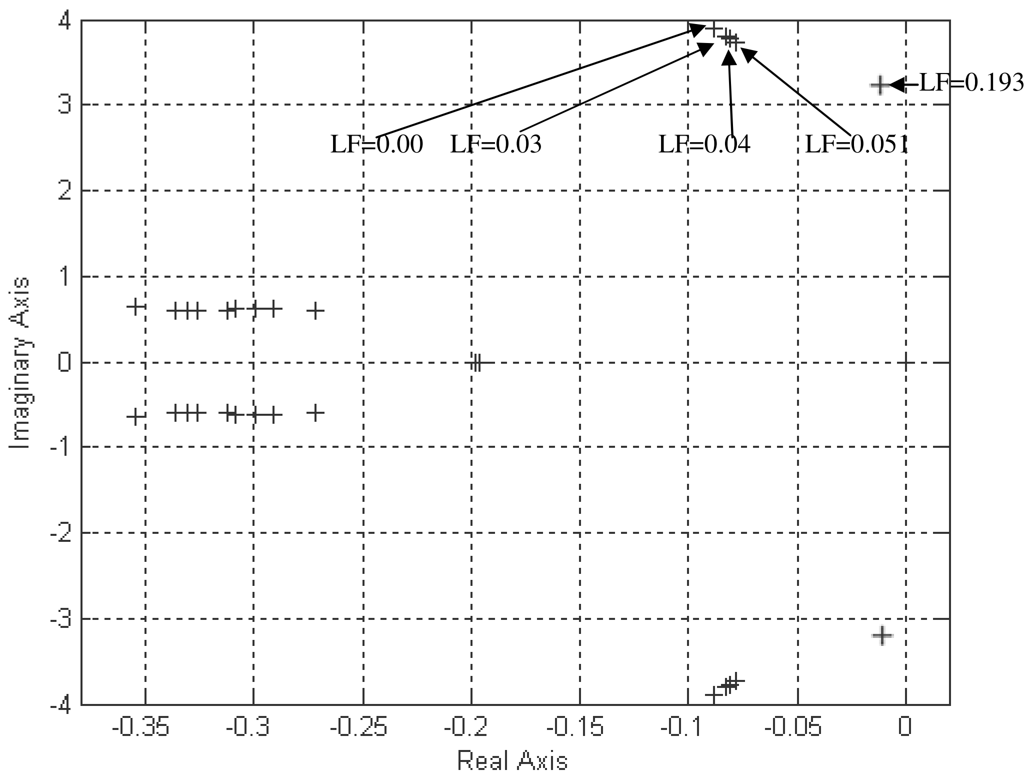

Figure 4.4: Critical eigenvalues of two area system with 40% series and shunt compensation

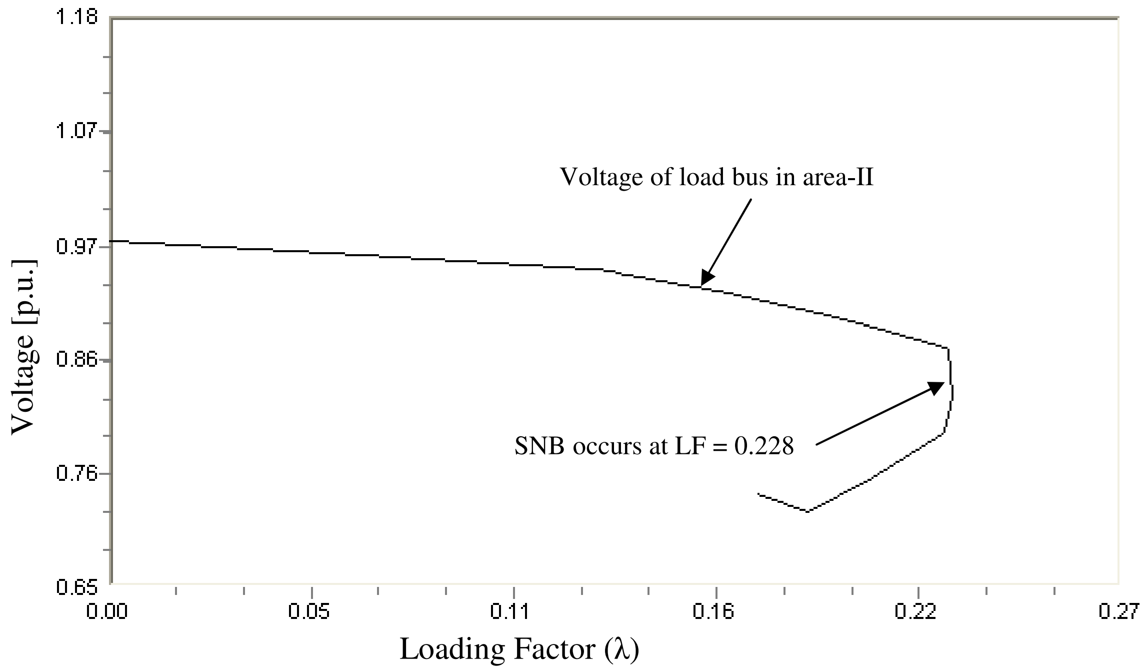

Figure 4.5: Bifurcation diagram of two area system with 70% series and shunt compensation

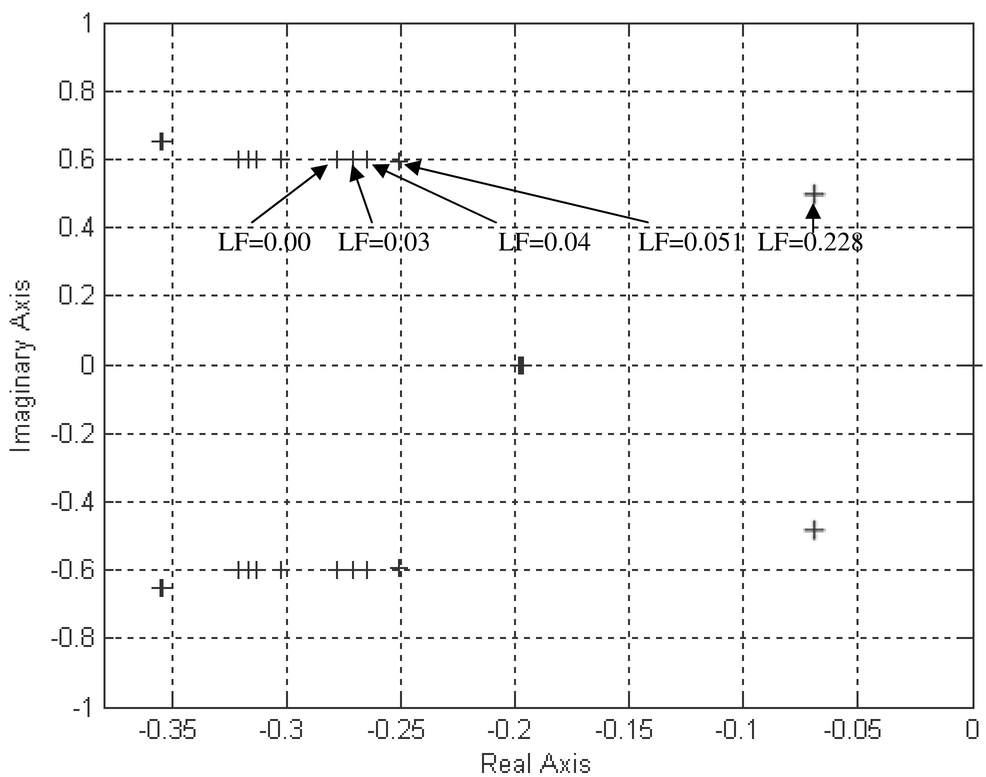

Figure 4.6: Critical eigenvalues of two area system with 70% series and shunt compensation

Figure 4.7 shows that with series-shunt compensation SNB occurs at higher loading factor than that of without compensation. Modal analysis shows that without compensation HB is triggered at a loading factor of 0.051 but no HB is triggered with series-shunt compensation up to SNB point.

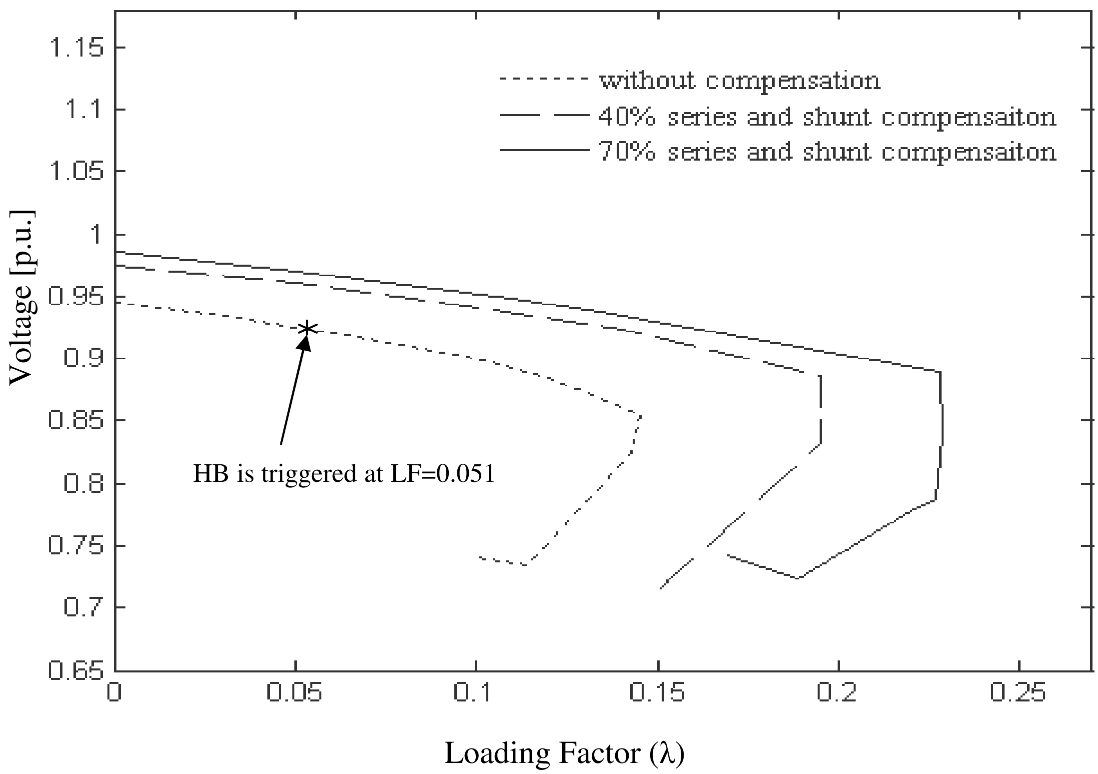

Figure 4.7: Comparison of bifurcation diagrams with different compensation levels

Application of fixed level of series or series-shunt compensation improves system dynamic stability. But system dynamic response can be further improved by setting up damping controller with TCSC and SVC. This controller will act to modulate compensation level upon occurrence of any fault on the system in order to damp low frequency oscillation. The damping controllers for TCSC and SVC used in this work have been presented in Chapter 3. Calculation of damping controller parameters involves eigenvalue analysis. Critical eigenvalues of two area system are shown in Table 4.1.

Table 4.1: Critical eigenvalues of two area system

Level of Compensation	Loading Factor (LF)	Critical Eigenvalue/Mode
Uncompensated	0.051	-0.0000 + 2.8189i
40% Series and 2 p.u. Shunt Compensation	0.051	-0.0777 + 3.7299i
70% Series and 2 p.u. Shunt Compensation	0.051	-0.4854 + 6.3250i

Typical accepTable damping ratio of oscillatory mode has been stated in the literature as 3% to 5% [55]. Some of the critical modes shown in Tables 4.2 and 4.3 have damping ratio lower than the accepTable range. Dynamic action of TCSC and SVC can improve the damping ratio of these critical modes.

Table 4.2 Damping ratio and frequency of critical mode with TCSC

Mode Number	Damping Ratio	Frequency (Hz)
22	2.01%	0.6041

Table 4.3 Damping ratio and frequency of critical mode with SVC

Mode Number	Damping Ratio	Frequency (Hz)
22	1.99%	0.6298

Using line active power flow as input to damping controller, controllability and observability analysis on this critical mode has been performed. Product of controllability and observability gives residue [56, 57] also known as sensitivity.

Table 4.4 Indices for TCSC controller using line active power as input

Controllability	Observability	Residue
0.0265 - 0.0380i	-0.4188 + 0.3776i	0.00325+j0.026

Table 4.5 Indices for SVC controller using line active power as input

Controllability	Observability	Residue
-0.8721 + j0.8996	0.7005 - j0.7270	0.0431 + j1.2642

Now phase compensation is required to shift this critical mode deeper into the left half region of the s-plane to improve damping ratio. Determination of phase compensation of critical mode and lag-lead time constant of controller is interrelated and can be found out from the following equations [56, 57].

$$\frac{T_{lead}}{T_{lag}} = \frac{1-\sin\left(\frac{\varphi_{comp}}{m}\right)}{1+\sin\left(\frac{\varphi_{comp}}{m}\right)} = \alpha \tag{4.1}$$

$$T_{lag} = \frac{1}{\omega_{to\ be\ damped}\sqrt{\alpha}} \tag{4.2}$$

Where,

φ_{comp} = 180°- (argument of residue) = required phase compensation

m = number of controller or compensator stage

Table 4.6: Controller parameters of TCSC in two area system

Gain (K)	Washout Time Constant (sec.)	T_{lag} (sec.)	T_{lead} (sec.)
30	10	0.6966	0.0966

Table 4.7: Controller parameters of SVC in two area system

Gain (K)	Washout Time Constant (sec.)	T_{lag} (sec.)	T_{lead} (sec.)
0.25	5	0.6251	0.1021

4.2.2 Steady State Analysis

Load flow analysis is performed on the base case and then loading in area-II is increased gradually. Table 4.8 shows power flow result without compensation.

Table 4.8: Steady state conditions of two area system without compensation

Percentage Increase in Loading in Area-II	Export From Area-I [MW+ J MVAR]	Voltage at Area-II Load Bus [P. U.]	Transmission Angle [Degree]
0.0%	400.44+ j 12.30	0.9712	27.48
1.5%	430.76+ j 26.72	0.9642	30.22

It is observed in Table 4.8 that without any compensation at 1.5% increased loading (LF=0.015) from the base case loading, transmission angle exceeds safe operating limit of 30 degree. Now application of series-shunt compensation will bring this transmission angle within safe operating limit and further loading will be possible.

Table 4.9: Steady state conditions of two area system with series-shunt compensation by means of TCSC and SVC

Percentage Increase in Loading in Area-II	Export From Area-I [MW+ J MVAR]	Voltage At Area-II Bus [P. U.]	Transmission Angle [Degree]	Percentage Series Compensation	Suscepta-nce of SVC [P.U.]
1.5%	427.34- j 93.68	1.0188	16.60	40%	2
1.5%	417.34- j169.4	1.0912	8.890	70%	2

Table 4.9 shows steady state condition of two area system with series-shunt compensation. Series compensation is applied up to 70% with TCSC, and 2 p.u. shunt compensation is applied on the load bus of area-II with a SVC of size 200 MVAR. Table 4.9 shows improvement of bus voltage and transmission angle by means of series-shunt compensation. Without any compensation as shown in Table 4.8, at 1.5% loading transmission angle exceeds its safe operating limit, at this loading level if 40% series and 2 p.u. shunt compensation is applied; transmission angle comes well within its acceptable operation range i.e. from 30.22 degree to 16.60 degree, and higher loading becomes possible. At this compensation level bus voltage is also improved form 0.9642 p.u. to 1.0188 p.u. Analysis has been performed up to 70% series compensation which is the practical maximum compensation level [32] and 2 p.u. shunt compensation.

4.2.3 Performance Analysis of Damping Controller

Transient analysis has been performed on the two area system without and with compensation to show positive effect of TCSC and SVC damping controller on damping power system oscillation. A three phase disturbance has been applied at t=0.3 second at a load bus of area two with subsequent tripping of line. Detailed switching data to apply disturbance has been provided in the Appendix A. Improvement in transient performance of the system is observed in time domain simulation with series or series-shunt compensation than that of without compensation.

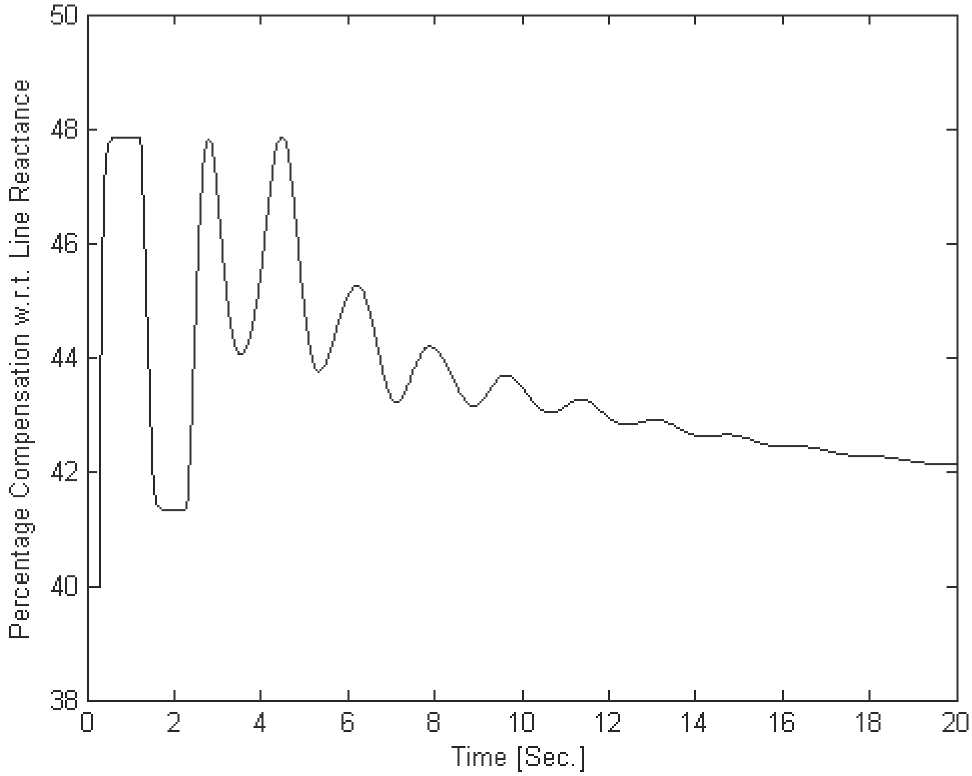

Figure 4.8: Dynamic compensation by TCSC in two area system

Dynamic action of TCSC and SVC controller is shown in Figure 4.8 and 4.9 respectively with active power as input signal to the controller. Figure 4.6 demonstrates that maximum level of series compensation is provided by the TCSC in the post fault scenario. Percentage compensation jumps up to 49% form its set point of 40% just after fault application and then gradually level of compensation decreases to reach its set point again.

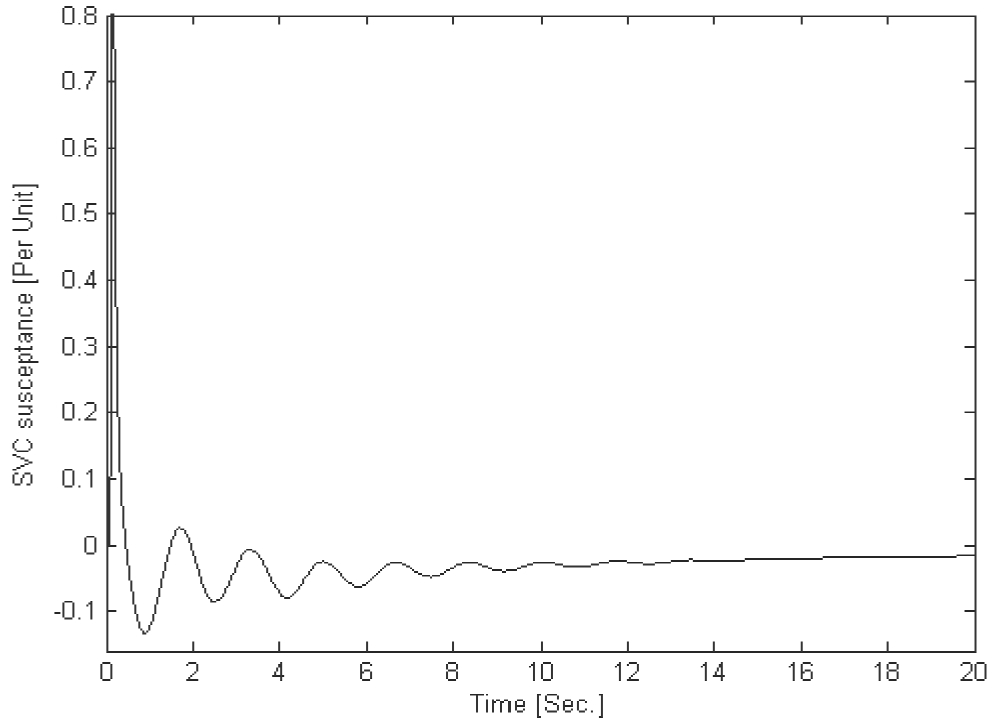

Figure 4.9: SVC susceptance profile in two area system

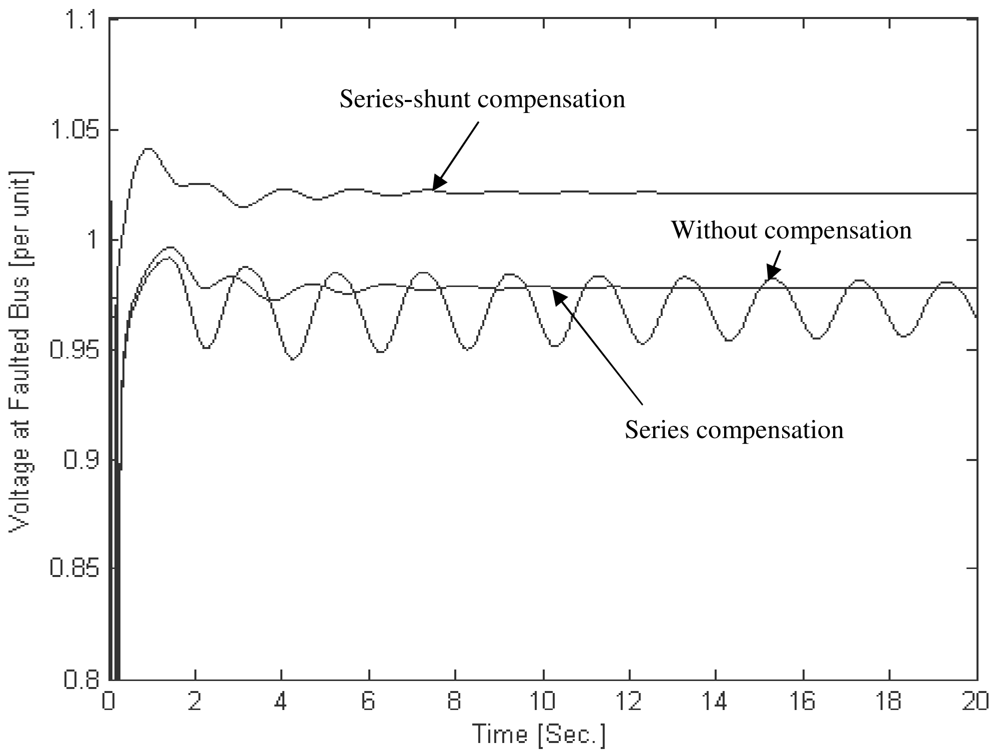

Figure 4.10: Faulted bus voltage profile in two area system

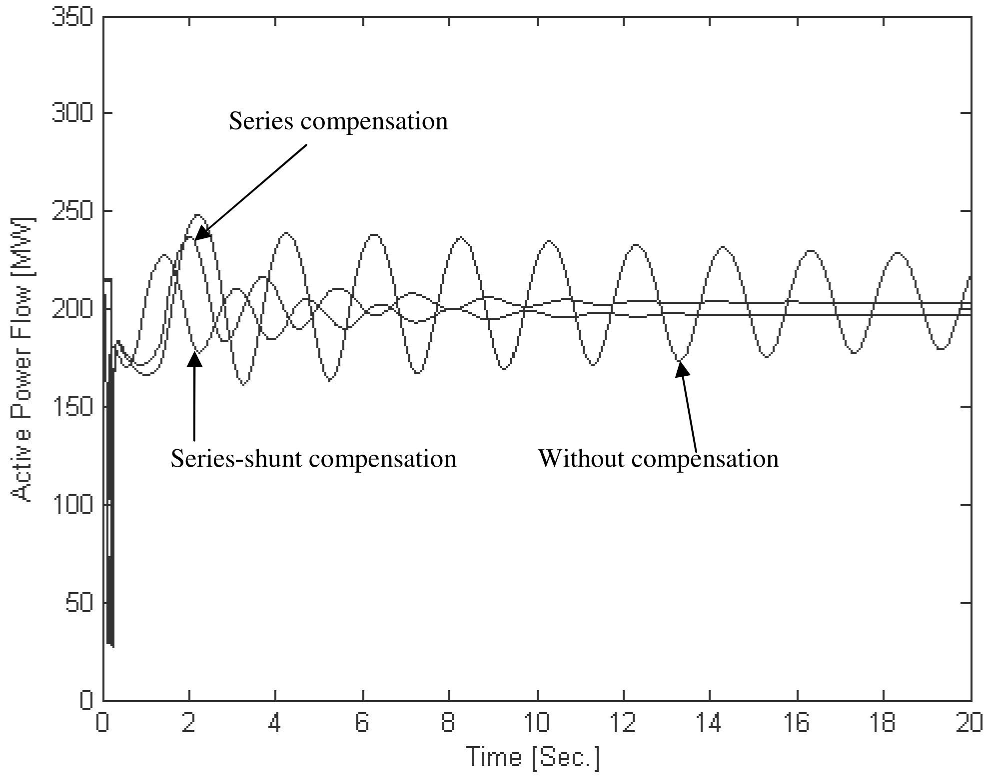

Figure 4.11: Tie line active power flow in two area system

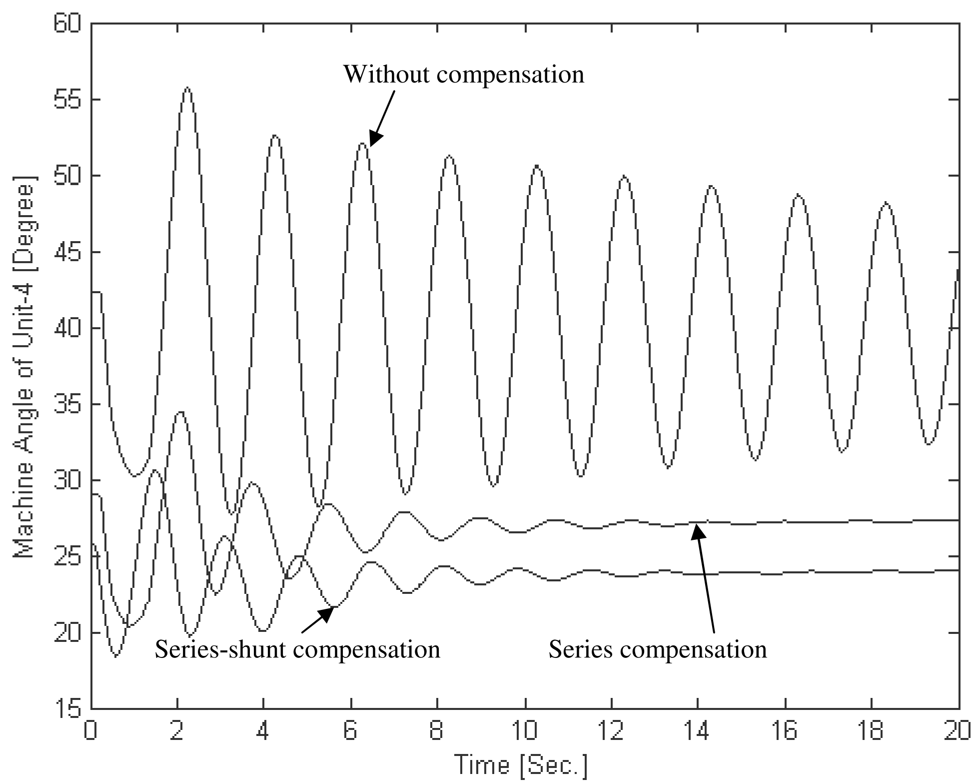

Figure 4.12: Machine angle in two area system

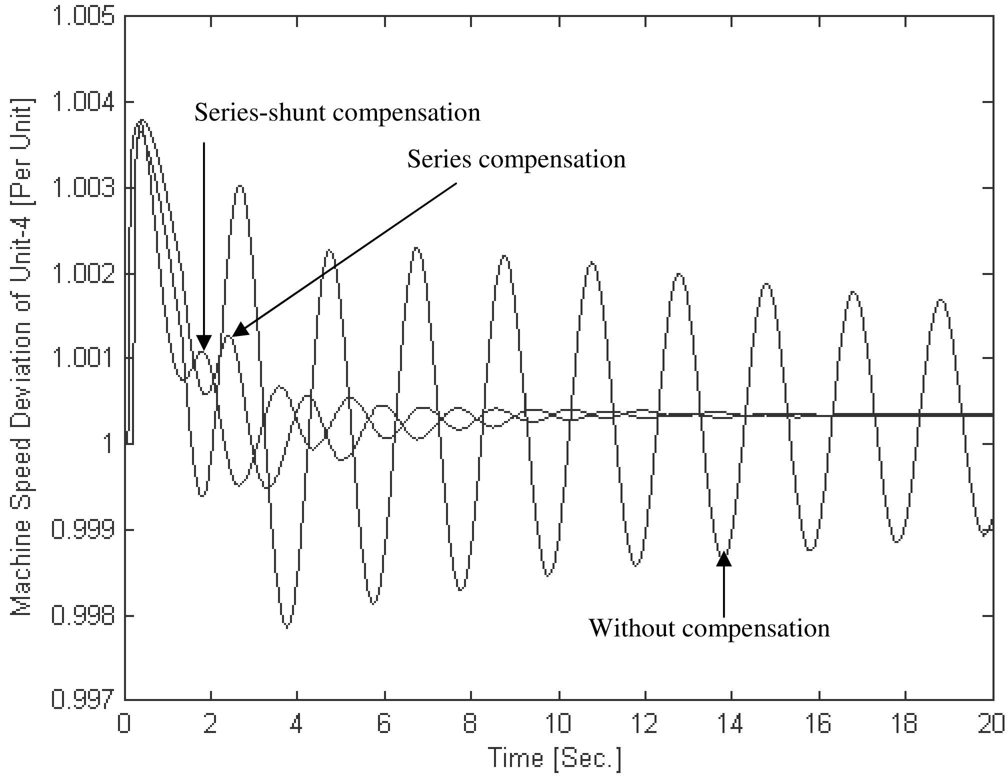

Figure 4.13: Machine speed deviation in two area system

Faulted bus voltage, tie line active power flow, angle of machine nearest to the faulted bus, and machine speed deviation nearest to the faulted bus have been plotted in Figures 4.10 to 4.13 to demonstrate the potential benefits of applying series or series-shunt compensation on transient stability of the system. With series compensation stability of the system is improved compared to the system without compensation. The system stability is improved further by application of series-shunt compensation with TCSC and SVC.

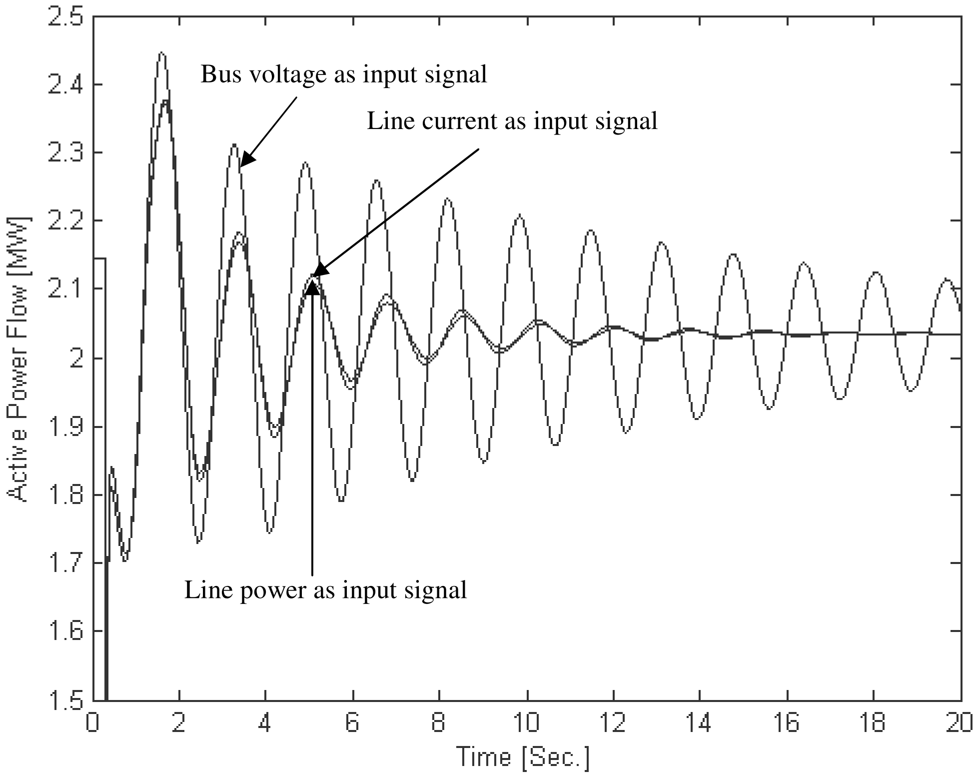

Figure 4.14: Tie line power flow with different input signals to TCSC and SVC controllers

Figure 4.14 depicts the controller action with voltage, current and power as input signal. Electromechanical power oscillation can not be damped well with the use of voltage as input signal to the controller. Line power as input to the controller has better damping effect on power oscillation than line current as depicted in Figure 4.14.

4.3 East West Interconnected System (EWIS)

Benefit of application of series-shunt compensation has been demonstrated with a standard two area system as a test bed in the previous section. This section presents the benefit of series-shunt compensation on the EWIS which is the main focus of this work. Series-shunt compensation is also compared without and with series compensation. EWIS data is provided in Appendix B.

4.3.1 Bifurcation and Steady State Analysis of EWIS

A. Without Compensation

Bifurcation diagram of EWIS without compensation shown in Figure 4.15 depicts, voltage collapse related to SNB occurs at LF=0.980.

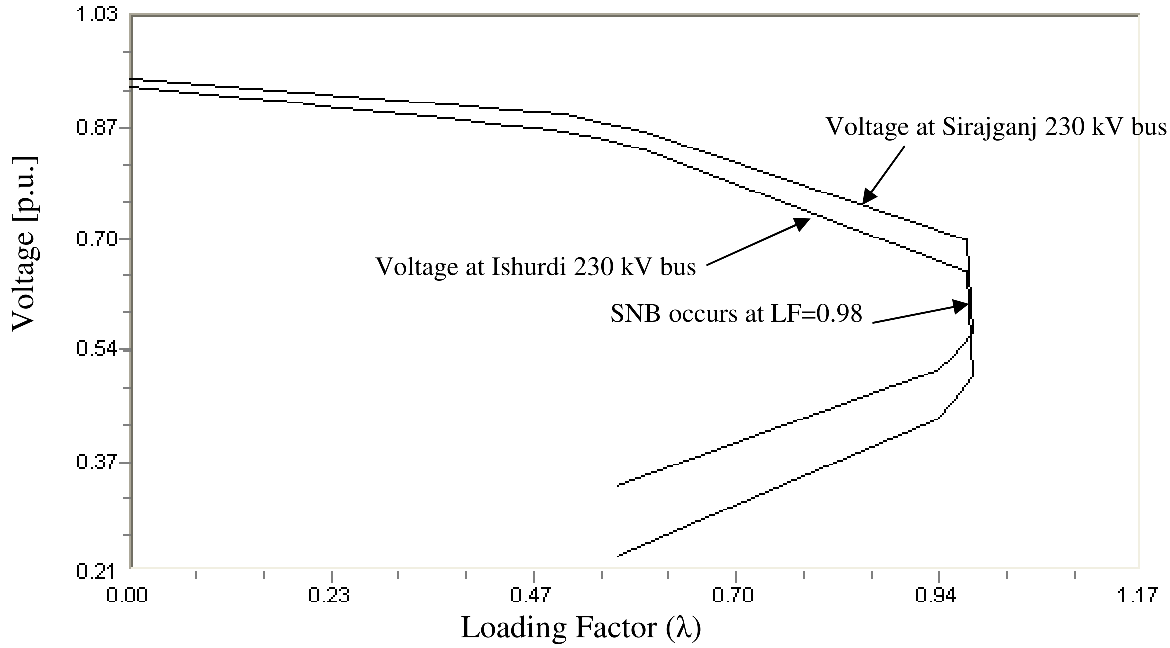

Figure 4.15: Bifurcation diagram of EWIS system without compensation

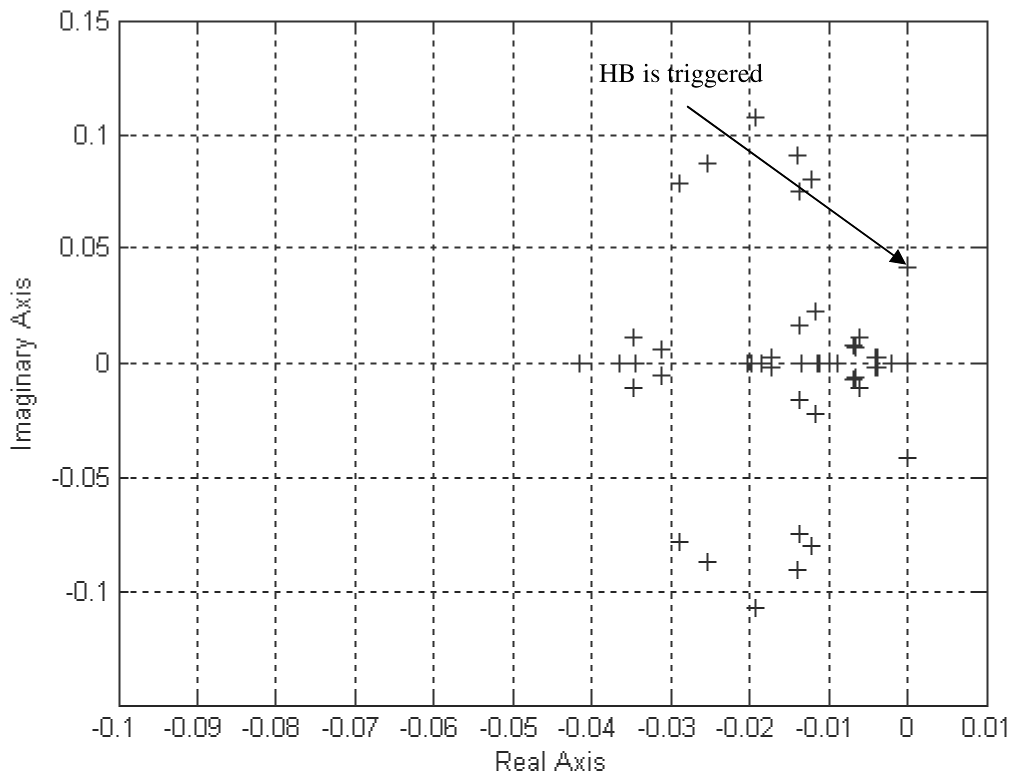

Figure 4.16: Critical eigenvalues of EWIS without compensation at LF=0.7

Modal analysis up to SNB point has been performed and it is observed that the system without any compensation at a loading factor of 0.7, a pair of complex conjugate eigenvalue crosses imaginary axis of s-plane showing oscillatory instability related to HB. Eigenvalues of EWIS without compensation at a LF=0.7 has been shown in Figure 4.16.

Load flow analysis of EWIS has been performed with loading factor of 0.7 and transmission angles between Ghorasal and Ishurdi , Ashuganj and Sirajgang have been shown in Table 4.10.

Table 4.10: Steady state condition of EWIS without compensation

LF	**Import to Western Grid [MW]**	**Export to Western Grid [MW+ j MVAR]**		**Bus Voltage [P.U.]**		**Transmission Angle [Deg.]**	
		G-I#	A-S*	I	S	G-I	A-S
0.7	384	165.33+j4.19	256.89+j4.08	0.8370	0.8542	17.82	15.30

Ghorasal-Ishurdi

*Ashugang-Sirajganj

From the Table 4.10 it is observed that voltages of Ishurdi and Sirajganj buses are satisfactory and transmission angles between Ghorasal-Ishurdi and Ashugang-Sirajganj are within safe operating limits up to HB point.

Summary of loading margins of EWIS without compensation is provided in the Table 4.11.

Table 4.11: Loading margins of EWIS without compensation

Compensation Level	**Static Loading Margin (SLM)**	**Dynamic Loading Margin (DLM)**
Uncompensated	0.98 (512.8 MW)	0.7 (384 MW)

B. Series Compensation

Maximum possible series compensation level of tie line is considered to be 70% [32]. This maximum level of compensation has been applied to EWIs with two TCSCs. CPF analysis has been performed to determine maximum loading factor at which SNB take places. Bifurcation diagram of EWIS with 70% series compensation has been shown in Figure 4.17.

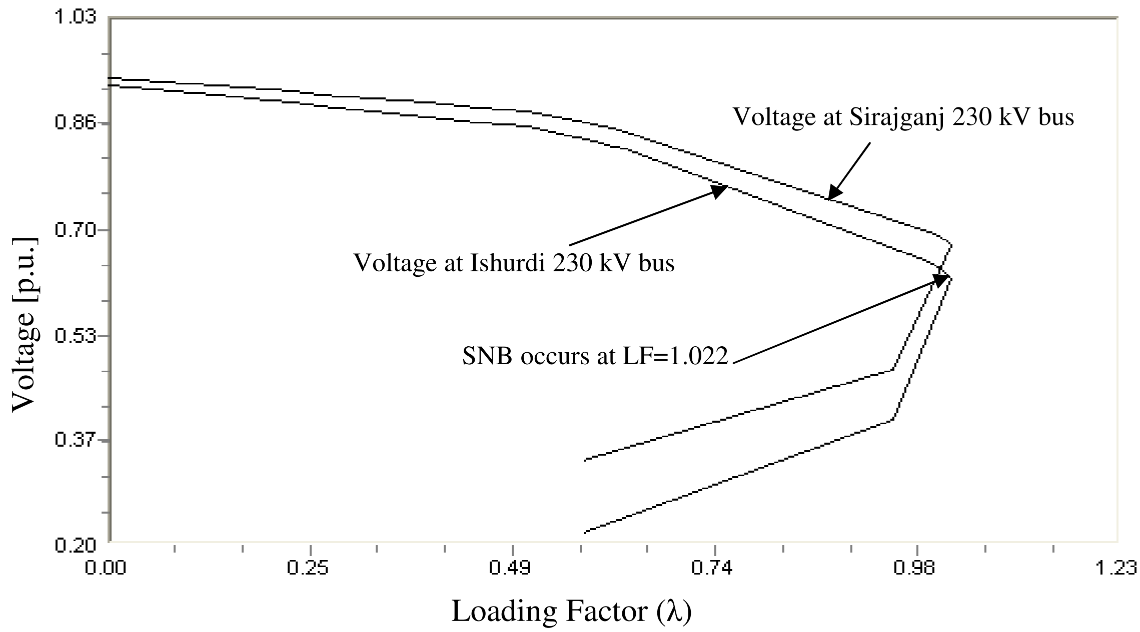

Figure 4.17: Bifurcation diagram of EWIS with 70% series compensation

Figure 4.17 depicts that EWIS with 70% series compensation experiences SNB at LF=1.022. Modal analysis of EWIS has been performed for base case loading. Then loading in the western grid has been increased gradually up to SNB point and no HB point has been found up to SNB point as shown in Figure 4.18.

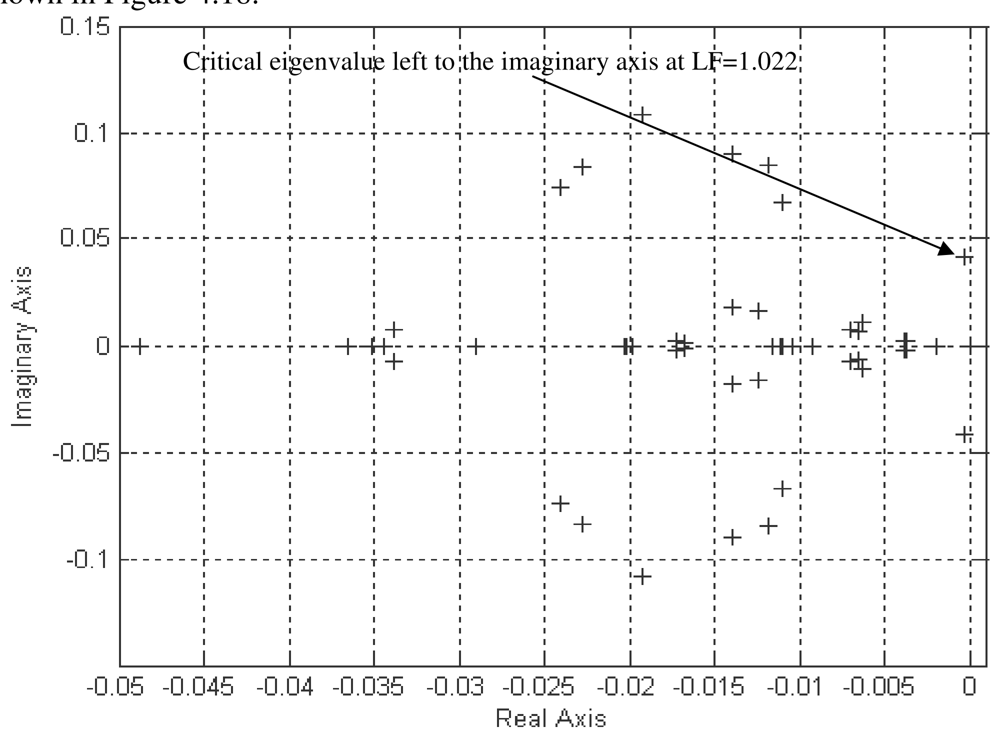

Figure 4.18: Critical eigenvalues of EWIS with 70% compensation at LF=1.022

Table 4.12: Steady state condition of EWIS with 70% series compensation

LF	Import to Western Grid [MW]	Export to Western Grid [MW+ jMVAR]		Bus Voltage [pu]		Transmission Angle [Deg.]	
		G-I	A-S	I	S	G-I	A-S
1.022	532.12	270.71+17.88	347.43+j55.65	0.8000	0.8183	9.050	6.050

Table 4.13: Loading margins of EWIS with series compensation

Compensation Level	Static Loading Margin (SLM)	Dynamic Loading Margin (DLM)
70% series compensation	1.022 (532.12MW)	--

Transmission angles between Ghorasal-Ishurdi and Ashugang-Sirajganj are within safe operating limits up to HB point as shown in Table 4.12. Summary of loading margins of EWIS with series compensation is provided in the Table 4.13.

C. Series-Shunt Compensation

Now series and shunt compensation has been applied to EWIS with TCSC and SVC respectively. Two SVCs of 200 MVAR have been connected to Ishurdi and Ghorasal buses. CPF analysis demonstrates that voltage collapse corresponding to SNB occurs at LF= 1.20 at the height level of series and shunt compensation as shown in Figure 4.19.

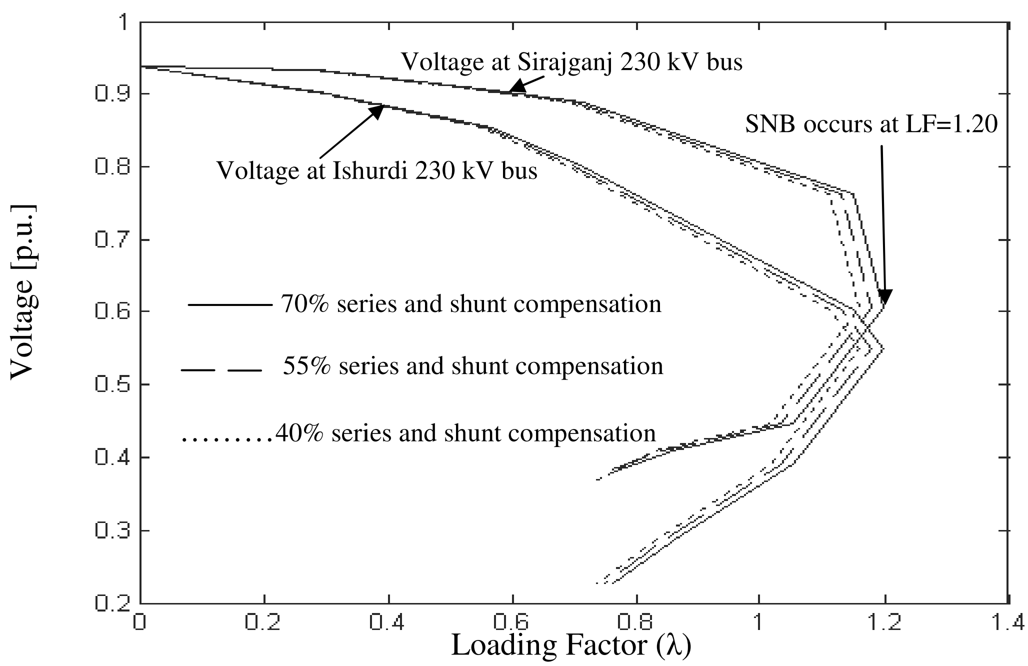

Figure 4.19: Bifurcation diagram EWIS system with series-shunt compensation

Modal analysis has been performed at LF=1.20 and no HB triggered at this loading level as shown in Figure 4.20. So transmission is only limited by SLM corresponding to collapse point.

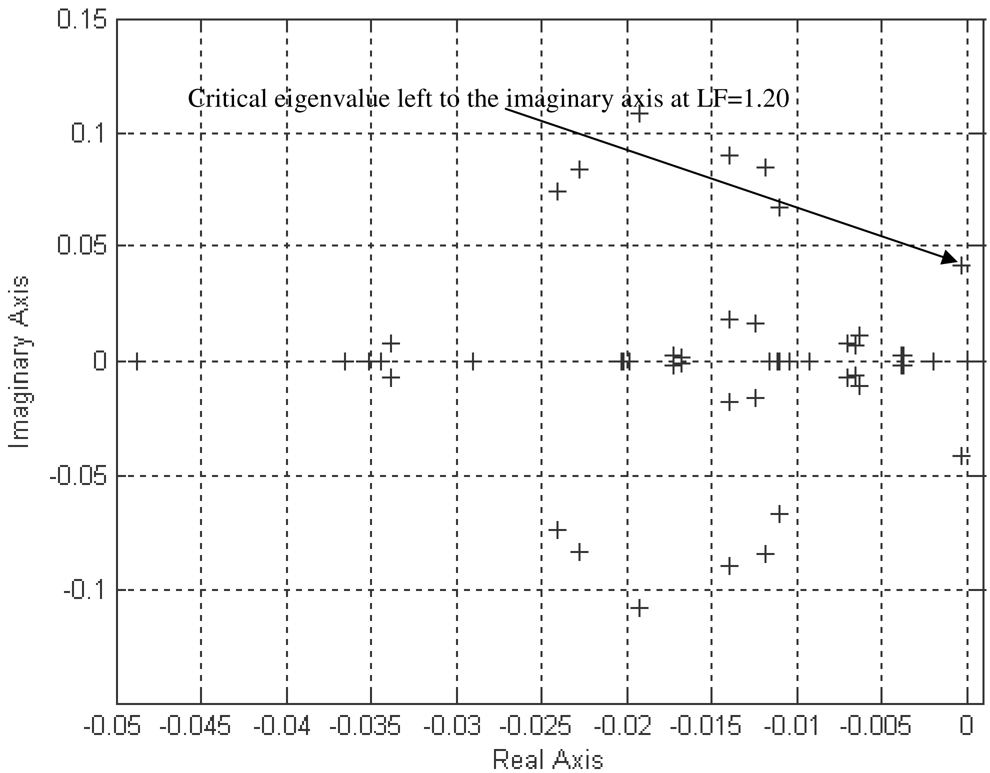

Figure 4.20: Critical eigenvalues of EWIS with 70% series and shunt compensation at LF=1.20

Table 4.14: Steady state condition of EWIS with 70% series and shunt compensation

LF	**Import to Western Grid [MW]**	**Export to Western Grid [MW+ jMVAR]**		**Bus Voltage [pu]**		**Transmission Angle [Deg.]**	
		G-I	A-S	I	S	G-I	A-S
1.20	614	309.44-j54.16	415.59-j51.76	0.8227	0.8440	11.587	8.062

Steady state analysis of EWIS with series-shunt compensation demonstrates that 309.44 MW and 415.59 MW are transmitted through first and second EWIs respectively. Bus voltage and transmission angle are also within the prescribed limits as shown in Table 4.14.

Table 4.15: Loading margins of EWIS with series-shunt compensation

Compensation Level	Static Loading Margin (SLM)	Dynamic Loading Margin (DLM)
70% series and shunt compensation	1.20 (614 MW)	--

614 MW is possible to transfer through the tie lines from eastern to western grid with series-shunt compensation corresponding to loading factor 1.20 as shown in Table 4.15. Dynamic stability is not needed to take into account because no HB is triggered up to this transmission level.

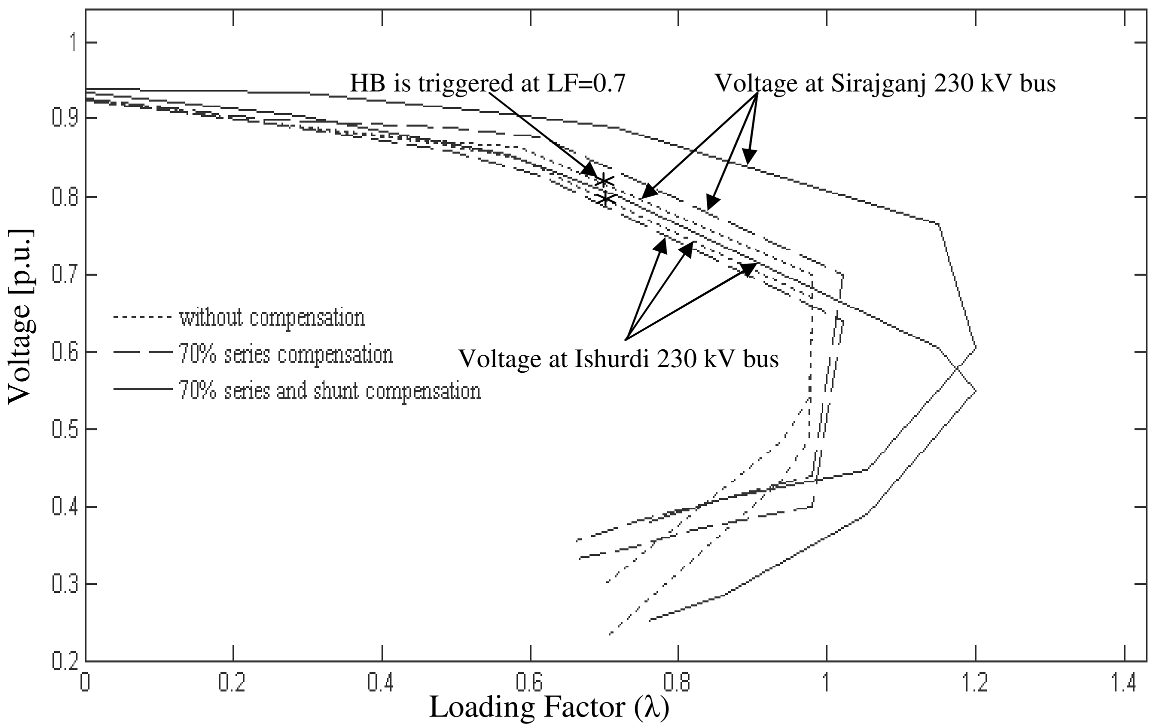

Figure 4.21: Comparison of bifurcation diagrams of EWIS with different compensation levels

Figure 4.21 shows that with series-shunt compensation SNB occurs at higher loading factor compared to the system without compensation. Modal analysis shows that without compensation HB is triggered at a loading factor of 0.7 but no HB is triggered with series or series-shunt compensation up to SNB point.

4.3.2 Performance of Damping Controller

Transient simulation has been performed to show performance of TCSC and SVC damping controllers. Improvement in transient stability with series-shunt compensation compared to the system without and with series compensation has been observed in EWIS. Simulation has been performed for the EWIS without compensation, with 70% series compensation, and with 70% series and 2 p.u. shunt compensation. All the simulations have been performed at LF= 0.7, which is the maximum loading factor of the EWIS without compensation considering dynamic stability limit. A three phase fault is applied in a load bus near the Ishurdi bus in the western grid during time domain simulation.

Time domain simulation profiles of dynamic compensation by TCSC and SVC, faulted bus voltage, active power flow, machine angle, and machine speed deviation presented in Figures 4.22 to 4.28 show improvements in system transient performance with series-shunt compensation compared to the system without and with series compensation.

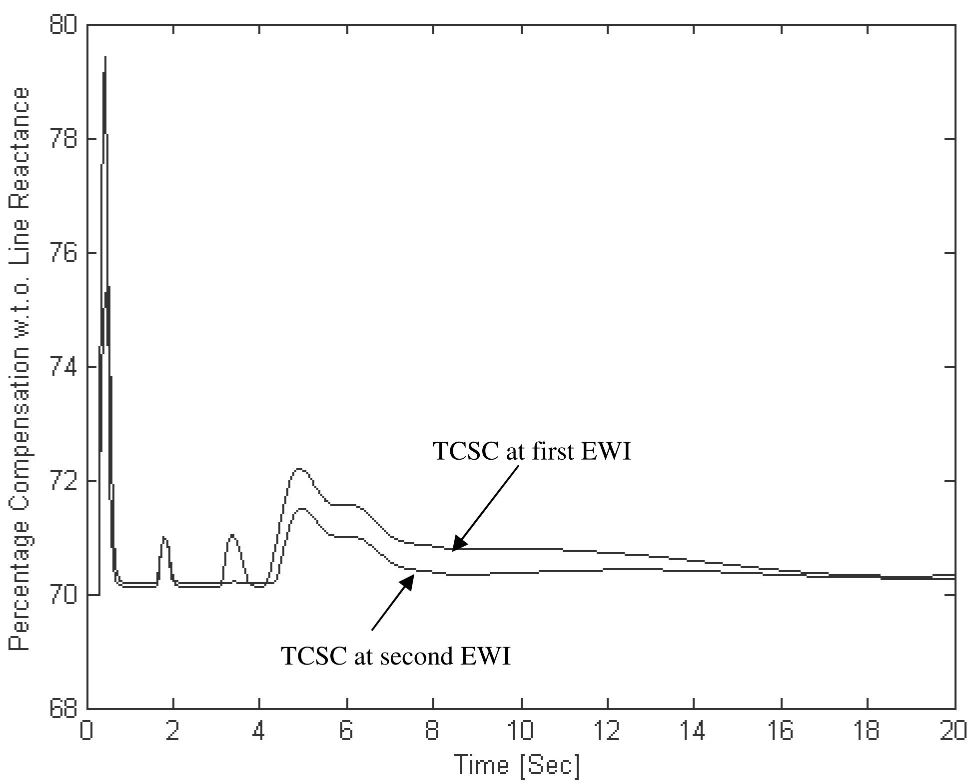

Figure 4.22: Dynamic compensation with TCSCs in EWIS

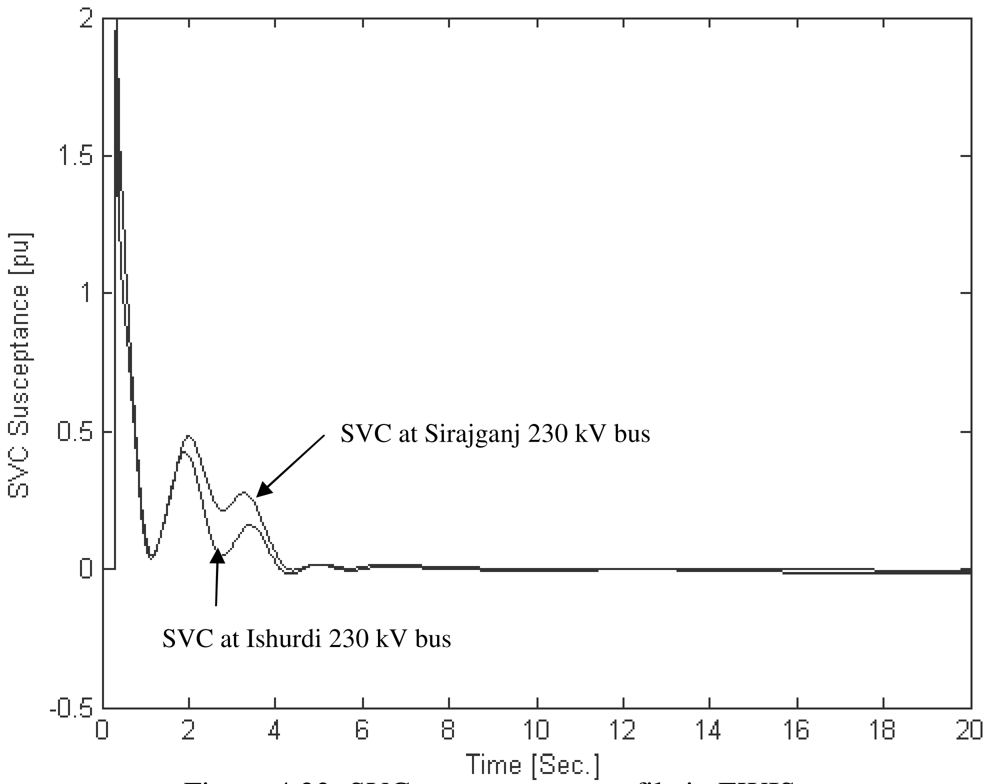

Figure 4.23: SVCs susceptance profile in EWIS

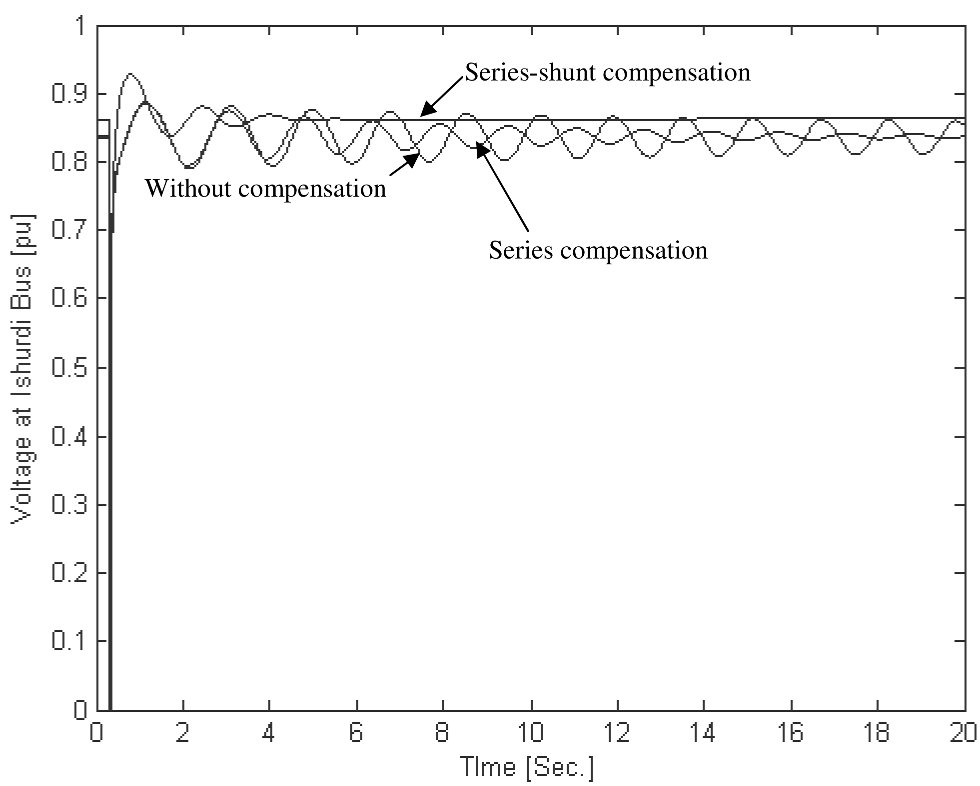

Figure 4.24: Voltage profile at Ishurdi bus

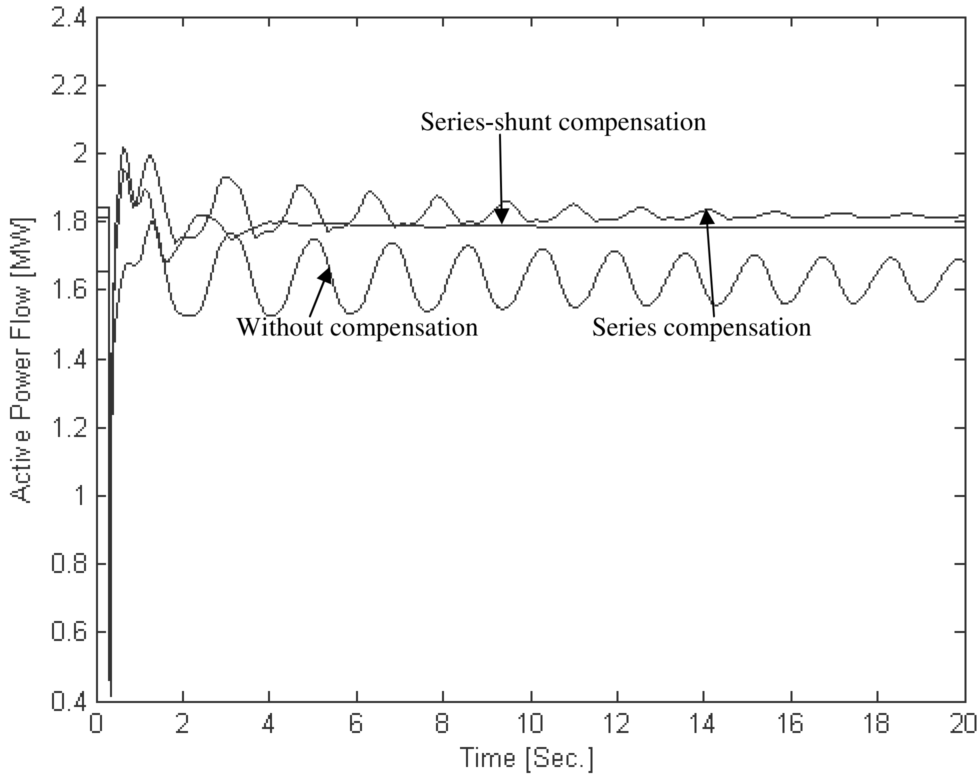

Figure 4.25: Active power flow through first EWI

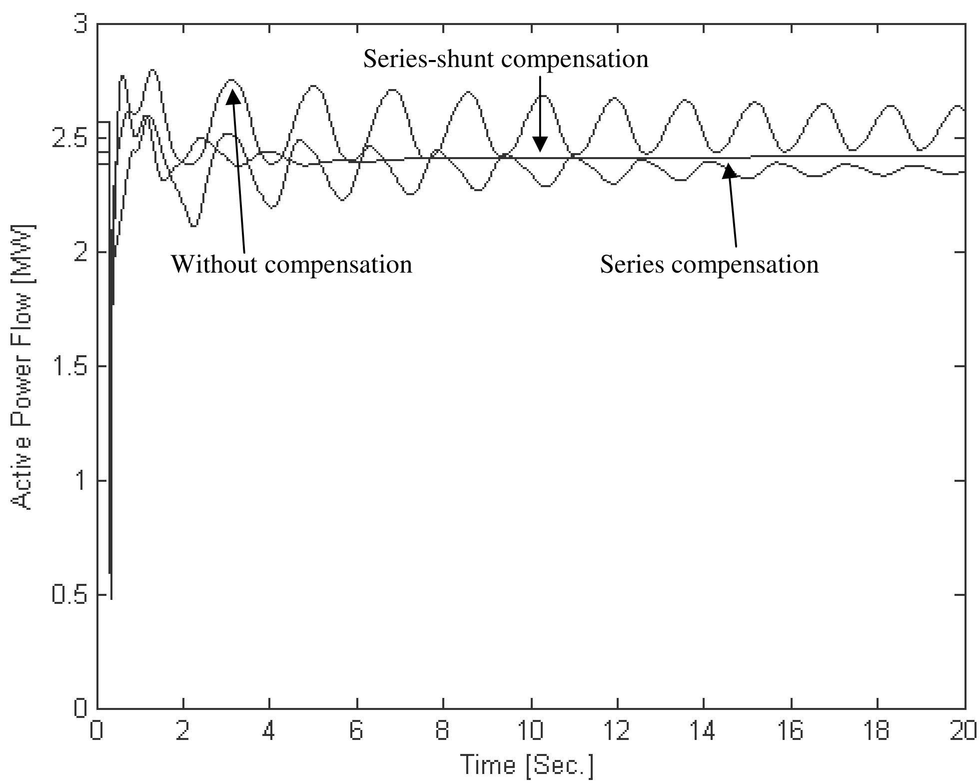

Figure 4.26: Active power flow through second EWI

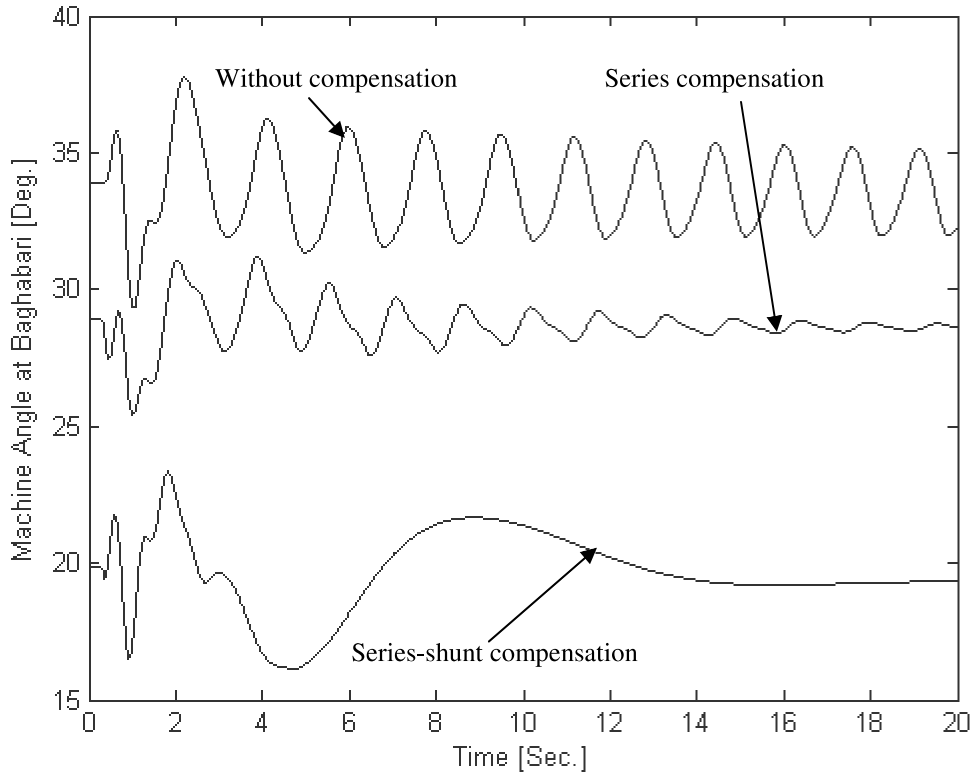

Figure 4.27: Machine angle in EWIS

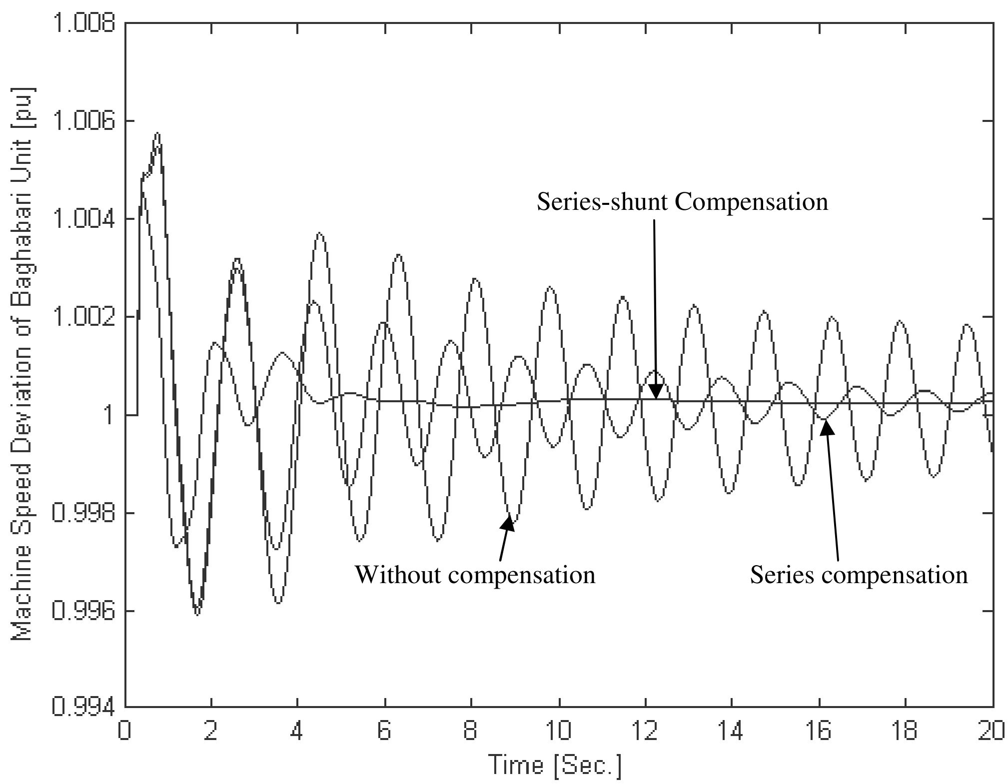

Figure 4.28: Machine speed deviation in EWIS

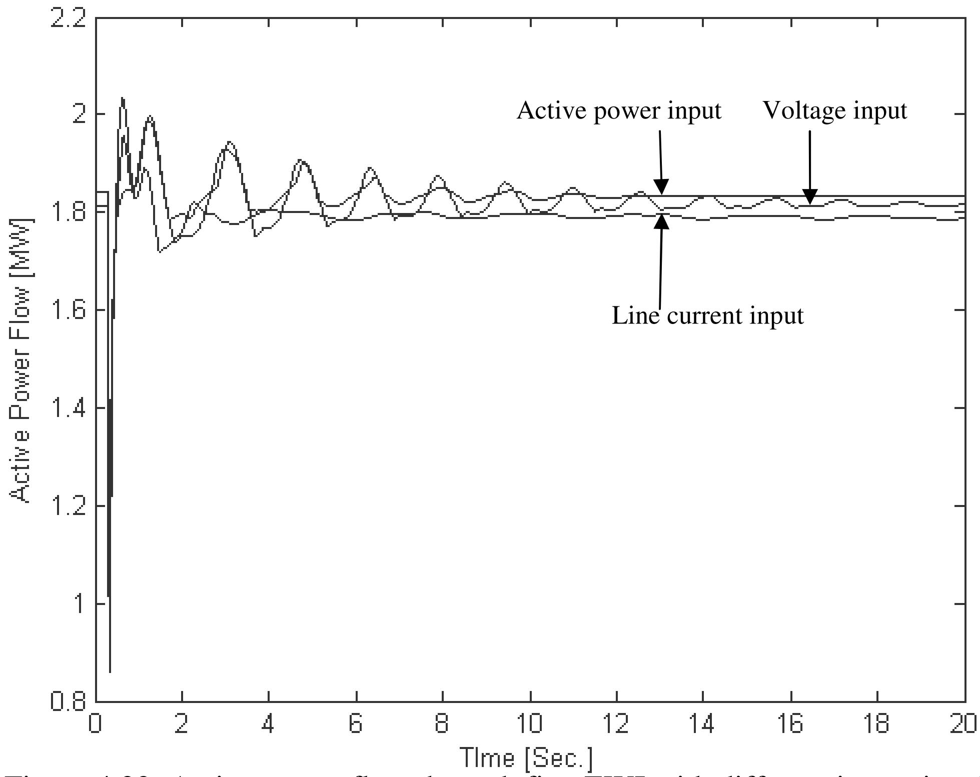

Figure 4.29: Active power flow through first EWI with different input signals

Effect of TCSC and SVC controllers on the damping of electromechanical oscillations with different input signals like voltage, active power and current, has also been studied in this work. Figure 4.29 depicts that the active power input to the controller can damp electromechanical oscillations of system well.

4.3.3 Summary of Capacity Enhancement of EWIs

Bifurcation, modal and load flow analyses presented in this chapter clearly demonstrate that application of series-shunt compensation enhances power transmission capacity of east-west interconnectors of BPS network.

Table 4.16: Comparison of capacity enhancement with different compensation levels

Compensation Level	**Static Loading Margin (SLM)**	**Dynamic Loading Margin (DLM)**
Uncompensated	0.98 (512.8 MW)	0.7 (384 MW)
70% series compensation	1.022 (532.12MW)	--
70% series and shunt compensation	1.20 (614 MW)	--

Table 4.16 shows that without any compensation in EWIS, voltage collapse occurs at a loading factor of 0.98. But before this collapse point, the system experiences oscillatory instability at loading factor of 0.7 which corresponds to 384 MW transfer from eastern to western area. Application of series compensation improves transmission level to 532.12 MW before reaching the collapse point. No oscillatory instability is experienced up to this collapse point. Finally, application of series-shunt compensation picks up transmission capacity to 614 MW up to voltage collapse point without any oscillatory instability.

Table 4.17: Percentage capacity enhancement with different compensation levels

Compensation Level	**Transmission Per Single Circuit [MW]**	**Transmission Per Double Circuit [MW]**	**Cause of Limitation**	**Enhancement [%]**
Uncompensated	384	768	HB	----
Series compensation	532.12	1064.24	SNB	38.57%
Series-shunt compensation	614	1228	SNB	59.89%

38.59% and 59.89% power transmission capacity enhancement have been observed with the application of series compensation and series-shunt compensation as shown in Table 4.17.

Table 4.18: Active power flow with series-shunt compensation at LF=1.20

Active Power Flow	
First EWI	Second EWI
309.44 MW	415.59 MW

Based on the conductor ampacity [3], thermal ratings of the first and second EWI are approximately 315 MVA and 630 MVA per circuit respectively. Active power flow with series-shunt compensation presented in Table 4.18 shows that 98% capacity of first EWI and 66% capacity of second EWI are exploited up to collapse point.

CHAPTER 5

Conclusion

5.1 Conclusions

The combined application of TCSC and SVC has been studied in this work to enhance power transmission capability of Ghorasal-Ishurdi and Ashuganj-Sirajganj tie lines of the BPS network. Improvement of system stability with these FACTS members has also been observed. A standard two area system has been considered as a test bed before using the EWIS of BPS network. The effect of the application of series-shunt compensation on this test system has been analyzed and considerable amount of power transmission capacity enhancement has been observed in both the test systems.

In this work CPF analysis on two area system has been performed with gradually increased loading in area-II, to determine the maximum loading point associated with the voltage collapse. Bifurcation diagram/PV curve of the analysis has been used to demonstrate the improvement in power transmission capacity with series-shunt compensation. In the two area system, without any compensation voltage collapse occurs at a loading factor of 0.145 associated with SNB. But transmission capability of the system is limited earlier than this point at loading factor 0.051 corresponding to HB. Application of 70% series and 2 p.u. shunt compensation improves loading factor to 0.228 and within this operating range no HB is triggered.

Steady state analysis has been performed to determine transmission angle between sending and receiving end buses. Without any compensation at 1.5% increased loading in the area-II, transmission angle exceeds safe operating limit whereas with 70% series and shunt compensation transmission angle is within safe operating limit.

Time domain simulation has been performed to observe the improvement in transient stability with series-shunt compensation. System dynamic performance i.e. damping of electromechanical oscillation has been further improved by adding TCSC and SVC damping controller. Controllability and observability analysis has been performed to calculate controller parameters. Effect of different input signals to TCSC and SVC damping controller like line bus voltage, active power, and line current magnitude has been observed on damping of electromechanical oscillation. Active power is found as the best input signal to damp electromechanical oscillation.

EWIS has been developed from the actual network configuration of BPS network. First CPF analysis has been performed on the EWIS and voltage collapse has been found to take place at a loading factor of 0.98 without compensation. Then modal analysis has been carried out with increased loading in the western grid and HB triggered at loading factor of 0.7. So without compensation only 768 MW is possible to transfer from eastern to western grid with dynamic stability consideration. 38.59% power transmission capacity enhancement has been observed with the application of series compensation by means of two TCSCs placed in first and second interconnectors. Power transmission capacity of EWIs has been further improved to 59.89% with two SVCs connected to Ishurdi and Sirajganj buses.

Steady state and transient analyzes have been performed on EWIS without and with compensation and better performance has been observed with series-shunt compensation. Time domain simulation has also been performed with different input signals to the controller and line active power has been found to be best candidate to damp system oscillation. Simulation results clearly demonstrate enhancement of transmission capacity and stability of the system with series-shunt compensation.

5.2 Further Works

In this work TCSCs and SVCs have been employed to enhance transmission capacity and stability. Both FACTS devices have been placed at the end of EWIs to enhance transmission capacity of EWIs. After application of these FACTS devices it has found that the most of the thermal capacity of first EWI is used but still about 34% thermal capacity of second EWI is unexploited. So the analysis may be conducted to find out optimal location of these FACTS devices to improve transmission capacity and system stability.

Co-ordination of control scheme between TCSC and SVC may be another work to enhance system stability.

Cost benefit analysis of applying series-shunt compensation may be another work.

Application of STATCOM may be analyzed in the EWIS to enhance transmission capacity and stability.

References

[1] Y. Qiuxia, G. Jianbo, X. Duan, *Elasticity Modeling For Transmission Network Expansion Planning in Deregulated Power System*, 42nd International Universities Power Engineering Conference, 4-6 September, 2007

[2] C. A. Canizares, *On Bifurcations, Voltage Collapse and Load Modeling*, IEEE Transactions on Power System, February 1995, Vol. 10, No. 1, pp. 512-522

[3] C. J. Duncan, M. S. Sarma, T. J. Overbye, *Power Systems Analysis and Design*, 4^{th} edition

[4] G. N. Kumar, M. S. Kalavathi, *Reactive Power Compensation for Large Disturbance Voltage Stability Using FACTS Controllers*, 3rd International Conference of Electronics Computer Technology (ICECT), Kanyakumari, 8-10 April, 2011

[5] C. A Canizares, Z. T. Faur, *Analysis of SVC and TCSC Controllers in Voltage Collapse*, IEEE Transactions on Power Systems, February 1999. Vol. 14, No. 1, pp. 158-165

[6] J. E. Alam, *Enhancement of Power Transmission Capacity of East-West Interconnector Using Controlled Series Compensation*, M. Sc. Engineering Thesis, BUET, Dhaka, October, 2009.

[7] R. E. Murbury, J.B. Owens, *New Series Capacitor Protective Devices*, AIEE Transactions, March 1946, Vol. 65, pp. 142-145

[8] E. C. Starr, R. D. Evans, *Series Capacitor for Transmission Circuits*, AIEE transactions, May 1942, Vol. 66, pp. 963-97

[9] S. B. Crary, L. E. Saline, *Location of Series Capacitors in High Voltage Transmission System*, AIEE transactions, December 1953, pp. 1140-1151.

[10] J. A. Maneatis, E.J. Hubacher, W.N. Rothenbuhler, J. Sabath, *500 kV Series Capacitor Installation In California*, IEEE Summer Power Meeting and EHV Conference, Los Angeles, July 17-17, 1970, pp.1138-1149

[11] N. G. Hingorani, *High Power Electronics and Flexible AC Transmission System*, IEEE Power Engineering Review, July 1998, pp. 3-4

[12] J. J. Paserba, N.W. Miller, E. V. Larsen, R. J. Piwko, *A Thyristor Controlled Series Compensation Model for System Stability Studies*, IEEE Transaction on Power Delivery, July 1995, Vol. 10 No. 3, pp. 1471-1478

[13] S. G. Jalali, R. Hedin, R. Johnson, M. Pereira, K. Sadek, *A Stability Model for the Advanced Series Compensation (ASC)*, IEEE Transactions on Power Delivery, April 1996, Vol. 11, No. 2, pp. 1128-1137

[14] Z. Xu, G. Jalali, R. Hedin, H. Liu, *Controller Impedance Range of TCSC and its TCR Reactance Constraints*, Power Engineering Society Summer Meeting, 2001, Vol. 2, pp. 939-943

[15] A. D. Rosso, C. A. Canizares, V. Quintana, and V. M. Dona, *Stability Improvement Using TCSC in Radial Power Systems*, Proceedings of the North American Power Symposium (NAPS), Waterloo, Ontario, October 2000, pp. 12-32 - 12-39

[16] A. D. Rosso, C. A. Canizares, and V. M. Dona, *A Study of TCSC Controller Design for Power System Stability Improvement*, IEEE Transaction on Power Systems, November 2003, Vol. 18 , No. 4, pp. 1487-1496

[17] L. Rouco, F. L. Pagola, *An Engenvalue Sensitivity Approach to Location And Controller Design of Controllable Series Capacitors for Damping Power System Oscillations*, IEEE Transaction on Power Systems, November 1997, Vol. 12, No. 4, pp. 1660-1660

[18] D. Jovcic, and G. N. Pillai, *Analytical Modeling of TCSC Dynamics*, IEEE Transactions on Power Delivery, April 2005, Vol. 20, No. 2, pp. 1097-1104

[19] J. X. Ling, Z. J. Guo, W. H. Feng, L. K. Jun, N. Lin, P. H. Chao, *Design of Adaptive TCSC Damping Controller Based on Oscillation Energy Analysis*, IEEE/PES Transmission and Distribution Conference and Exhibition: Asia and Pacific Dalian, China, 2005, pp. 1-5

[20] Q. Liu, V. Vittal, N. Elia, *LPV Supplementary Damping Controller Design for a Thyristor Controlled Series Capacitor (TCSC) Device*, IEEE Transactions On Power Systems, August 2006, Vol. 21, No. 3, pp. 1242-1249

[21] X. Zheng, Z. Xu, J. Zhang, *A Supplementary Damping Controller of TCSC for Mitigating SSR*, IEEE Power and Energy Society General Meeting, 2009, pp. 1-5

[22] L. Gyugyi, E. R.Taylor, *Characteristics of Static, Thyristor-Controlled Shunt Compensators for Power Transmission System Applications*, IEEE Transactions on Power Apparatus and Systems, September 1980, Vol. 5 No. 10, pp. 1795-1804

[23] A. A. Edris, *Controllable Var Compensator: A Potential Solution to Loadability Problem of Low Capacity Power Systems* , IEEE Transactions on Power Systems, August 1987, Vol. 2, No. 3, pp. 561-567

[24] E. V. Larsen, J. H. Chow, *SVC Control Concepts for System Dynamic Performance*, in IEEE Tutorial Course: Application of Static Var Systems for System Dynamic Performance, 87TH0187-5-PWR, 1987, pp. 36-53

[25] E. Lerch, D. Povh, L. Xu, *Advanced SVC Control for Damping Power System Oscillations*, IEEE Transaction on Power Systems, May 1991, Vol. 6, No. 2, pp. 524-535

[26] Q. Zhao, J. Jiang, *Robust SVC Controller Design for Improving Power System Damping*, IEEE Transaction on Power Systems, November 1995, Vol. 10, No. 4, pp. 1927-1932

[27] Q. Wang, S. S. Choi, M. H. Haque, *Transfer Capability of Long Transmission Lines as Affected by Shunt Compensation*, International Conference on Power System Technologh, Chongqing , 2006, pp. 1-8

[28] R. Yan, Z. Y. Dong, T. K. Saha, J. Ma, *Nonlinear Robust Adaptive SVC Controller Design For Power Systems*, IEEE Power and Energy Society General Meeting - Conversion and Delivery of Electrical Energy in the 21st Century, 2008, pp. 1-7

[29] H. K. Tyll, *Application of SVCs to Satisfy Reactive Power Needs of Power Systems*, IEEE PES Transmission and Distribution Conference and Exhibition, 2005/2006, pp. 887-892.

[30] M. Noroozian, M. Ghandhari, G. Andersson, J. Gronquist, I. Hiskens, *A Robust Control Strategy for Shunt and Series Reactive Compensations to Damp Electromechanical Oscillation*, IEEE Transactions on Power Delivery, October 2001, Vol. 16, No. 4, pp. 812-817

[31] R. Griinbaum, M. D. Grijp, V. Moshi, *Enabling Long Distance AC Power Transmission by Means of FACTS*, IEEE AFRICON, 23-25 September 2009, Nairobi, Kenya

[32] C. A. Canizares, A. Berizzi. P. Marannino, *Using FACTS Controllers to Maximize Available Transfer Capability*, Bulk Power Systems Dynamics and Control IV-Restructuring, August 24-28, 1998, Santorini, Greece

[33] Z. T. Faur, , *Effects of FACTS Devices on Static Voltage Collapse Phenomena*, M. Sc. Engineering Thesis, University of Waterloo, Canada, 1996.

[34] T. J. Miller, *The Theory of Steady State Reactive Power Control in Electric Power Transmission System*, Reactive Power Control In Electric System, John Willey and Sons, Inc. pp. 35-62

[35] J. J. Grainger, W. D. Stevenson, *Power System Analysis*, Mc-Graw-Hill, Edition 2003

[36] C. A. Canizares, *Conditions for Saddle-Node Bifurcations in AC/DC Power Systems*, International Journal of Electric Power and Energy Systems, February 1995, vol. 17, No. 1, pp. 61-68

[37] P. Kundur, *Power System Stability and Control*, McGraw-Hill, New York, 1994

[38] I. J. Nagrath, D. P. Kothari, *Modern Power System Analysis*, McGraw-Hill, 2nd Edition, 2002

[39] C. A. Ayasum and R. Fischl, *On The Region-Wise Analysis of Available Transfer Capability (ATC)*, Proc. NAPS, Wyoming, October 1997, pp. 464-469.

[40] C. A. Canizares, S. Hranilovic, *Transcritical and Hopf Bifurcations in AD/DC Systems*, PROC. Bulk Power System Voltage Phenomena III Seminar, Davos, Switzerland, August 1994, pp. 105-114

[41] C. A. Canizares, F. L. Alvarado, *Point of Collapse and Continuation Methods for Large AC/DC Systems*, IEEE Transactions on Power Systems, February 1993, Vol. 8, No. 1, pp. 1-8

[42] R. Seydel, *From equilibrium to Chaos-Practica1 Bifurcation and Stability Analysis*, Elsevier Science Publishers, North-Holland, 1988

[43] C. A. Canizares, N. Mithulananthan, F. Milano, J. Reeve, *Linear Performance Indices to Predict Oscillatory Stability Problems in Power Systems*, IEEE Transactions on Power Systems, May 2004, Vol. 19, No. 2, pp. 1104-1114

[44] N. Mithulananthan, C. A. Canizares, J. Reeve, *Hopf Bifurcation Control in Power Systems Using Power System Stabilizers and Static Var Compensators*, North American Power Symposium (NAPS), San Luis Obispo, California, October 1999

[45] C. A. Canizares, S. K. M. Kodsi, *Modeling and Simulaiton if IEEE 14 Bus System with FACTS Controllers*, Technical Report 2003-3, University of Waterloo, Canada, March 2003

[46] N. Johansson, L Angquist, H. P. Nee, *An Adaptive Controller for Power System Stability Improvement and Power Flow Control by Means of A Thyristor Switched Series Capacitor (TSSC)*, IEEE Transactions on Power Systems, February 2010 Vol. 25, No. 1, pp. 381-391

[47] J. H. Chow, G. Rogers, *Power System Toolbox Version 3.0*, available at http://www.eps.ee.kth.se/personal/vanfretti/pst/Power_System_Toolbox_Webpage/PST.html

[48] P. M. Anderson, A. A. Fouad, *Power System Control and Stability*, The Iowa State University Press, Ames, Iowa, USA, Indian English Language Edition, 1984

[49] IEEE Committee Report, *IEEE Recommended Practice for* Excitation *System Models for Power System Stability Studies*, IEEE std. 5-2005, April 2006

[50] Nexant, *Power System Master Plan Update 2005*, Ministry of Power, Energy and Mineral Resources, Asian Development Bank TA No. 4379-BAN: Power Sector Development Program II, Component B, Section-3

[51] Laszlo Gyugyi, *Power Electronics in Electric Utilities: Static Var Compensators*, Proc. Of IEEE, April 1988, Vol. 76, No. 4, pp. 383-394

[52] N. Christl, R. Heiden, R. Johnson, P. Krause, and A. Montoya, *Power System Studies And Modeling for The Kayenta 230 kV Substation Advanced Series Compensation*, AC and DC Power Transmission IEEE Conference Publication 5: International Conferenc on AC and DC Power Transmission, September 1991, pp. 33-37

[53] L. A. Erinmez, editor, *Static Var Compensators*, Technical Report of Task Force 2, CIGRE, 1986

[54] C. A. Canizares, S. Zhang, F. L. Alavarado, *UWPFLOW: Continuation and Direct Methods to Locate Fold Bifurcation in AC/DC/FACTS Power System*, available at www.power.uwterloo.com

[55] J. Paserba, P. Kundur, J. Sanchez-Gasca, E. Larsen, *The Electric Power Engineering Handbook*, article 11.3, CRC and IEEE Press, 2011

[56] R. Sadikovic, P. Korba, G. Anderson, *Application of FACTS Devices for Damping of Power System Oscillations*, IEEE Power Tech Conference, St. Petersburg, Russia, 2005

[57] M. E. Aboul-Ela, A. A. Sallam, J. D. McCally, A. A. Fouad, *Damping Controller Design for Power System Oscillations Using Global Signals*, IEEE Transactions on Power System, May 1996, Vol. 11, No. 2, pp. 767-773

Appendix A

Two Area Data

A-1. PST Data Format

Bus Data Format:

Column 1 : Bus Number
Column 2 : Voltage Magnitude (pu)
Column 3 : Voltage Angle (degree)
Column 4 : Generator Active power (pu)
Column 5 : Generator Reactive power (pu)
Column 6 : Load Active power (pu)
Column 7 : Load Reactive Power (pu)
Column 8 : Shunt Conductance (pu)
Column 9 : Shunt Susceptance (pu)
Column 10 : Bus Type (1-for swing bus, 2-for generator bus, 3-for load bus)
Column 11 : Maximum Reactive Power Generation (pu)
Column 12 : Minimum Reactive Power Generation (pu)
Column 13 : Rated Voltage (kV)
Column 14 : Maximum Voltage (pu)
Column 15 : Minimum Voltage (pu)

Line Data Format:

Column 1 : From Bus
Column 2 : To Bus
Column 3 : Resistance (pu)
Column 4 : Reactance (pu)
Column 5 : Line Charging (pu)
Column 6 : Tap Ratio
Column 7 : Tap Phase
Column 8 : Tap Max
Column 9 : Tap Min
Column 10 : Tap Size

Machine Data Format:

Column 1 : Machine Number
Column 2 : Bus Number
Column 3 : Base MVA
Column 4 : Leakage Reactance (pu)
Column 5 : Resistance (pu)
Column 6 : Direct Axis Synchronous Reactance (pu)
Column 7 : Direct Axis Transient Reactance (pu)
Column 8 : Direct Axis Sub-transient Reactance
Column 9 : Direct Axis Open Circuit Time Constant (sec)
Column 10 : Direct Axis Open Circuit Sub-Transient Time Constant (sec)
Column 11 : Quadrature Axis Synchronous Reactance (pu)
Column 12 : Quadrature Axis Transient Reactance (pu)
Column 13 : Quadrature Axis Sub-Transient Reactance (pu)
Column 14 : Quadrature Axis Open Circuit Time Constant (sec)
Column 15 : Quadrature Axis Open Circuit Sub-Transient Time Constant (sec)
Column 16 : Inertia Constant (sec)
Column 17 : Damping Co-efficient d_o (pu)
Column 18 : Damping Co-efficient d_l (pu)

IEEE Type-1 DC Exciter Data Format:

Column 1 : Type
Column 2 : Machine Number
Column 3 : T_R
Column 4 : K_A
Column 5 : T_A
Column 6 : T_B
Column 7 : T_C
Column 8 : V_{RMAX}
Column 9 : V_{RMIN}
Column 10 : K_E
Column 11 : T_E
Column 12 : E_1
Column 13 : $S_E(E_1)$
Column 14 : E_2
Column 15 : $S_E(E_2)$
Column 16 : K_F
Column 17 : T_F

Turbine-Governor Data Format:

Column 1 : Turbine Model (=1)
Column 2 : Machine Number
Column 3 : Speed Set Point w_f (pu)
Column 4 : Steady State Gain (pu)
Column 5 : Maximum Power order Tmax (pu)
Column 6 : Serveo Time Constant T_s (sec)
Column 7 : Governor Time Constant T_C (sec)
Column 8 : Transient Gain Time Constant T_3 (sec)
Column 9 : HP Section Time Constant T_4 (sec)
Column 10 : Reheater Time Constant T_5 (sec)

Non-Conforming Load Bus Data Format to Define TCSC and SVC:

Column 1 : Bus Number
Column 2 : Fraction Constant Active Power Load
Column 3 : Fraction Reactive Active Power Load
Column 4 : Fraction Constant Active Current Load
Column 5 : Fraction Constant Reactive Current Load

TCSC Data Format:

Column 1 : TCSC Number
Column 2 : From Bus Number
Column 3 : To Bus Number
Column 4 : Control Gain
Column 5 : Control Time Constant
Column 6 : Maximum Susceptance B-on System Base (pu)
Column 7 : Minimum Susceptance B-on System Base (pu)

SVC Data Format:

Column 1 : SVC Number
Column 2 : Bus Number
Column 3 : SVC Base MVA
Column 4 : Maximum Susceptance Bcvmax (pu)
Column 5 : Minimum Susceptance Bcvmin (pu)
Column 6 : Regulator Gain
Column 7 : Regulator Time Constant (sec)

Switching Data Format for Transient Simulation:

Row 1	: Column 1 - Simulation Start Time (sec)
	: Column 2 to Column 6- zeros
	: Column 7 - Initial Time Step (sec)
Row 2	: Column 1 - fault application time (s)
	: Column 2- Bus Number at Which Fault is Applied
	: Column 3- Bus Number Defining Far End of Faulted Line
	: Column 4- Zero Sequence Impedance on System Base (pu)
	: Column 5- Negative Sequence Impedance on System Base (pu)
	: Colunm 6- Fault Type (0 for three phase fault)
	: Column 7- Time Step for Fault Period (sec)
Row 3	: Column 1- Near End Fault Clearing Time (sec)
	: Column 2 to Column 6- zeros
	: Column 7 - Time Step for Second Part of Fault (sec)
Row 4	: Column 1- Far End Fault Clearing Time (sec)
	: Column 2 to Column 6- zeros
	: Column 7 - Time Step for Fault Cleared Simulation (sec)
Row 5	: Column 1- Time to Change Step Length (sec)
	: Column 2 to Column 6- zeros
	: Column 7 - Time Step (sec)
Column n	: Total Simulation Period (sec)

(n Indicates that Intermediate Rows May be Inserted)

A-2. UWPFLOW Data Format

Bus Data Format:

T |Ow|Name |kV |Z|PL |QL |MW |Mva|PM |P |QM |Qm |Vpu|Vm |Name |kV |%Q
T- Type (A2) - "B " for PQ Load Bus
"BQ" for PV Generator Bus with Q Limits
Ow (A3)- Owner
Name (A8)- Bus Name
kV (F4.0) - Bus kV base
Z (2A) -Zone
PL (F5.0)- Active Load in MW
QL (F5.0) -Reactive Load in MVAR
SHUNT (2F4.0) -MW and MVAR Shunts (+ for Capacitors)
PM (F4.0) –Maximum Generator Active Power in MW
P (F5.0) - Generator Active Power in MW
QM (F5.0) - Maximum Generator Reactive Power in MVAR
Qm (F5.0) - Minimum Generator Reactive Power in MVAR
Vpu (F4.3)-> Desired Voltage Magnitude in pu for PV Bus

Line Data Format:

T |Ow|Name_1 |kV1||Name_2 |kV2|||In || R | X | G/2 | B/2 |Mil|
T-Type (A2) -"L for Line "
Ow (A3) -Owner
Name_1 (A8) -Name of Sending Bus
kV1 (F4.0) - kV Base for Sending Bus
M (I1)-Metered Bus for Flow Interchange
Name_2 (A8) - Name of Receiving Bus
kV2 (F4.0) - kV Base for Receiving Bus
C (I1) -Circuit ID
S (I1) -Section Number
In (F4.0) -Rated Ampere
N (I1) - Circuit Number
R (F6.5) - Series Resistance of PI Equivalent (p.u.)
X (F6.5) - Series Reactance of PI Equivalent (p.u.)
G/2 (F6.5) - Shunt G/2 of PI Equivalent (p.u.)
B/2 (F6.5) - Shunt B/2 of PI Equivalent (p.u.)
Mil (F4.1) - Length in Miles

Transformer Data Format:

T |Ow|Name_1 |kV1||Name_2 |kV2|||Sn | R | X | G | B |Tap1|Tap2|
T-Type (A2) – “T for Transformer”

Ow (A3) - Owner
Name_1 (A8) -Name of Sending Bus
kV1 (F4.0) - kV Base for Sending Bus
M (I1) -Metered Bus for Flow Interchange
Name_2 (A8) - Name of Receiving Bus
kV2 (F4.0) - kV Base for Receiving Bus
C (I1) -Circuit ID
S (I1) -Section Number
Sn (F4.0) - Rated MVA
N (I1) - Circuit Number
R (F6.5) -p.u. Series R of Equivalent Circuit
X (F6.5) - p.u. Series X of Equivalent Circuit
G (F6.5) - p.u. Shunt G of Equivalent Circuit
B (F6.5) - p.u. Shunt B of Equivalent Circuit
Tap1 (F5.2) - kV Tap for Sending Bus
Tap2 (F5.2) - kV Tap for Receiving Bus

TCSC Data Format:

T |Bus1 |kV1 |Bus2 |kV2|Xc |Xl |am|aM|cont ||MVA|al |M1 |
T-Type (A2) - "FC" (F for FACTS, C for TCSC)
Bus1 (A8) - Sending Bus Where TCSC is Connected
kV1 (F4.0)- Bus 1 kV Base
Bus2 (A8) - Receiving Bus Where TCSC is Connected
kV2 (F4.0)- Bus 2 kV Base
Xc (F8.7) - Per Unit TCSC Capacitive Reactance w.r.t MVA and kV1 Base
Xl (F8.7) - Per unit TCSC Inductive Reactance w.r.t MVA and kV1 Base
am (F3.0) - Minimum Firing Angle Alpha in Degrees
aM (F3.0) - Maximum Firing Angle Alpha in Degrees
cont (F8.3)- TCSC Control Value: % of X; MW for P; KA for I; Degrees for D
Mode (A1) - Control mode: X for Reactance; P for Power; I for Current; D for Angle
MVA (F4.0)- TCSC Rating in MVA. Defaults to MVA System Base
al (F5.1) - Initial Value of Firing Angle in Degrees (optional)
M1 (F4.0) - Needed for Determining Series Line Reactance for % X , $M1=Xc/X_{line}$

SVC Data Format:

T |Ow|Bus1 |kV1 |Bus2 |kV2|Xc |Xl |am|aM|s|MVA|Vrf|kV |Xth |al
T- Type (A2) - "FS" (F for FACTS, S for SVC)
Ow (A3) -Owner
Bus1 (A8) - System Bus Where SVC is Connected

kV1 (F4.0) - Bus 1 kV Base
Bus2 (A8) - System Bus that SVC Controls
kV2 (F4.0) - Bus 2 kV Base
Xc (F8.7) - Per Unit SVC Capacitive X w.r.t. MVA and kV1 Base
Xl (F8.7) - Per Unit SVC Inductive X w.r.t. MVA and kV1 Base
am (F3.0) - Minimum Firing Angle Alpha in Degrees
aM (F3.0) - Maximum Firing Angle Alpha in Degrees
s (F2.0) - SVC Control Slope in % w.r.t. to MVA and kV1 Base
MVA (F4.0) -SVC Maximum Rating in MVAr (capacitive)
Vrf (F4.3) -p.u. Reference Control Voltage
kV (F4.0) - Low kV Side of Step-Down Transformer (optional)
Xth (F8.7) - Step-Down Transformer Reactance in p.u. w.r.t. to SVC MVA; Rating and kV1 (optional)
al (F5.1) - Initial Value of Firing Angle in Degrees (optional)

A-3. PST Data of Two Area System

```
bus=[...
 1  1.0300  20.2000 7.0000 1.8500 0.00         0.00   0.00 0.00 1 10.0 -10.0 230.0 1.1 0.9;
 2  1.0100  10.5000 7.0000 2.3500 0.00         0.00   0.00 0.00 2 5.0  -5.0  230.0 1.1 0.9;
 3  1.0300 -6.8000  7.1900 1.7600 0.00         0.00   0.00 0.00 2 5.0  -5.0  230.0 1.1 0.9;
 4  1.0100 -17.0000 7.0000 2.0200 0.00         0.00   0.00 0.00 2 5.0  -5.0  230.0 1.1 0.9;
 5  1.0074  20.3799 0.0000 0.0000 0.00         0.00   0.00 0.00 3 0.0   0.0  230.0 1.1 0.8;
 6  0.9804  10.3201 0.0000 0.0000 0.00         0.00   0.00 0.00 3 0.0   0.0  230.0 1.1 0.8;
 7  0.9652  1.9560  0.0000 0.0000 9.67         1.00   0.00 2.00 3 0.0   0.0  230.0 1.1 0.8;
 8  1.0000 -11.7915 0.0000 0.0000 0.00         0.00   0.00 2.00 3 0.0   0.0  230.0 1.1 0.8;
 9  0.9763 -25.2580 0.0000 0.0000 1.015*17.17 1.015*1 0.00 3.50 3 0.0   0.0  230.0 1.1 0.8;
 10 0.9862 -16.8988 0.0000 0.0000 0.00        0.00    0.00 0.00 3 0.0   0.0  230.0 1.1 0.8;
 11 1.0093 -6.6276  0.0000 0.0000 0.00        0.00    0.00 0.00 3 0.0   0.0  230.0 1.1 0.8;
 12 0.9763 -25.2580 0.0000 0.0000 1.015*0.5   0.00    0.00 0.00 3 0.0   0.0  230.0 1.1 0.8;
 13 0.9763 -25.2580 0.0000 0.0000 1.015*0.5   0.00    0.00 0.00 3 0.0   0.0  230.0 1.1 0.8;]
line=[...
 1   5   0.00     0.0167   0.00      1 0 0 0 0;
 5   6   0.0025   0.025    0.04375   1 0 0 0 0;
 2   6   0.00     0.0167   0.00      1 0 0 0 0;
 6   7   0.001    0.01     0.0175    1 0 0 0 0;
 7   8   0.011    0.11     0.1925    1 0 0 0 0;
 12  9   0.011    0.11     0.1925    1 0 0 0 0;
 12  9   0.011    0.11     0.1925    1 0 0 0 0;
 7   8   0.011    0.11     0.1925    1 0 0 0 0;
 9  10   0.001    0.01     0.0175    1 0 0 0 0;
 10  4   0.00     0.0167   0.00      1 0 0 0 0;
 10 11  0.0025   0.025    0.04375    1 0 0 0 0;
 3  11   0.00    0.0167    0.00      1 0 0 0 0;
 9  13   0.00     0.01     0         1 0 0 0 0;
 8  12   0.0    -0.11*0.4  0.1925    1 0 0 0 0;
  ];
mac_con=[...
1 1 900 0.200 0.0025 1.8 0.30 0.25 8.00 0.03 1.7 0.55 0.25 0.4 0.05 6.5   2 0 1 0.039 0.267;
2 2 900 0.200 0.0025 1.8 0.30 0.25 8.00 0.03 1.7 0.55 0.25 0.4 0.05 6.5   2 0 2 0.039 0.267;
3 3 900 0.200 0.0025 1.8 0.30 0.25 8.00 0.03 1.7 0.55 0.25 0.4 0.05 6.175 2 0 3 0.039 0.267;
4 4 900 0.200 0.0025 1.8 0.30 0.25 8.00 0.03 1.7 0.55 0.25 0.4 0.05 6.175 2 0 4 0.039 0.267;];
exc_con=[...
1 1 0.01 46.0 0.06 0 0 1.0 -0.9 0.0 0.46 3.1 0.33 2.3 0.1 0.07 1.0 0 0 0;
1 2 0.01 46.0 0.06 0 0 1.0 -0.9 0.0 0.46 3.1 0.33 2.3 0.1 0.07 1.0 0 0 0;
1 3 0.01 46.0 0.06 0 0 1.0 -0.9 0.0 0.46 3.1 0.33 2.3 0.1 0.07 1.0 0 0 0;
1 4 0.01 46.0 0.06 0 0 1.0 -0.9 0.0 0.46 3.1 0.33 2.3 0.1 0.07 1.0 0 0 0;];
tg_con=[...
    1 1 1 25.0 1.0 0.1 0.5 0.0 1.25 5.0;
    1 2 1 25.0 1.0 0.1 0.5 0.0 1.25 5.0;
    1 3 1 25.0 1.0 0.1 0.5 0.0 1.25 5.0;
    1 4 1 25.0 1.0 0.1 0.5 0.0 1.25 5.0;];

load_con =[ 8 0 0 0 0
            12 0 0 0 0];

svc_con = [...
        1   9   100  2 -2 2 0.05 ];

tcsc_con=[...
    1 8 12 1.0 0.05 0 -3;
    ]

rlmod_con = [...

    1  9 100 2 -2 2 0.05;
];
% damping controller function of SVC
svc_dc=[];
svc_dc{1,1}=0.25.*wo_stsp(10).*(ldlg_stsp(1,0.6251,0.1021).^1);
svc_dc{1,2}=1;
svc_dc{1,3}=9;
svc_dc{1,4}=2;
svc_dc{1,5}=-2;
svc_dc{1,6}=2;
```

```
%damping controller function of TCSC
tcsc_dc=[];
tcsc_dc{1,1}=30.*wo_stsp(10).*(ldlg_stsp(1,0.6966,0.0966).^1);
tcsc_dc{1,2}=1;
tcsc_dc{1,3}=8;
tcsc_dc{1,4}=0;
tcsc_dc{1,5}=-3;
tcsc_dc{1,6}=2;

sw_con = [...
0    0    0    0    0    0    0.01;
0.1  9   13    0    0    0    0.005;
0.15 0    0    0    0    0    0.005556;
0.20 0    0    0    0    0    0.005556;
0.50 0    0    0    0    0    0.01;
1.0  0    0    0    0    0    0.01;
20.0 0    0    0    0    0    0];
lmon_con=[1:length(line(:,1))]';
```

A-4. UWPFLOW Data Two Area System

```
HDG

TWO AREA TEST SYSTEM

BAS
C 34567890123456789012345678901234567890123456789012345678901234567890123456789
BQ   BUS_1    230              4000700.01000.-10001.03
BQ   BUS_2    230                800700.0500.0-500.1.01
BQ   BUS_3    230                800719.0500.0-500.1.03
BQ   BUS_4    230                800700.0500.0-500.1.01
B    BUS_5    230
B    BUS_6    230
B    BUS_7    230  967.0100.0    200.0
B    BUS_8    230
B    BUS_9    230  1717.100.0    350.0
B    BUS_10   230
B    BUS_11   230
B    BUS_12   230
B    BUS_13   230    50.
C
C 34567890123456789012345678901234567890123456789012345678901234567890123456789
L    BUS_1    230 BUS_5    2301            .0167
L    BUS_2    230 BUS_6    2302            .0167
L    BUS_5    230 BUS_6    2302     .0025 .025       .02178
L    BUS_6    230 BUS_7    2302     .001   .01       .00875
L    BUS_7    230 BUS_8    2302     .011   .11       .09625
L    BUS_7    230 BUS_8    2302     .011   .11       .09625
L    BUS_12   230 BUS_9    2302     .011   .11       .09625
L    BUS_12   230 BUS_9    2302     .011   .11       .09625
L    BUS_9    230 BUS_13   2302            .01
L    BUS_9    230 BUS_10   2302     .001   .01       .00875
L    BUS_10   230 BUS_11   2302     .0025.025        .02178
L    BUS_4    230 BUS_10   2302            .0167
L    BUS_3    230 BUS_11   2302            .0167
C 34567890123456789012345678901234567890123456789012345678901234567890123456789
FC   BUS_8    230 BUS_12   230 .03300 .003300 144175  70.0  X        3.33
FS   BUS_9    230 BUS_9    230  1.1708  0.4925 90175 2 200  1. 26.     0.1
SOL                 50  BUS_1    230      20.2
ZZ
END
```

East-West Interconnected System Data

B-1. PST Data of East-West Interconnected System

```
bus=[...
1  0.87   00.0  0.0  0.0 0.0       0.0           0.0   0.0   1  5.0   -5.0   230  1.01  0.5;
2  0.86  -10.0  0.0  0.0 0.00      0.00000       0.0   0.0   3  0.0    0.0   230  1.01  0.5;
3  0.86  -10.0  0.0  0.0 0.00      0.00000       0.0   0.0   3  0.0    0.0   230  1.01  0.5;
4  0.86  -10.0  0.0  0.0 1.7*0.00  0.400*1.7*0.00 0.0  2.0   3  0.0    0.0   230  1.01  0.5;
5  0.86  -10.0  0.0  0.0 1.7*0.24  0.400*1.7*0.24 0.0  0.1   3  0.0    0.0   132  1.01  0.5;
6  0.86  -10.0  0.0  0.0 1.7*0.37  0.400*1.7*0.37 0.0  0.05  3  0.0    0.0   132  1.01  0.5;
7  0.86  -10.0  0.0  0.0 1.7*0.00  1.7*0.00000000 0.0  0.00  3  0.0    0.0   132  1.01  0.5;
8  0.86  -10.0  0.0  0.0 1.7*0.00  0.400*1.7*0.00 0.0  2.00  3  0.0    0.0   230  1.01  0.5;
9  0.86  -10.0  0.0  0.0 1.7*0.00  0.400*1.7*0.00 0.0  0.00  3  0.0    0.0   230  1.01  0.5;
10 0.86  -10.0  0.0  0.0 1.7*0.20  0.400*1.7*0.20 0.0  0.00  3  0.0    0.0   132  1.01  0.5;
11 0.86  -10.0  0.0  0.0 1.7*0.30  0.400*1.7*0.30 0.0  0.10  3  0.0    0.0   132  1.01  0.5;
12 0.86  -10.0  0.0  0.0 1.7*0.20  0.400*1.7*0.20 0.0  0.075 3  0.0    0.0   132  1.01  0.5;
13 0.86  -10.0  0.0  0.0 0.100000  0.000000000000 0.0  0.000 3  0.0    0.0   132  1.01  0.5;
14 0.86  -10.0  0.0  0.0 1.7*0.20  0.400*1.7*0.20 0.0  0.025 3  0.0    0.0   132  1.01  0.5;
15 0.86  -10.0  0.0  0.0 1.7*0.20  0.400*1.7*0.20 0.0  0.025 3  0.0    0.0   132  1.01  0.5;
16 0.86  -10.0  0.0  0.0 1.7*0.20  0.400*1.7*0.20 0.0  0.0   3  0.0    0.0   132  1.01  0.5;
17 0.86  -10.0  0.0  0.0 1.7*0.10  0.400*1.7*0.10 0.0  0.00  3  0.0    0.0   132  1.01  0.5;
18 0.86  -10.0  0.0  0.0 1.7*0.10  0.400*1.7*0.10 0.0  0.075 3  0.0    0.0   132  1.01  0.5;
19 0.86  -10.0  0.0  0.0 1.7*0.05  0.400*1.7*0.05 0.0  0.000 3  0.0    0.0   132  1.01  0.5;
20 0.86  -10.0  0.0  0.0 1.7*0.05  0.400*1.7*0.05 0.0  0.000 3  0.0    0.0   132  1.01  0.5;
21 0.86  -10.0  0.0  0.0 1.7*0.10  0.400*1.7*0.10 0.0  0.000 3  0.0    0.0   132  1.01  0.5;
22 0.86  -10.0  0.0  0.0 1.7*0.20  0.400*1.7*0.20 0.0  0.000 3  0.0    0.0   132  1.01  0.5;
23 0.86  -10.0  0.0  0.0 1.7*0.25  0.400*1.7*0.25 0.0  0.200 3  0.0    0.0   132  1.01  0.5;
24 0.86  -10.0  0.0  0.0 1.7*0.26  0.400*1.7*0.26 0.0  0.075 3  0.0    0.0   132  1.01  0.5;
25 0.86  -10.0  0.0  0.0 1.7*0.38  0.400*1.7*0.38 0.0  0.075 3  0.0    0.0   132  1.01  0.5;
26 0.86  -10.0  0.0  0.0 1.7*0.10  0.400*1.7*0.10 0.0  0.000 3  0.0    0.0   132  1.01  0.5;
27 0.86  -10.0  0.0  0.0 1.7*0.10  0.400*1.7*0.10 0.0  0.150 3  0.0    0.0   132  1.01  0.5;
28 0.86  -10.0  0.0  0.0 1.7*0.10  0.400*1.7*0.10 0.0  0.000 3  0.0    0.0   132  1.01  0.5;
29 0.86  -10.0  0.0  0.0 1.7*0.15  0.400*1.7*0.15 0.0  0.350 3  0.0    0.0   132  1.01  0.5;
30 0.86  -10.0  0.0  0.0 1.7*0.35  0.400*1.7*0.35 0.0  0.000 3  0.0    0.0   132  1.01  0.5;
31 0.86  -10.0  0.0  0.0 1.7*0.10  0.400*1.7*0.10 0.0  0.100 3  0.0    0.0   132  1.01  0.5;
32 0.86  -10.0  0.0  0.0 1.7*0.10  0.400*1.7*0.10 0.0  0.000 3  0.0    0.0   132  1.01  0.5;
33 0.86  -10.0  0.0  0.0 1.7*0.00  0.400*1.7*0.00 0.0  0.000 3  0.0    0.0   230  1.01  0.5;
34 0.86  -10.0  0.0  0.0 1.7*0.00  0.400*1.7*0.00 0.0  0.000 3  0.0    0.0   230  1.01  0.5;
35 0.86  -10.0  0.0  0.0 1.7*0.10  0.400*1.7*0.10 0.0  0.000 3  0.0    0.0   132  1.01  0.5;
36 0.86  -10.0  0.0  0.0 1.7*0.00  0.400*1.7*0.00 0.0  0.000 3  0.0    0.0   230  1.01  0.5;
37 0.86  -10.0  0.0  0.0 1.7*0.00  0.400*1.7*0.00 0.0  0.000 3  0.0    0.0   230  1.01  0.5;
38 0.86  -10.0  0.0  0.0 1.7*0.00  0.400*1.7*0.00 0.0  0.000 3  0.0    0.0   33   1.01  0.5;
39 0.95  -10.0  0.1  0.0 1.7*0.00  0.400*1.7*0.00 0.0  0.000 2  0.075 -0.075 11   1.01  0.5;
40 0.87  -10.0  1.25 0.0 1.7*0.00  0.400*1.7*0.00 0.0  0.000 2  1.27  -1.27  11   1.01  0.5;
41 0.95  -10.0  1.20 0.0 1.7*0.00  0.400*1.7*0.00 0.0  0.000 2  1.22  -1.22  11   1.01  0.5;
42 0.87  -10.0  0.23 0.0 1.7*0.00  0.400*1.7*0.00 0.0  0.000 2  0.2   -0.2   11   1.01  0.5;
43 0.85  -10.0  1.05 0.0 1.7*0.00  0.400*1.7*0.00 0.0  0.000 2  1.07  -1.07  11   1.01  0.5;
44 0.85  -10.0  0.15 0.0 1.7*0.00  0.400*1.7*0.00 0.0  0.000 2  0.13  -0.13  11   1.01  0.5;
45 0.86   0.0   0.0  0.0 1.7*0.00  0.400*1.7*0.00 0.0  0.000 3  0.000  0.000 230  1.01  0.5;
46 0.86   0.0   0.0  0.0 1.7*0.00  0.400*1.7*0.00 0.0  0.000 3  0.000  0.000 230  1.01  0.5;
];
```

```
line=[...
1    2     0.000         0.001           0.00        1.0  0.0 0.0 0.0 0.0;
1    3     0.000         0.001           0.00        1.0  0.0 0.0 0.0 0.0;
2   45     0.0267        0.1371          0.2647      1.0  0.0 0.0 0.0 0.0;
45   4     0.000        -0.7*0.1371      0.000       1.0  0.0 0.0 0.0 0.0;
3   46     0.011         0.077           0.2954      1.0  0.0 0.0 0.0 0.0;
31   5     0.0174        0.066           2*0.0078    1.0  0.0 0.0 0.0 0.0;
31  17     0.0093        0.0352          2*0.0042    1.0  0.0 0.0 0.0 0.0;
46   8     0.000        -0.7*0.0770      0.00        1.0  0.0 0.0 0.0 0.0;
17  26     0.0232        0.088           2*0.0104    1.0  0.0 0.0 0.0 0.0;
7   26     0.00462       0.0135          2*0.00155   1.0  0.0 0.0 0.0 0.0;
26  32     0.0197        0.0748          2*0.00884   1.0  0.0 0.0 0.0 0.0;
4   33     0.0044        0.03025         0.1161      1.0  0.0 0.0 0.0 0.0;
31  7      0.0385        0.1125          2*0.0127    1.0  0.0 0.0 0.0 0.0;
6   25     0.0261        0.099           2*0.0117    1.0  0.0 0.0 0.0 0.0;
5   6      0.0377        0.143           2*0.0169    1.0  0.0 0.0 0.0 0.0;
31  23     0.0261        0.099           2*0.0115    1.0  0.0 0.0 0.0 0.0;
5   23     0.0308        0.090           2*0.0102    1.0  0.0 0.0 0.0 0.0;
23  24     0.0275        0.104           2*0.0122    1.0  0.0 0.0 0.0 0.0;
33  8      0.00320       0.022           0.0844      1.0  0.0 0.0 0.0 0.0
7   32     0.0232        0.088           2*0.01044   1.0  0.0 0.0 0.0 0.0;
34  8      0.00544       0.03740         0.1435      1.0  0.0 0.0 0.0 0.0;
6   32     0.0383        0.1452          2*0.0172    1.0  0.0 0.0 0.0 0.0;
6   16     0.0291        0.1104         2*0.0131     1.0  0.0 0.0 0.0 0.0;
16  27     0.0304        0.11528         2*0.0136    1.0  0.0 0.0 0.0 0.0;
34  9      0.008         0.05775         0.20        1.0  0.0 0.0 0.0 0.0;
27  35     0.0222        0.0839          2*0.00985   1.0  0.0 0.0 0.0 0.0;
27  28     0.0222        0.0839          2*0.00985   1.0  0.0 0.0 0.0 0.0;
35  29     0.033         0.264           2*0.0116    1.0  0.0 0.0 0.0 0.0;
27  29     0.02378       0.0902          2*0.0106    1.0  0.0 0.0 0.0 0.0;
29  30     0.01212       0.0459          2*0.0054    1.0  0.0 0.0 0.0 0.0;
4   36     0.0008        0.0055          0.021       1.0  0.0 0.0 0.0 0.0;
31  10     0.0058        0.022           2*0.0026    1.0  0.0 0.0 0.0 0.0;
10  14     0.01305       0.0495          2*0.0058    1.0  0.0 0.0 0.0 0.0;
14  18     0.02517       0.09548         2*0.0113    1.0  0.0 0.0 0.0 0.0;
18  20     0.0261        0.099           2*0.0117    1.0  0.0 0.0 0.0 0.0;
20  11     0.02767       0.1049          2*0.0124    1.0  0.0 0.0 0.0 0.0;
36  37     0.013         0.090           0.34        1.0  0.0 0.0 0.0 0.0;
10  15     0.0805        0.2353          2*0.0253    1.0  0.0 0.0 0.0 0.0;
15  22     0.0495        0.1449          2*0.0165    1.0  0.0 0.0 0.0 0.0;
22  12     0.0433        0.1267          2*0.0145    1.0  0.0 0.0 0.0 0.0;
11  19     0.0251        0.09526         2*0.0112    1.0  0.0 0.0 0.0 0.0;
19  21     0.0246        0.072           2*0.0083    1.0  0.0 0.0 0.0 0.0;
21  12     0.0385        0.1125          2*0.013     1.0  0.0 0.0 0.0 0.0;
31  13     0.0000        0.0303          0.0         1.0  0.0 0.0 0.0 0.0;
4   31     0.0000        0.01            0.0         1.0  0.0 0.0 0.0 0.0;
33  7      0.0000        0.01            0.0         1.0  0.0 0.0 0.0 0.0;
8   32     0.0000        0.01            0.0         1.0  0.0 0.0 0.0 0.0;
34  6      0.0000        0.01            0.0         1.0  0.0 0.0 0.0 0.0;
36  10     0.0000        0.01            0.0         1.0  0.0 0.0 0.0 0.0;
37  11     0.0000        0.01            0.0         1.0  0.0 0.0 0.0 0.0;
9   35     0.0000        0.01            0.0         1.0  0.0 0.0 0.0 0.0;
38  39     0.0000        0.01            0.0         1.0  0.0 0.0 0.0 0.0;
6   38     0.0000        0.01            0.0         1.0  0.0 0.0 0.0 0.0;
7   40     0.0000        0.01            0.0         1.0  0.0 0.0 0.0 0.0;
9   41     0.0000        0.01            0.0         1.0  0.0 0.0 0.0 0.0;
10  42     0.0000        0.01            0.0         1.0  0.0 0.0 0.0 0.0;
11  43     0.0000        0.01            0.0         1.0  0.0 0.0 0.0 0.0;
12  44     0.0000        0.01            0.0         1.0  0.0 0.0 0.0 0.0;
];
mac_con=[...
1 1  768 0.240 0.0012 2.100 0.400 0.250 4.50 0.034 2.05 1.200 0.250 1.50  0.15  2.40 2.0 0 1;
2 39 25  0.134 0.0014 1.250 0.232 0.120 4.75 0.059 1.22 0.715 0.120 1.50  0.210 5.02 2.0 0 39;
3 40 192 0.102 0.0026 1.651 0.232 0.171 5.90 0.033 1.59 0.380 0.171 0.535 0.078 3.30 2.0 0 40;
4 41 192 0.102 0.0026 1.651 0.232 0.171 5.90 0.033 1.59 0.380 0.171 0.353 0.078 3.30 2.0 0 41;
5 42 35  0.134 0.0014 1.250 0.232 0.120 4.75 0.059 1.22 0.715 0.120 1.500 0.210 5.02 2.0 0 42;
6 43 160 0.110 0.0031 1.700 0.245 0.185 5.90 0.033 1.64 0.380 0.185 0.540 0.076 3.96 2.0 0 43;
7 44 25  0.134 0.0014 1.250 0.232 0.120 4.75 0.059 1.22 0.715 0.120 1.500 0.210 5.02 2.0 0 44;
 ];
```

```
exc_con=[...
1 1 0.01 46.0 0.06 0 0 1.0 -0.9  0.0  0.4  4.5  0.267  3.4  0.07  0.02  1.0  0  0  0;
1 2 0.01 46.0 0.06 0 0 1.0 -0.9  0.0  0.4  4.5  0.267  3.4  0.07  0.02  1.0  0  0  0;
1 3 0.01 46.0 0.06 0 0 1.0 -0.9  0.0  0.4  4.5  0.267  3.4  0.07  0.02  1.0  0  0  0;
1 4 0.01 46.0 0.06 0 0 1.0 -0.9  0.0  0.4  4.5  0.267  3.4  0.07  0.02  1.0  0  0  0;
1 5 0.01 46.0 0.06 0 0 1.0 -0.9  0.0  0.4  4.5  0.267  3.4  0.07  0.02  1.0  0  0  0;
1 6 0.01 46.0 0.06 0 0 1.0 -0.9  0.0  0.4  4.5  0.267  3.4  0.07  0.02  1.0  0  0  0;
1 7 0.01 46.0 0.06 0 0 1.0 -0.9  0.0  0.4  4.5  0.267  3.4  0.07  0.02  1.0  0  0  0;
];

tg_con=[...
1  1  1  25.0  1.0  0.1  0.5  0.0  1.25  5.0;
1  2  1  25.0  1.0  0.1  0.5  0.0  1.25  5.0;
1  3  1  25.0  1.0  0.1  0.5  0.0  1.25  5.0;
1  4  1  25.0  1.0  0.1  0.5  0.0  1.25  5.0;
1  5  1  25.0  1.0  0.1  0.5  0.0  1.25  5.0;
1  6  1  25.0  1.0  0.1  0.5  0.0  1.25  5.0;
1  7  1  25.0  1.0  0.1  0.5  0.0  1.25  5.0;
];

load_con=[...
         4   0   0   0   0;
         45  0   0   0   0;
         46  0   0   0   0;
         8   0   0   0   0;
         ];

svc_con = [...

    1  4 100  2  0  20  0.02 0.0905 0.6460 0.5;
    2  8 100  2  0  20  0.02 0.0905 0.6460 0.5;
];

tcsc_con=[...
         1  45  4 1.0  0.05  0  -1.3;
         2  46  8 1.0  0.05  0  -1.3;
         ];

rlmod_con = [1  4 100 2 -2 2 0.2;
             2  8 100 2 -2 2 0.2];


% damping controller function

%SVC-1
svc_dc=[];
svc_dc{1,1}=0.25.*wo_stsp(5).*(ldlg_stsp(1,0.6460,0.0905.^1));
svc_dc{1,2}=1;
svc_dc{1,3}=4;
svc_dc{1,4}=2;
svc_dc{1,5}=0;
svc_dc{1,6}=2;


% SVC-2
svc_dc{2,1}=0.25.*wo_stsp(5).*(ldlg_stsp(1,0.6460,0.0905.^1));
svc_dc{2,2}=2;
svc_dc{2,3}=8;
svc_dc{2,4}=2;
svc_dc{2,5}=0;
svc_dc{2,6}=2;


% TCSC-1
tcsc_dc=[];
tcsc_dc{1,1}=70.*wo_stsp(10).*(ldlg_stsp(1,0.4009,0.1509)).^1;
tcsc_dc{1,2}=1;
tcsc_dc{1,3}=45;
tcsc_dc{1,4}=0;
tcsc_dc{1,5}=-1.3;
tcsc_dc{1,6}=2;
```

```
 % TCSC-2
tcsc_dc{2,1}=70.*wo_stsp(10).*(ldlg_stsp(1,0.4009,0.1509)).^1;
tcsc_dc{2,2}=2;
tcsc_dc{2,3}=46;
tcsc_dc{2,4}=0;
tcsc_dc{2,5}=-1.3;
tcsc_dc{2,6}=2;

sw_con=[...
0    0  0  0 0 0 0.01;
0.3  31 13 0 0 0 0.005;
0.35 0  0  0 0 0 0.005;
0.4  0  0  0 0 0 0.01;
0.5  0  0  0 0 0 0.01;
1.0  0  0  0 0 0 0.01;
20.0 0  0  0 0 0 0;
];
lmon_con=[1:length(line(:,1))]';
```

B-2. UWPFLOW Data East-West Interconnected System

```
HDG

EAST-WEST INTERCONNECTED SYSTEM WITH SERIES-SHUNT COMPENSATION

BAS
C       1        2        3        4        5        6        7        8
C 34567890123456789012345678901234567890123456789012345678901234567890123456789 0
C
BQ   BUS_1     230                          500.0-500..870
B    BUS_2     230
B    BUS_3     230
B    BUS_4     230
B    BUS_5     132  24.00 9.60      10
B    BUS_6     132  37.0014.80       5
B    BUS_7     132
B    BUS_8     230
B    BUS_9     230
B    BUS_10   132  20.00 8.00
B    BUS_11   132  30.0012.00      10
B    BUS_12   132  20.00 8.00      7.5
B    BUS_13   132  10.00
B    BUS_14   132  20.00 8.00      2.5
B    BUS_15   132  20.00 8.00      2.5
B    BUS_16   132  20.00 8.00
B    BUS_17   132  10.00 4.00
B    BUS_18   132  10.00 4.00      7.5
B    BUS_19   132  5.00  2.00
B    BUS_20   132  5.00  2.00
B    BUS_21   132  10.00 4.00
B    BUS_22   132  20.00 8.00
B    BUS_23   132  25.0010.00
B    BUS_24   132  26.0010.40      7.5
B    BUS_25   132  38.0015.20      7.5
B    BUS_26   132  10.00 4.00
B    BUS_27   132  10.00 4.00       15
B    BUS_28   132  10.00 4.00
B    BUS_29   132  15.00 6.00       35
B    BUS_30   132  35.0014.00
B    BUS_31   132  10.00  4.00      10
B    BUS_32   132  10.00  4.00
B    BUS_33   230
B    BUS_34   230
B     BUS_35   132  10.00 4.00
B     BUS_36   230
B     BUS_37   230
B     BUS_38     33
```

```
BQ   BUS_39   11                    10.00 7.50    -7.5.950
BQ   BUS_40   11                    125.0127.0-127..870
BQ   BUS_41   11                    120.0122.0-122..950
BQ   BUS_42   11                    23.00 20.0    -20..850
BQ   BUS_43   11                    105.0107.0-107..850
BQ   BUS_44   11                    15.0013.00-13.0.850
B    BUS_45  230
B    BUS_46  230
C
C
C       1        2        3        4        5        6        7        8
C 34567890123456789012345678901234567890123456789012345678901234567890123456789890
C
L    BUS_1    230  BUS_2    2301              .001
L    BUS_1    230  BUS_3    2301              .001
L    BUS_2    230  BUS_45   2301     .0267  .1371       .13240
L    BUS_3    230  BUS_46   2301     .0110  .0770       .14770
L    BUS_31   132  BUS_5    1321     .0174  .066        .00780
L    BUS_31   132  BUS_17   1321     .0093  .0352       .00420
L    BUS_17   132  BUS_26   1321     .0232  .088        .01040
L    BUS_7    132  BUS_26   1321     .00462 .0135       .00155
L    BUS_26   132  BUS_32   1321     .0197  .0748       .00884
L    BUS_31   132  BUS_7    1321     .0385  .1125       .01270
L    BUS_4    230  BUS_33   2301     .0044  .03025      .05810
L    BUS_6    132  BUS_25   1321     .0261  .099        .01170
L    BUS_5    132  BUS_6    1321     .0377  .1430       .01690
L    BUS_31    132 BUS_23   1321     .0261  .099        .01100
L    BUS_5    132  BUS_23   1321     .0308  .09         .01020
L    BUS_23   132  BUS_24   1321     .0275  .104        .01220
L    BUS_7    132  BUS_32   1321     .0232  .088        .01044
L    BUS_33   230  BUS_8    2301     .0032  .022        .04220
L    BUS_6    132  BUS_32   1321     .0383  .1452       .01720
L    BUS_34   230  BUS_8    2301     .00544.0374        .07170
L    BUS_6    132  BUS_16   1321     .0291  .1104       .01310
L    BUS_16   132  BUS_27   1321     .0304  .11528      .01360
L    BUS_34   230  BUS_9    2301     .008   .0577       .08000
L    BUS_27   132  BUS_35   1321     .0222  .0839       .00985
L    BUS_27   132  BUS_28   1321     .0222  .0839       .00985
L    BUS_35   132  BUS_29   1321     .033   .264        .01160
L    BUS_27   132  BUS_29   1321     .02378.0902        .01060
L    BUS_29   132  BUS_30   1321     .01212.0459        .00540
L    BUS_31   132  BUS_10   1321     .0058  .022        .00260
L    BUS_4    230  BUS_36   2301     .0008  .0055       .01050
L    BUS_10   132  BUS_14   1321     .01305.0495        .00580
L    BUS_14   132  BUS_18   1321     .02587.09548       .01330
L    BUS_18   132  BUS_20   1321     .0261  .099        .01170
L    BUS_20   132  BUS_11   1321     .02767.1049        .01240
L    BUS_36   230  BUS_37   2301     .013   .09         .10000
L    BUS_10   132  BUS_15   1321     .0805  .2353       .02530
```

```
L    BUS_15   132  BUS_22   1321     .0495  .1449       .01650
L    BUS_22   132  BUS_12   1321     .0433  .1267       .01450
L    BUS_11   132  BUS_19   1321     .0251  .09526      .01220
L    BUS_19   132  BUS_21   1321     .0246  .072        .00830
L    BUS_21   132 BUS_12   1321      .0385  .1125       .01300
L    BUS_31   132  BUS_13   1321            .0303
T    BUS_4    230  BUS_31   1321            .01
T    BUS_33   230  BUS_7    1321            .01
T    BUS_8    230  BUS_32   1321            .01
T    BUS_34   230  BUS_6    1321            .01
T    BUS_36   230  BUS_10   1321            .01
T    BUS_37   230  BUS_11   1321            .01
T    BUS_9    230  BUS_35   1321            .01
T    BUS_6    132  BUS_38    331            .01
T    BUS_38    33  BUS_39    111            .01
T    BUS_7    132  BUS_40    111            .01
T    BUS_9    230  BUS_41    111            .01
T    BUS_10   132  BUS_42    111            .01
T    BUS_11   132  BUS_43    111            .01
T    BUS_12   132  BUS_44    111            .01
C
C
C       1       2       3       4       5       6       7       8
C 345678901234567890123456789012345678901234567890123456789012345678901234567890
C
FS   BUS_8    230  BUS_8    230  1.1708  0.4925 90175 2 200  1. 26.    0.1
FS   BUS_4    230  BUS_4    230  1.1708  0.4925 90175 2 200  1. 26.    0.1
FC   BUS_45  230 BUS_4    230 .04113 .004113 144180  70.0  X          3.33
FC   BUS_46  230 BUS_8    230 .02310 .002310 144180  70.0  X          3.33
SOL                  50  BUS_1    230      0.
ZZ
END
```